YEAR END TECHNICAL REPORT
September 29, 2020 to September 28, 2021

Waste and D&D Engineering and Technology Development

Date submitted:

December 3, 2021

Principal Investigator:

Leonel E. Lagos, Ph.D., PMP®

Florida International University Collaborators:

Leonel E. Lagos, Ph.D., PMP® (Project Manager)
Himanshu Upadhyay, Ph.D., PMP®
Joseph Sinicrope, M.S., MBA
Walter Quintero, M.S.
Santosh Josh, M.S.
Tushar Bhardwaj, Ph.D.
Suresh Peddoju, Ph.D.
Masudur Siddiquee, Ph.D.
Clint Miller, MCSE+Security
Mellissa Komninakis, B.S.
Kexin Jiao, Ph.D.
DOE Fellows

Submitted to:

U.S. Department of Energy
Office of Environmental Management
Under Cooperative Agreement No. DE-EM0005213

FIU Applied Research Center
FLORIDA INTERNATIONAL UNIVERSITY

Addendum:

This document represents one (1) of five (5) reports that comprise the Year End Reports for the period of September 29, 2020 to September 28, 2021 prepared by the Applied Research Center at Florida International University for the U.S. Department of Energy Office of Environmental Management (DOE-EM) under Cooperative Agreement No. DE-EM0005213.

The complete set of FIU's Year End Reports for this reporting period includes the following documents:

Project 1: Chemical Process Alternatives for Radioactive Waste
Document number: FIU-ARC-2020-800012997-04b-009

Project 2: Environmental Remediation Science and Technology
Document number: FIU-ARC-2020-800013918-04b-004

Project 3: Waste and D&D Engineering and Technology Development
Document number: FIU-ARC-2020-800013919-04b-008

Project 4: DOE-FIU Science & Technology Workforce Development Initiative
Document number: FIU-ARC-2020-800013920-04b-017

Project 5: Long-Term Stewardship of Environmental Remedies: Contaminated Soils and Water and STEM Workforce Development
Document number: FIU-ARC-2020-800013922-04b-007

Each document will be submitted to OSTI separately under the respective project title and document number as shown above. In addition, the documents are available at the DOE Research website for the Cooperative Agreement between the U.S. Department of Energy Office of Environmental Management and the Applied Research Center at Florida International University: https://doeresearch.fiu.edu

TABLE OF CONTENTS

LIST OF FIGURES

LIST OF TABLES

PROJECT 3 EXECUTIVE SUMMARY

The Waste and D&D Engineering and Technology Development Project (Project 3) focuses on delivering solutions under the waste, D&D and IT areas for the DOE Office of Environmental Management. This work directly supports D&D activities being conducted across the DOE EM complex to include Oak Ridge, Savannah River, Hanford, Idaho and Portsmouth. This project included the following tasks during the September 29, 2020 to September 28, 2021 period of performance:

Task 1: Waste Information Management System (WIMS)

This task provides direct support to DOE EM for the management, development, and maintenance of a Waste Information Management System (WIMS). WIMS was developed to receive and organize the DOE waste forecast data from across the DOE complex and to automatically generate waste forecast data tables, disposition maps, GIS maps, transportation details, and other custom reports. WIMS is successfully deployed and can be accessed from the web address https://emwims.org/. The waste forecast information is updated annually. WIMS has been designed to be extremely flexible for future additions and is being enhanced on a regular basis.

Task 2: D&D Support for DOE EM for Technology Innovation, Development, Evaluation and Deployment

This task provides direct support to DOE EM for D&D technology innovation, development, evaluation, and deployment in several key areas based on high priority operational requirements, for which FIU will provide support by expanding its research in technology test and evaluation to: 1) Support SRNL and SRS 235-F in completion of the final data collection and Technical Report for the onsite hot demonstration of the FD intumescent fixative at the SRS 235-F PUFF Facility; 2) Confirm the experimental designs intended to certify fixative technology performance when exposed to various stressors (e.g., fire, thermal, environmental, water) that are postulated in contingency scenarios in DOE EM-wide Safety Basis Documents; 3) Investigate the application of a down-selected intumescent foam technology and other fire retardant materials to mitigate contaminate release during nuclear pipe dismantling and other D&D activities; 4) Collaborate with ASTM to continue development of standards and testing protocols in support of D&D technologies; and 5) Investigate the potential for multi-functional fixatives intended for mercury abatement during D&D Activities. FIU will further support the EM D&D program by participating in D&D workshops, conferences, and serving as subject matter experts.

Task 3: D&D Knowledge Management Information Tool (KM-IT)

The Knowledge Management Information Tool (KM-IT) is a web-based system developed to maintain and preserve the EM knowledge base. The system was developed by Florida International University's Applied Research Center with the support of the D&D community, including DOE-EM, the former DOE ALARA centers, and with the active collaboration and support of the DOE's Energy Facility Contractors Group (EFCOG). The KM-IT is a community driven system tailored to serve the technical issues faced by the workforce across the DOE Complex. The KM-IT can be accessed from web address http://www.dndkm.org.

Task 6: AI for EM Problem Set (D&D): Structural health monitoring of D&D facility to identify cracks and structural defects for Surveillance and Maintenance (SRNL)

This task is focused on investigating specific applications of artificial intelligence and big data technologies to solve DOE-EM problem sets and challenge areas, including potential applications of existing state-of-the-art technologies (e.g., imaging, robotics, big data, and machine learning/deep learning) to assess the structural integrity of aging facilities in support of ongoing surveillance and maintenance (S&M) across the DOE complex.

Task 7: AI for EM Problem Set (Soil and Groundwater) - Exploratory data analysis and machine learning model for Hexavalent Chromium (Cr [VI]) concentration in 100-H area (PNNL) (NEW)

The overall goal of this research task is to couple long-term monitoring data of hexavalent chromium [Cr(VI)] with AI/ML models to identify temporal and spatial relationships of subsurface chromium transport that reduces uncertainties in the conceptual site model (CSM).

Task 8: AI for EM Problem Set (Soil and Groundwater) – Data analysis and visualization of sensor data from wells at the SRS F-Area using machine learning (LBNL, SRNL) (NEW)

The main objective of this task is to determine the most optimal locations to place an additional 10 to 15 Aqua TROLL 500 sensors. The well locations should be chosen with the aim of capturing the overall contamination and groundwater movement.

MAJOR TECHNICAL ACCOMPLISHMENTS

Task 1: Waste Information Management System (WIMS) (HQ)

- FIU successfully ensured a consistent high level of performance of the WIMS application through day-to-day maintenance and administration tasks.
- FIU received a new set of waste stream forecast and transportation forecast data from DOE and completed the data import and all the necessary code updates to the back-end and front-end of the application to accommodate the new waste streams. This subtask was completed ahead of schedule on April 29, 2021.
- FIU developed a new GIS Map module using Google map APIs to display waste stream disposition information. This module provides enhanced features by integrating the latest web technology. Disposition paths are dynamically generated based on latitude and longitude coordinates of sites and disposition facilities. DOE was notified of the completion of this task on April 29, 2021.
- FIU successfully deployed Power BI report server with SQL server 2019 in DOE-EM infrastructure to publish WIMS reports. This milestone was completed on January 29, 2021. Power BI report server is a reliable and efficient platform, which is hosted on a new server with web facing interface. This server replaced the existing SQL reporting server for 2021 waste stream reports.
- FIU successfully ensured the WIMS application remained secure and reliable by consistently engaging with the external FIU security team to do independent testing and with the DOE Fellows to do internal testing. The DOE Fellows are learning to use the latest cyber security tools to get them ready for the workforce as they contribute to this task.
- A poster based on the WIMS application was presented at the Waste Management Symposia 2021 (WM2021) and was awarded “Best Poster Presentation in Track #3” at the conference.

Task 2: D&D Support to DOE EM for Technology Innovation, Development, Evaluation and Deployment

- Mr. Joseph Sinicrope accepted an invitation from ASTM International Board of Directors to serve a three-year term on the ASTM Committee on Technical Committee Operations starting January 1, 2021.
- The final report outline for the SRNL Hot Demo was approved and an associated POAM has been developed for the closeout activities.
- The SRS 235-F Risk Reduction team took the final thickness measurements of the FD Intumescent Fixative in the entry hood of Process Cell #1 on December 3, 2020. This will provide SRNL and FIU with the needed data points to press forward with the collaborative final report on the FD Intumescent Fixative research activity.
- FIU completed Milestone 2020-P3-M3 through participation in the ASTM E10 Committee Meeting. All comments made during the balloting process for the latest ASTM International standard, "Standard Practice for Preparation of Loose Radiological/Surrogate Contamination on Nonporous Test Coupon Surfaces for Evaluation of Decontamination Techniques", were addressed and adjudicated during the ASTM E10.03 subcommittee meeting.
- FIU completed the final report (deliverable 2020-P3-D10) for the onsite hot demonstration of intumescent fixative at SRS 235-F PUFF Facility. The technical report, titled “A Novel

Approach to Mitigating the Potential Release of Radioisotopes Under Fire Conditions - Enhancing Fire Resiliency of Radiological Contamination Fixatives During Deactivation & Decommissioning Activities", was also posted to OSTI by SRNL at: https://www.osti.gov/servlets/purl/1772363.

- DOE-EM released an article on the newly announced ASTM standard for the work under the FIU CA and the overall collaborative efforts with ASTM International to facilitate the introduction of new decommissioning technologies: https://www.energy.gov/em/articles/em-collaboration-leads-new-standards-fixatives.
- FIU participated in an initial meeting with SRNL and the F/H Lab Deactivation Site Team to discuss the Cold Demo Test Plan for Project 3 Subtask 2.2. General test objectives were outlined and there is a desire to conduct an onsite hot demo o/a FY'23, pending the results of the cold demo.
- FIU completed the Technical Progress Report on Certifying Fixative Technology Performance under Task 2 (deliverable 2020-P3-D11).
- Mr. Joseph Sinicrope was nominated for the 2nd Vice Chair on the ASTM E10 Main Committee. Voting for the E10 Main Committee Officer Election Ballot will be open from October 6, 2021 to November 6, 2021.
- DOE Fellow, Derek Gabaldon, won the Undergraduate Student Poster competition at the WM2021 Symposia for his poster which was based on Task 2 Fixative Technologies research.
- A professional paper, also based on Task 2 Fixative Technologies research, was presented at the WM2021 Symposia and was awarded the designation of "Superior".

Task 3: D&D Knowledge Management Information Tool (KM-IT) (HQ, SRNL, INL, ANL)

- The team enhanced the KM-IT application by making it mobile-friendly providing a better user experience on mobile devices. All the modules of the KM-IT application have been modified to take advantage of the responsive design. The team no longer needs to maintain two separate code bases (desktop and mobile) for the D&D KM-IT application. FIU successfully completed this deliverable (2020-P3-D6) D&D KM-IT - Responsive Design on August 20, 2021.
- FIU successfully completed the deliverable (2020-P3-D3) KM-IT Development - Enhance D&D Research Module for Multiple DOE EM Sites and National Laboratories back in January 2021. The team has enhanced the research module framework to publish D&D research being performed at various national labs and universities.
- FIU has successfully completed the Milestone 2020-P3-M4, Software Upgrades - Database and .NET Framework for D&D KM-IT in February 2021. This involved migration of the SQL server database and KM-IT modules to the .NET Framework 4.2.
- FIU published additional technologies, vendors and lessons learned on the KM-IT platform in addition to other relevant resources for the community, such as D&D related training, conferences and workshops. There were 72 technologies published on the D&D KM-IT website. The content management efforts continue to keep the website current and informative for the D&D community.
- FIU presented the research accomplishments on D&D KM-IT for the year 2020 during a poster session at the 2021 Waste Management Symposia virtual conference.
- The team performed 3 Tech Talks during this period of performance (in January, April, and July 2021). This involved collaboration with Savannah River National Laboratory (SRNL),

Washington River Protection Solutions (WRPS), and Lawrence Berkeley National Laboratory (LBNL) to present topics relevant to the DOE EM Complex.

- The team has successfully kept the D&D KM-IT application and production environment running with optimal performance. In addition, the team continued to test, maintain, secure and administer the KM-IT system to keep it secured and up to date with industry standards.

Task 6: AI for EM Problem Set (D&D): Structural health monitoring of D&D facility to identify cracks and structural defects for Surveillance and Maintenance (SRNL)

- A CNN deep learning approach was implemented for structural healing monitoring.
- YOLOv3 (You Only Look Once V3) neural network architecture has been implemented, which is a Real-Time object detection mechanism suitable for streaming videos, static videos, and static images.
- A One Class Classifier (OCC), which is a hybrid approach with a combination of Auto Encoder (AE) and CNN, was implemented.
- FIU proved their ability to generate 3D point clouds from mesh files that are like LiDAR scans.
- The FIU team designed an AE to reconstruct 3D point clouds from synthetic and LiDAR data capable of detecting some cracks.
- A Convolutional Auto Encoder (CAE) was implemented for anomaly detection, which can visually highlight the cracks in imagery data.

Task 7: AI for EM Problem Set (Soil and Groundwater) – Exploratory data analysis and machine learning model for Hexavalent Chromium (Cr [VI]) concentration in 100-H area (PNNL) (NEW)

- FIU developed an AI-based algorithm to resolve the key issue of missing values in soil and groundwater legacy datasets.
- Deep learning-based anomaly detection system was implemented using the 100 Area Cr (IV) dataset.
- A data filtering method was developed to filter the usable subset of the dataset for time-series pattern recognition and analyze the overall statistical features using metrics such as cosine similarity and Pearson correlation coefficient.
- A method was developed to explore any probable spatiotemporal relationships between inland monitoring wells and shoreline Cr(VI) concentrations using data filter and machine learning models.

Task 8: AI for EM Problem Set (Soil and Groundwater) - Data analysis and visualization of sensor data from wells at the SRS F-Area using machine learning (LBNL, SRNL) (NEW)

- FIU developed a suite of preprocessing and visualization tools to understand the pattern of the data for processing.
- Key analytes were identified for the sensor placement optimization by finding the correlation between in-situ sensors and contaminant.
- A spatial estimation pipeline was developed to optimize its parameters based on the given input.
- Thirteen (13) well locations were selected by LBNL that appeared in the recommended top 20 and another two that appeared in the top 22 to install new Aqua TROLL 500 sensors.

TASK 1: WASTE INFORMATION MANAGEMENT SYSTEM (WIMS) (HQ)

Subtask 1.1 WIMS System Administration - Database Management, Application Maintenance & Performance Tuning

Subtask 1.1: Introduction

This subtask includes the day-to-day maintenance and administration of the application and the database servers. FIU maintains the WIMS application system to ensure a consistent high level of performance. In addition, the database administrators perform routine maintenance in order to keep the WIMS database and server in a stable condition. The WIMS application is also maintained on the web server by the Web Server Administrator. This administrator monitors the network and server traffic and performs changes necessary to optimize the application performance. In addition, as part of this subtask, FIU will provide application and database security, as well as Help Desk support to DOE site waste managers, HQ managers and other users who need assistance in using WIMS.

Subtask 1.1: Objectives

The objective of this task is to secure the WIMS application (software and hardware) and make it more resilient to cyber-attacks. Cyber threats continue to increase at an exponential rate. The FIU team secures the application by performing routine maintenance and performance tuning. This helps prevent cyber breaches and also improves the user experience by allowing the application to run at optimal performance.

Subtask 1.1: Methodology

FIU is constantly updating the physical environment of the WIMS application. This requires the updates of the servers and software, including IIS (application server), SQL Server (database server), and Microsoft Visual Studio (development tool). This effort supports system availability, security, maintenance, backup and disaster recovery, etc. Keeping software and hardware up to date facilitates future migration/upgrade processes which also reduces overall maintenance costs.

In addition, FIU continues to perform certain security tasks, including antivirus engine and definitions updates on both the web and database servers. Other maintenance tasks included Windows OS updates and patches that were applied to the servers running the emwims.org application.

Additional effort was expended on the system administration task resulting in the completion of two milestones during the month of April 2021 (Task 1.2 and 1.3). This included backing up and restoring the production application and database to the development environment, setting up a staging server for unit and integration testing for FIU and DOE, and deploying the final version to the production server.

After completing Tasks 1 & 2, the team proceeded to back up the application and database development servers used during the development of those tasks. In addition, the team cleaned up the database from previous waste stream data.

Subtask 1.1: Results and Discussion

FIU continued to perform day-to-day maintenance and administration of the application and the database servers to ensure a consistent high level of performance of the WIMS application system. FIU continued to execute certain security tasks, including antivirus engine and definitions updates on both the web and database servers. Other maintenance tasks included Windows OS updates and patches that were applied to the servers running the emwims.org application. This routine maintenance is necessary in order to keep the WIMS database and server in a stable condition and to monitor the network and server traffic to optimize the application's performance.

Subtask 1.1: Conclusions

This is a continuous task. The objective of this task to secure the WIMS application (software and hardware) is an ongoing process. The FIU team has reduced cyber-attacks by securing the application through routine maintenance and performance tuning. This has contributed to the prevention of cyber breaches and improves the user experience by allowing the application to run at optimal performance.

Subtask 1.1: References

Waste Information Management System (WIMS), https://emwims.org/, Applied Research Center, Florida International University.

Subtask 1.2: Waste Stream Annual Data Integration

Subtask 1.2: Introduction

Under this subtask, FIU receives revised waste forecast data as well as transportation data as formatted data files on an annual basis. To incorporate these new files, FIU built a data interface to allow the files to be received by the WIMS application and imported into SQL Server. SQL server is the database server where the actual WIMS data is maintained. This data is typically received from DOE in the April/May timeframe.

Subtask 1.2: Objectives

The objective of this subtask is to consolidate waste forecast information from separate DOE sites and build forecast data tables, disposition maps, and GIS maps on the web. An integrated system is needed to receive and consolidate waste forecast information from all DOE sites and facilities and to make this information available to all stakeholders and to the public. As there was no off-the-shelf computer application or solution available for creating disposition maps and forecast data, FIU built a DOE complex-wide, high performance, n-tier web-based system for generating waste forecast information, disposition maps, GIS Maps, successor stream relationships, summary information and custom reports based on DOE requirements.

Subtask 1.2: Methodology

FIU receives revised waste forecast data and transportation data as formatted data files from DOE EM on an annual basis. To incorporate these new files, FIU built a data interface to allow the files to be received by the WIMS application and imported into SQL Server. SQL server is the database server where the actual WIMS data is maintained. Once integrated, reviewed and verified, the new waste data replaces the existing/previous waste data and becomes fully viewable and operational in WIMS.

Subtask 1.2: Results and Discussion

Once the new annual waste forecast dataset was received from DOE EM in March 2021, the team worked on importing the data into the development database environment and updated the application to consume the new waste stream data. Changes were made to the front-end and back-end of the application to accommodate new data that was imported into the database. The team completed updating the Forecast, Disposition Map, GIS Map and Transportation Map modules with the new waste stream data. All changes made in the development environment were moved to staging for the DOE to review.

In early April, the team worked on importing the data into the development database environment and updated the application to consume the new waste stream data. Changes were made to the front-end and back-end of the application to accommodate new data that was imported into the database. Finally, at the end of April, the team completed updating the Forecast, Disposition Map, GIS Map and Transportation Map modules with the new waste stream data, ensuring all the feedback from DOE HQ was incorporated.

After a final review, the FIU team moved the application from the staging server to the production server and made all the data live at https://emwims.org/. This subtask was actually completed ahead of schedule on April 29, 2021. Figure 1 and Figure 2 below show a few screenshots representing the new data from 2021.

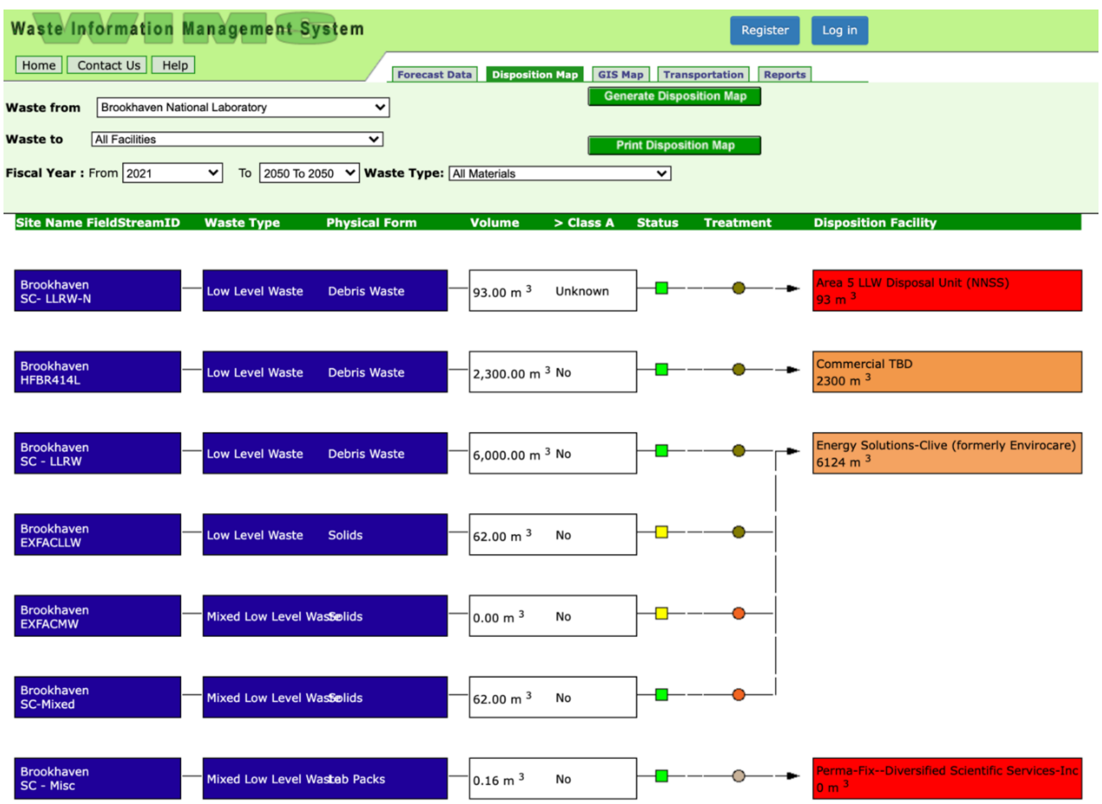

Figure 1. Disposition map module showing the waste forecast from Brookhaven National Laboratory to all facilities.

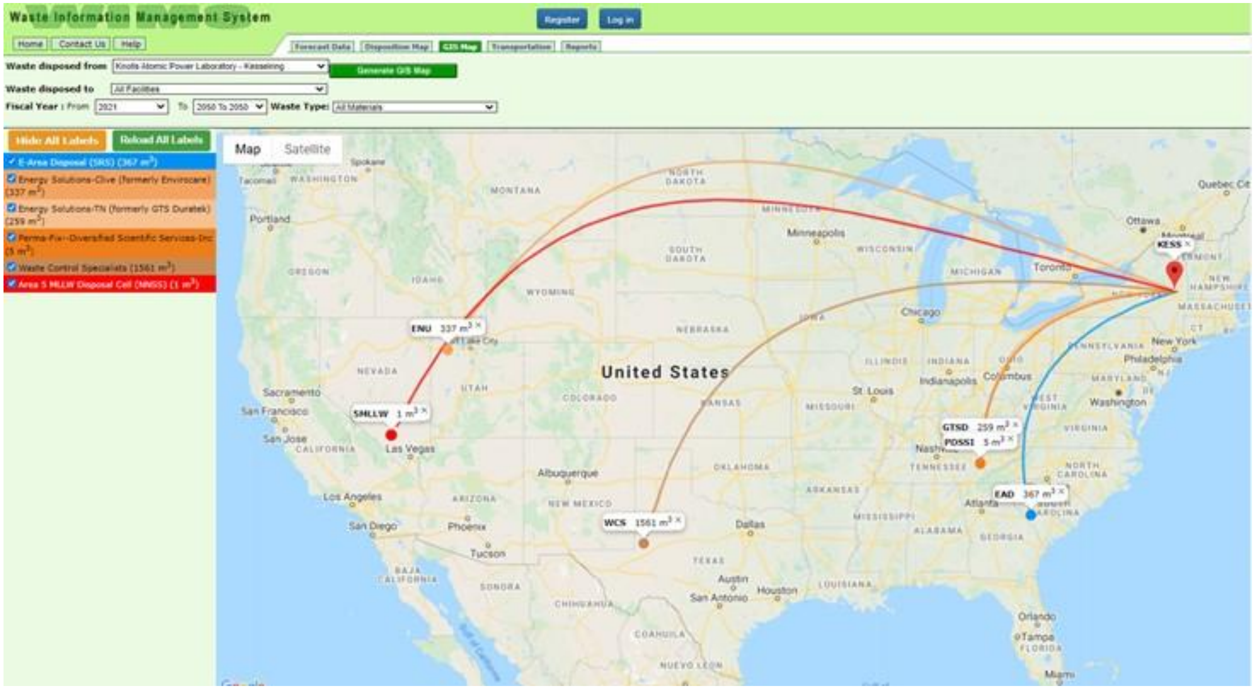

Figure 2. GIS Map module showing forecast data from Knolls Atomic Power Laboratory - Kesselring to all facilities.

As of the end of this period, the WIMS application supported the following waste types:

- All Materials
- Unknown
- Low-Level Waste
- Mixed Low-Level Waste
- 11e.(2) Byproduct Material
- Other Material

In addition, the waste can be forecasted among 36 sites and 34 disposition facilities. The names of each of the locations are listed below. These include a new disposition facility named US Ecology-Idaho.

Table 1. List of Sites and Facilities Supported by WIMS

	SITES		**FACILITIES**
1	Ames Laboratory	1	200 Area Burial Ground (HANF)
2	Argonne National Laboratory	2	746-U Landfill (Paducah)
3	Bettis Atomic Power Laboratory	3	Alaron
4	Brookhaven National Laboratory	4	Area 5 LLW Disposal Unit (NTS)
5	Energy Technology Engineering Center	5	Area 5 MLLW Disposal Cell (NTS)
6	Fermi National Accelerator Laboratory	6	Clean Harbors
7	Hanford Site-RL	7	Commercial TBD
8	Hanford Site-RP	8	E-Area Disposal (SRS)
9	Idaho National Laboratory	9	EMWMF Disposal Cell (ORR)
10	Kansas City Plant	10	Energy Solutions-Clive (formerly Envirocare)

11	Knolls Atomic Power Laboratory - Kesselring	11	Energy Solutions-TN (formerly GTS Duratek)
12	Knolls Atomic Power Laboratory - Schenectady	12	ERDF (HANF)
13	Lawrence Berkeley National Laboratory	13	Impact Services-TN
14	Lawrence Livermore National Laboratory	14	INL CERCLA Cell (INL)
15	Los Alamos National Laboratory	15	Integrated Disposal Facility (HANF)
16	Naval Reactor Facility	16	New RH LLW Vaults (INL)
17	Nevada Test Site	17	Omega Waste Logistics
18	NG Newport News	18	OSWDF(Portsmouth)
19	Norfolk Naval Shipyard	19	Paducah CERCLA
20	Nuclear Fuel Services, Inc. (cleanup site)	20	Perma-Fix Gainesville
21	Oak Ridge Reservation	21	Perma-Fix--Diversified Scientific Services, Inc.
22	Paducah Gaseous Diffusion Plant	22	Perma-Fix--Northwest (formerly PEcoS)
23	Pantex Plant	23	Perma-Fix/Materials & Energy Corp
24	Pearl Harbor Naval Shipyard	24	Remote Waste Disposition Project (INL)
25	Pacific Northwest National Laboratory	25	River Metals
26	Portsmouth Gaseous Diffusion Plant	26	RMW Trenches (MLLW/LLW) (HANF)
27	Portsmouth Naval Shipyard	27	RMW Trenches/IDF (HANF)
28	Princeton Plasma Physics Laboratory	28	RWMC (LLW disposal) (INL)
29	Puget Sound Naval Shipyard	29	Siemens
30	Sandia National Laboratories - NM	30	Smokey Mountain Solutions
31	Savannah River Site	31	TA 54/Area G (LLW disposal) (LANL)
32	Stanford Linear Accelerator Center	32	To Be Determined
33	Separations Process Research Unit	33	US Ecology-Idaho
34	Thomas Jefferson National Accelerator Facility	34	Waste Control Specialist
35	Waste Isolation Pilot Plant		
36	West Valley Demonstration Project		

Subtask 1.2: Conclusions

WIMS continues to successfully accomplish the goals and objectives set forth by DOE. WIMS has replaced the historic process of each DOE site gathering, organizing, and reporting their waste forecast information utilizing different database and display technologies. In addition, WIMS meets DOE's objective to have the complex-wide waste forecast information available to all stakeholders and the public in one easy-to-navigate system. The data includes low-level and mixed low-level radioactive waste forecast data supplied by all DOE programs in addition to transportation information. After a final review, the FIU team published the application to the production server running live at https://emwims.org/. This subtask (2020-P3-M6) was completed ahead of schedule on April 29, 2021.

Finally, the team prepared a poster for the Waste Management Symposia 2021 (WM2021), shown in the image below (Figure 3), titled *"Waste Information Management System (WIMS) with 2020-21 Waste Streams"* which was presented by Dr. Himanshu Upadhyay. On March 30, 2021, FIU was notified that the poster had won "Best Poster Presentation in Track #3" at the conference. The poster presentation for Poster/Paper #21356 was presented in Session #74 and was selected based on the poster judging criteria which demonstrated knowledge, understanding and a foundation for future waste management endeavors. The team was also informed that this poster is eligible to win the "Best Poster Presentation of WM2021 Conference" award. If selected, the winner(s) will be invited to accept their award(s) at the Honors and Awards Ceremony at WM2022.

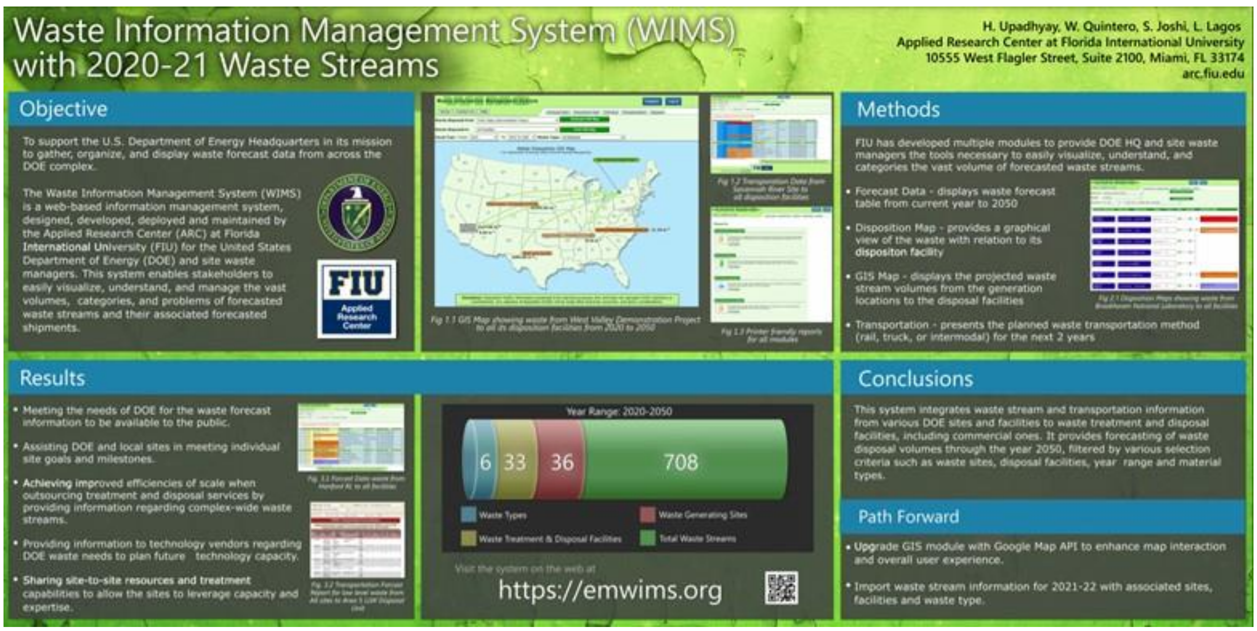

Figure 3. WIMS Poster for WM2021 titled "Waste Information Management System (WIMS) with 2020-21 Waste Streams".

Subtask 1.2: References

Office of Environmental Management (DOE-EM), https://www.energy.gov/em/office-environmental-management, U.S. Department of Energy.

Waste Information Management System (WIMS), https://emwims.org/, Applied Research Center, Florida International University.

Subtask 1.3: Upgrade GIS module with Google Map API

Subtask 1.3: Introduction

The current GIS module needs to be upgraded to make it mobile friendly and to reduce the development time when adding new disposition sites and facilities to the module. By incorporating the Google Map API, the module will be more interactive, and the user experience will be greatly improved, especially on mobile devices. These API calls can be used to add markers, polygons, and overlays to a basic map, and to change the user's view of a particular map area. These objects provide additional information for map locations and allow user interaction with the map.

Subtask 1.3: Objectives

The objective of this task is to upgrade the GIS module to use the Google Map API in order to improve the performance, stability, and user experience of the GIS module. Another advantage of replacing the existing GIS module with Google Map is that new updates to yearly waste streams data will be deployed much quicker because all the location information (latitude, longitude) will be stored on the database.

Subtask 1.3: Methodology

FIU created a development environment to develop this module where it started to incorporate the Google Maps API onto the WIMS application. The DOE Fellows assisted with getting GIS coordinates (latitude and longitude) for each site and disposition location. The existing database was modified to include this new information for each site and facility. The team proceeded to rewrite the GIS module code using a new approach to display the information with the help of new custom Javascript and Google Map API.

The team began by incorporating the Google Maps API with the data structure of the GIS module. This enabled the application to display the Google Maps by using the following code with different configuration settings. The team was also able to display the initial map by entering a value in the ‘zoom’ parameter of the Map class; center the map by binding Lat/Lng; and also choose different Map types as one of the settings for Map class to display different Map patterns.

```
var map = new google.maps.Map(document.getElementById("map_canvas"), {
    zoom: 5,
    center: new google.maps.LatLng(52.395715,4.888916),
    mapTypeId: google.maps.MapTypeId.ROADMAP
});
```

Later, the team was able to create markers for selected sites and facilities on the Map with the help of the google.maps.Marker class. The name of the site and facility can be displayed as text in the Marker. The infoWindow class was also added to include additional information about the site and facility.

```
var markerP1 = new google.maps.Marker({
    position: p1,
    map: map
});
```

Finally, it was possible to draw a line between site and facility with the help of the Polyline Class of the Google Maps API. By using polyline for a given site and chosen facility, the team was able to draw lines from one site to many facilities. This made it possible to assign different parameters as part of Polyline class, providing different options such as color of the line, thickness of the line, brightness of the line and many more.

```
var flightPath=new google.maps.Polyline({
        path:myfacilitypaths,
        strokeColor:"#0000FF",
        strokeOpacity:0.8,
        strokeWeight:2,
        map:map
  });
```

After this implementation, the team modified the functionality of Polyline in combination with Marker class to make it a curved instead of a straight line. This made it possible for any site-to-facility line or vice versa to be drawn in a curved manner, which improved the visibility of the line between the site and facility. This was achieved with the google.maps.Point() function and Icon parameter of the Marker whereby the Path parameter is used to draw the curved line between the site and facility.

```
Icon: {
                path: “M 0 0 q “ +   c.x + “ “ + c.y + “ “ + e.x + “ “ + e.y,
                scale: 24,
                strokeWeight: 2,
                fillColor: ‘#009933’,
                fillOpacity: 0,
                rotation: 180,
                anchor: new google.maps.Point(0, 0)
}
```

Apart from drawing lines (straight or curved) between site and facility, the team was also able to display Volume of the transfer as a Label at either site or facility, as per the requirement of the user selection. This Label class is customized and additional functionality was added to display the quantity at site or facility. User defined functions are created to give additional functionality to the Label class. The primary class for customizing the Label is initially defined by the overlay which is derived from google.maps.OverlayView, then the additional functionality was extended to the Label.

The team performed a rigorous unit test and integration testing on the new Google GIS module. The team, with the help of DOE Fellows, has tested each data combination between site and disposition facility. The application was moved to a staging server where DOE got a chance to review and provide feedback. After all the DOE comments and feedback were addressed, the team moved the application to the production server at https://emwims.org/.

Subtask 1.3: Results and Discussion

The result is a new Google GIS module using the latest technology, which provides a fast and more stable application with a better user experience. Users can filter their results and hide/show labels using the new sidebar capability, which also serves as a color legend for each location being displayed on the map. The Figure 4 below shows the new GIS module with the Google GIS API. The data shown is the waste stream data from Los Alamos National Laboratory to all facilities from 2021 to 2050.

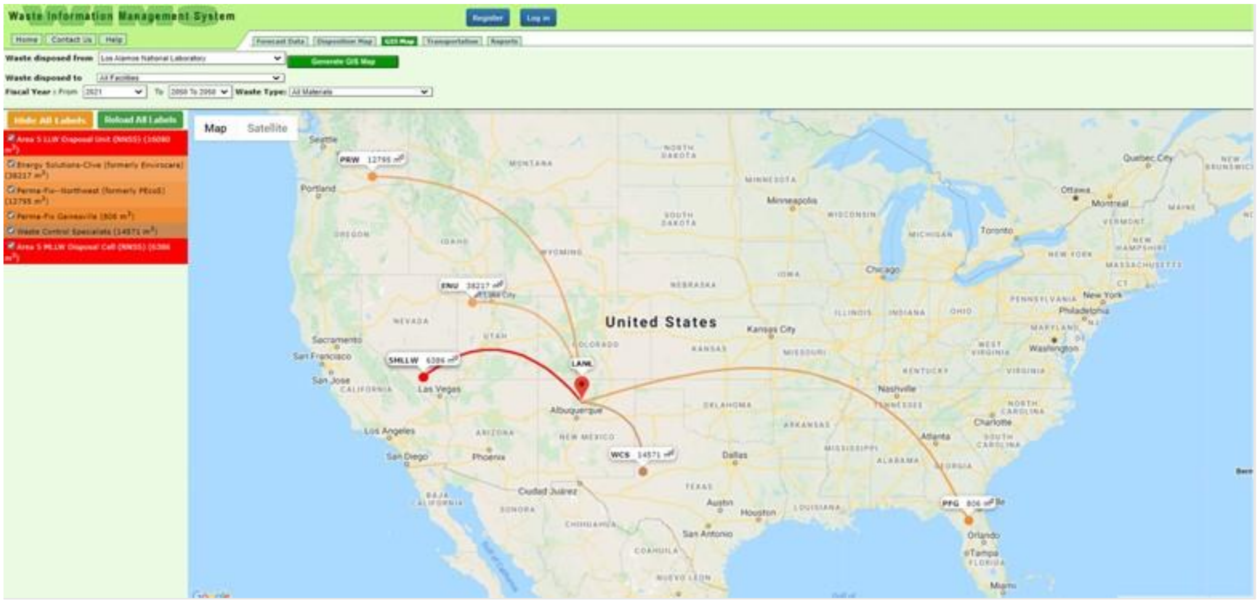

Figure 4. WIMS GIS Module with stream data from Los Alamos National Laboratory to all facilities from 2021 to 2050.

One of the more noticeable changes to the GIS module is the addition of a sidebar that serves as a map legend and helps the users interact with the map by allowing them to hide all labels and reload all the labels on the map. Also, when the user rolls his/her mouse over each of these locations, the location icon on the map bounces to help the user identify the facility. The sidebar is hidden when the map is first loaded before the user makes a selection (Figure 5 below).

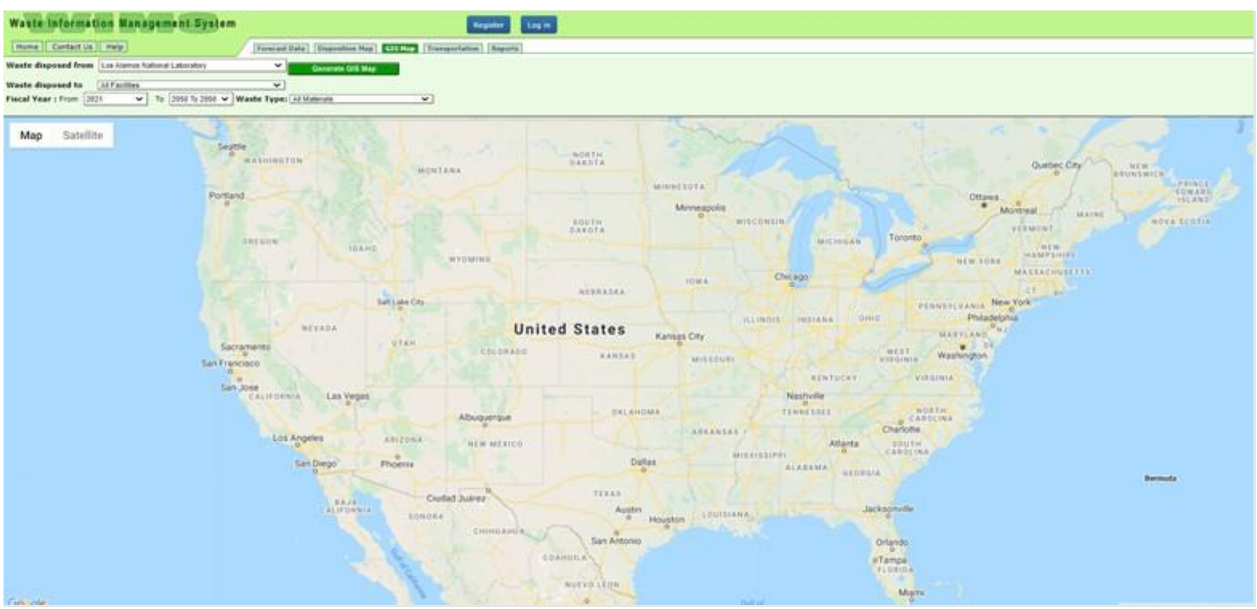

Figure 5. Default view of the GIS module before user makes a selection.

Subtask 1.3: Conclusions

FIU has developed a new GIS Map module using Google map APIs to display waste stream disposition information. This module provides enhanced features by integrating the latest web technology. Disposition paths are dynamically generated based on latitude and longitude coordinates of sites and disposition facilities. Users can filter their results and hide/show labels using the new sidebar capability, which also serves as a color legend for each location being displayed on the map. DOE was notified of the completion of this task on April 29, 2021. The updated module is available at the following link: https://emwims.org/GoogleGISMap. The team continues to monitor the API as it may require code adjustments to ensure its performance and stability are maintained.

Subtask 1.3: References

Waste Information Management System (WIMS), https://emwims.org/, Applied Research Center, Florida International University.

Google Maps Platform APIs by Platform Retrieved November, 2021 from https://developers.google.com/maps/apis-by-platform

Subtask 1.4: Deploy Power BI Reporting Server for Waste Stream Reports

Subtask 1.4: Introduction

Power BI is a powerful reporting server. It has proven to be very reliable, efficient and easy to use. It also provides a pleasant user interface that facilitates a very enjoyable user experience. This task replaces the existing SQL reporting server with Power BI reporting server. Power BI reporting server will be deployed with SQL Server 2019 to publish reports. This will provide a foundation for authoring existing reports using Power BI desktop.

Subtask 1.4: Objectives

The objective of this task is to replace the existing SQL reporting server with Power BI reporting server. This upgrade allows for a more reliable reporting platform for the WIMS application. The Power BI reporting server will make deploying new reports more efficient. It will also bring the reporting module of the WIMS application to the latest industry standards

Subtask 1.4: Methodology

The process of upgrading the WIMS application with the new Power BI reporting server involved setting up a development environment to perform this upgrade. After the development environment was in place, the team backed up a copy of the production environment which included the WIMS application and database. Next, the Power BI reporting server was installed on the same server running the SQL database. The Power BI reporting server was configured to use the WIMS SQL database and each of the existing reports were recreated using the new features of the Power BI reporting server. The WIMS application was updated so the Reports module was replaced to use the Power BI reporting server. The team proceeded to test the WIMS application, specifically the Power BI Reports module. After successful testing, the production application was updated and deployed at https://emwims.org/Reports.

Subtask 1.4: Results and Discussion

In January 2021, FIU successfully deployed Power BI report server with SQL server 2019 in DOE-EM infrastructure to publish WIMS reports. This completed milestone (2020-P3-M2) Deploy Power BI Reporting Server for Waste Stream Reports. Power BI report server is a reliable and efficient platform, which is hosted on a new server with web facing interface. This server replaced the existing SQL reporting server for 2021 waste stream reports. This will provide a foundation for authoring existing reports using Power BI desktop in future.

The new Power BI report server supports four types of reports. Below is the list of the reports supported and the following figure is a screen capture of the Report module on the WIMS application. There is also a sample of the Transportation Forecast Report incorporated on the WIMS application using a Report Viewer control. Figure 6 and Figure 7 below show the Report module landing page and a Transportation report from all sites to Waste Control Specialist. The list of current available reports are:

- Transportation Forecast Report
- Waste Stream Report
- Waste Stream Information Report
- Waste Stream Forecast Report

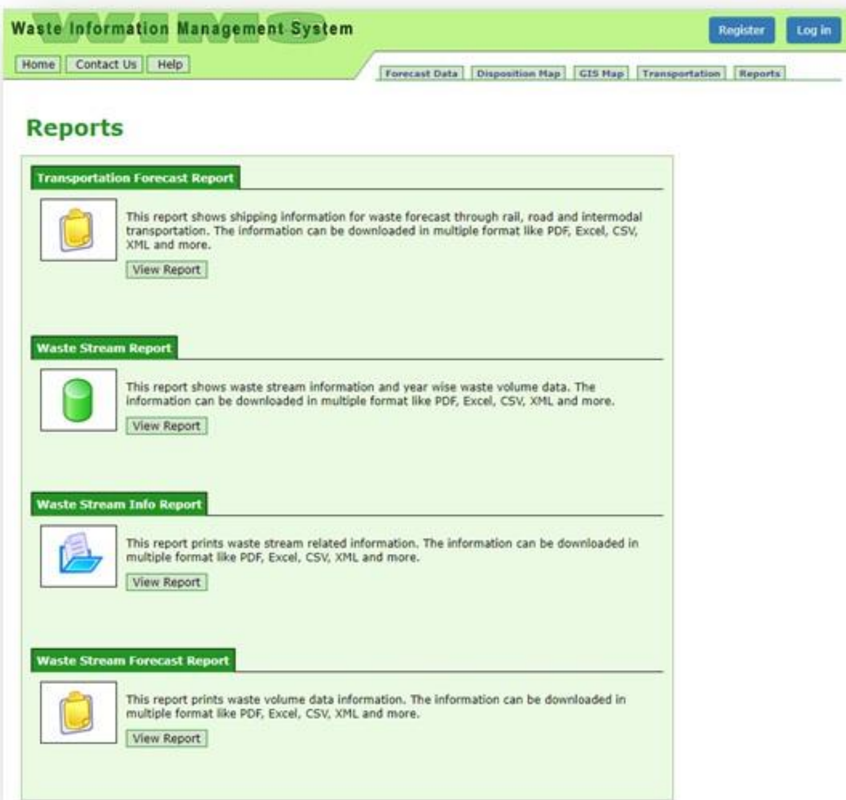

Figure 6. Screen capture of Report module landing page on WIMS.

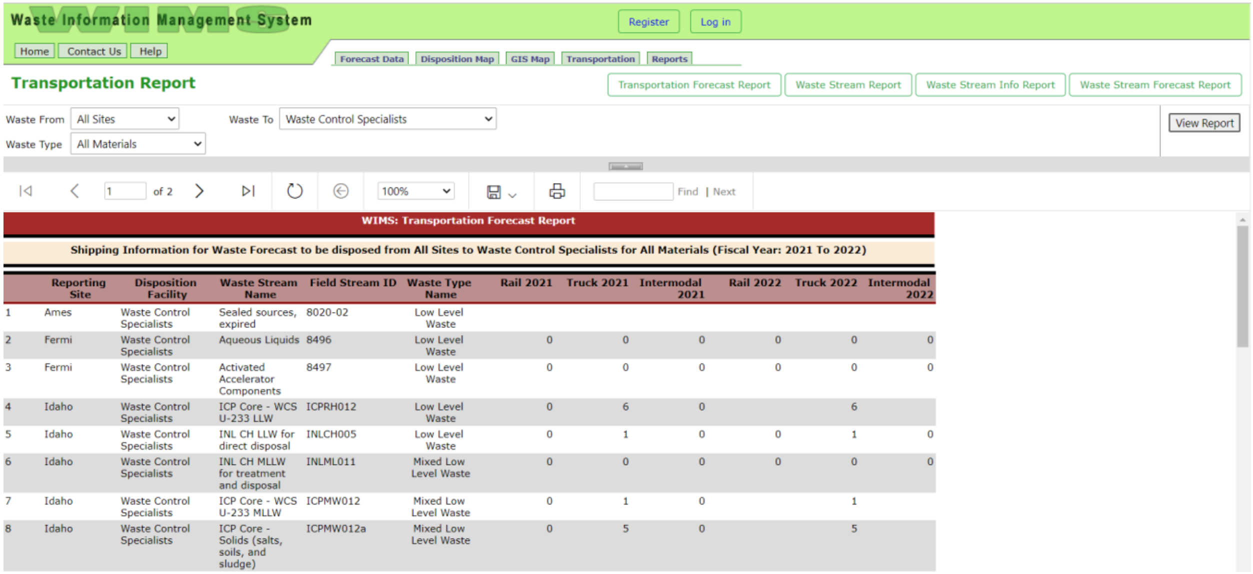

	Reporting Site	Disposition Facility	Waste Stream Name	Field Stream ID	Waste Type Name	Rail 2021	Truck 2021	Intermodal 2021	Rail 2022	Truck 2022	Intermodal 2022
1	Ames	Waste Control Specialists	Sealed sources, expired	8020-02	Low Level Waste						
2	Fermi	Waste Control Specialists	Aqueous Liquids	8496	Low Level Waste	0	0	0	0	0	0
3	Fermi	Waste Control Specialists	Activated Accelerator Components	8497	Low Level Waste	0	0	0	0	0	0
4	Idaho	Waste Control Specialists	ICP Core - WCS U-233 LLW	ICPRH012	Low Level Waste	0	6	0		6	
5	Idaho	Waste Control Specialists	INL CH LLW for direct disposal	INLCH005	Low Level Waste	0	1	0	0	1	0
6	Idaho	Waste Control Specialists	INL CH MLLW for treatment and disposal	INLML011	Mixed Low Level Waste	0	0	0	0	0	0
7	Idaho	Waste Control Specialists	ICP Core - WCS U-233 MLLW	ICPMW012	Mixed Low Level Waste	0	1	0		1	
8	Idaho	Waste Control Specialists	ICP Core - Solids (salts, soils, and sludge)	ICPMW012a	Mixed Low Level Waste	0	5	0		5	

Figure 7. Screen capture of Transportation Report from all sites to Waste Control Specialist on WIMS.

Subtask 1.4: Conclusions

The team met the objective of replacing the existing SQL reporting server with Power BI reporting server. This upgrade allowed for a more reliable reporting platform for the WIMS application. The Power BI reporting server makes it easier for deploying new reports on the WIMS application. This upgrade also brought the reporting module of the WIMS application to the latest industry standards.

Subtask 1.4: References

Waste Information Management System (WIMS), https://emwims.org/, Applied Research Center, Florida International University.

Microsoft Power BI [Wikipedia] Retrieved November, 2021 from https://en.wikipedia.org/wiki/Microsoft_Power_BI

Subtask 1.5: Cyber Security of WIMS Infrastructure

Subtask 1.5: Introduction

The cyber security of WIMS Infrastructure involves securing the network not only by system administration tasks mentioned above (Subtask 1.3), but also by conducting routine cyber security tasks to test the network's vulnerability. This involves coordination between the FIU security team and DOE Fellows who also learn cybersecurity skills while assisting staff do penetration testing and other tasks to test the overall security of the system at the application, database, and infrastructure levels.

Subtask 1.5: Objectives

The objective of this task is to focus on specific cyber security threats that could affect the WIMS application and framework. The team achieves this by implementing the latest industry security standards on the application and network in order to protect the WIMS application from malicious attacks.

Subtask 1.5: Methodology

Cyber security of WIMS involves securing the network infrastructure by performing routine cyber security tasks to test the network's vulnerability. The team involves coordination between the FIU security team and DOE Fellows to achieve this goal. The FIU security team performs independent security scans to test the vulnerability of the system. The reports of these scans are shared with the developer team which uses the information to focus on critical areas. The DOE Fellows perform internal tests on the environment. They use commonly used industry cyber security tools to test system vulnerability. By using these tools, the DOE Fellows are trained on the latest penetration test standards performed in the industry.

Some specific tasks include:

- Updating the DOE server room network switch from 24-port unmanaged switch to 50-port to managed switch. This switch supports the network connectivity of the server running the WIMS application.
- Updating security patches and applications for the servers and firewall of the DOE server room. This includes the server hosting the WIMS application.
- Updating Secure Socket Layer (SSL) security protocol each year.
- Performing penetration testing on the application and network.

Subtask 1.5: Results and Discussion

The teams continued to secure the application on a constant basis. This effort needs to be performed regularly as new security treads are developed daily. The team has engaged with the external FIU security team to do independent testing and engaged the DOE Fellows to do internal testing. As a result, the WIMS application has remained secure and reliable. The DOE Fellows are learning to use the latest cyber security tools to get them ready for the workforce as they contribute to this task.

Subtask 1.5: Conclusions

As mentioned above, this is a continuous task in which multiple teams work together to achieve the goal of securing the WIMS application. The team has been successful in keeping the application secured and are always looking for new tools to use in order to test the application security. As new threats are identified on the internet, the team tests the application against those threats and quickly applies the appropriate patches and software updates to minimize the system vulnerability.

Subtask 1.5: References

Waste Information Management System (WIMS), https://emwims.org/, Applied Research Center, Florida International University.

TASK 2: D&D SUPPORT TO DOE EM FOR TECHNOLOGY INNOVATION, DEVELOPMENT, EVALUATION AND DEPLOYMENT

Subtask 2.1: Development of Uniform Testing Protocols and Standard Specifications for D&D Technologies

Subtask 2.1: Introduction

The U.S. Department of Energy's Office of Environmental Management (DOE EM) has taken a leading role in investing the research and development (R&D) of critical technologies to support the safe and efficient decommissioning of legacy nuclear facilities. To facilitate the complex-wide deployment and adoption of those technologies from the laboratory to end users, and to maximize return on investment of government-sponsored R&D projects, DOE EM proactively solicits and evaluates initiatives intended to enhance achievement of these goals. One such case study emerged and involved the successful deployment of an intumescent fixative technology in support of the SRS 235-F PuFF Facility Risk Reduction Program. A detailed analysis confirmed that a critical enabler and key contributor to this effort was a deliberate, methodical approach to leverage an international, consensus-based standards organization from the onset. This approach ensured uniform standard specifications and testing protocols were used to confirm technology performance, which correspondingly mitigated the risk to the end user for acceptance and adoption of the new technological solution. There is a substantial body of literature that supports the crucial role of standards in technology programs across all phases of development - from concept, to deployment, to large-scale diffusion - in other industries. There are several federal directives that recognize the essential role of standards. For example, Section 12(d) of the National Technology Transfer and Advancement Act (Public Law 104-113), directs federal departments to achieve a greater reliance on voluntary consensus standards, and this mantra is also required by the Office of Management and Budget’s Circular A-119, “Federal Participation in the Development and Use of Voluntary Consensus Standards and in Conformity Assessment Activities.”

Given that standards-based testing and evaluation is a critical enabler to the successful transition and deployment of D&D technologies from the lab to the end user, FIU will continue to actively participate in ASTM International’s E10 and E10.03 Committees to develop and promulgate uniform performance metrics and testing protocols for D&D technologies, with a particular emphasis on fixatives and foams. To date, this effort has produced five (5) new international standard specifications and testing practices for fixative technologies which have been fully integrated into D&D technology test plans across the DOE EM complex. Another is currently under development that is intended to facilitate uniform testing protocols in order to evaluate and compare the operational performance of commercial fixatives. Furthermore, this initiative has been identified as a critical component to the successful transition of intumescent fixative technologies from the lab to the operational environment in support of end user requirements.

These efforts help to ensure that the FIU three-phased Technology Test and Evaluation Model is uniform in its application and defensible in its findings and results. As part of these efforts, FIU will attend and participate in the two planned ASTM International Conferences per year throughout this period of performance. The ultimate outcome of these efforts is to reduce the risks associated with implementing new technologies and further support the update of existing directives and guidance handbooks to account for the recent advancements in technology development in D&D.

Subtask 2.1: Objectives

Under this task, FIU ARC continued to actively participate in ASTM International's E10 and E10.03 Committees to develop and promulgate uniform performance metrics and testing protocols for D&D technologies, with a particular emphasis on fixatives and foams. This activity directly supports the planned operational deployment of those technologies on site, as well as establishes the groundwork for updating the DOE-HDBK-3010. Providing a uniform certification methodology for fixative technologies has been deemed an essential goal under this activity.

Subtask 2.1: Methodology

Leveraging the incombustible fixatives research and development activity being led by Savannah River National Laboratory (SRNL) and Florida International University's Applied Research Center (FIU ARC) on behalf of DOE EM's Office of Infrastructure and D&D, a holistic technology deployment approach was devised for the adoption of intumescent technologies as fire resistant fixatives. SRNL's close relationship with the SRS 235-F PuFF Facility Risk Reduction Team and FIU's involvement with the American Society for Testing and Materials (ASTM) International's E10.03 Subcommittee on Radiological Protection for D&D of Nuclear Facilities and Components provided an ideal vehicle to test the initiative. New international standard specifications for fixative technologies have been formally published and promulgated by ASTM. More importantly, this effort has been an important pillar for the test and evaluation of a fixative technology that has been successfully deployed in the entry hood and process cell #7 at the SRS 235-F PuFF Facility, and serves as the basis for promoting the planned deployment of the intumescent foam technology on site in FY'23/24.

Subtask 2.1: Results and Discussion

FIU, in collaboration with SRNL, introduced a fixative technology that mitigates the potential release of radioactive contamination under thermal and seismic stressors, and during the test and evaluation component of the activity it became readily apparent that the end-users at the site desired a more formal process that would assist in mitigating their risk exposure. In discussions with DOE EM, as well as commercial entities conducting the environmental restoration of various nuclear sites, it was determined that many of these human factor concerns could be alleviated by:

1. Leveraging an international, consensus-based organization that develops and promulgates international standards and testing protocols for fixative technologies used in D&D, and
2. Referencing these new standards to update dated regulations and directives guiding the environmental restoration of nuclear sites.

Immediately addressing these concerns would provide tremendous credibility to the R&D effort and yield a significant return on investment as the fixative technology would be tested, evaluated, and compared to a set of uniformly accepted standards and metrics that ensure it satisfactorily addresses the three pillars of test and evaluation – quality, productivity, and safety. This requirement becomes even more pressing and prominent when technologies are on the higher end of the technology readiness level (e.g., 7-9) and are ready for acquisition and deployment.

The ASTM International E10.03 Subcommittee on Radiological Protection during Decontamination and Decommissioning of Nuclear Facilities and Components is answering this challenge. It boasts a robust international membership that spans the entire spectrum of stakeholders and is perfectly postured to lead a collaborative process that bridges the organizational boundaries and cultures to achieve consensus on industry standards to facilitate uniform testing and evaluation of technologies and processes.

The E10.03 Subcommittee formed a D&D Fixatives Working Group that subsequently developed and published international standard specifications for fixative technologies that aim to immobilize radioactive contamination, minimize worker exposure, and protect uncontaminated areas against the spread of radioactive contamination during the decommissioning of nuclear facilities. The first specification, Specification for Strippable & Removable Coatings to Mitigate Spread of Radioactive Contamination (E 3104-17), establishes performance specifications for a coating that is intended to be removable during subsequent decontamination operations. The second specification, Specification for Permanent Coatings Used to Mitigate Spread of Radioactive Contamination (E 3105-17), is for coatings that are intended to be permanent, non-removable, long-term material for fixing contamination in place during decommissioning. These successes have ignited increased interest in the effort, and over the course of this performance year, one (1) additional standard has been developed, balloted, and formally promulgated, Standard Practice for Preparation of Loose Radiological/Surrogate Contamination on Nonporous Test Coupon Surfaces for Evaluation of Decontamination (E3283-21).

Subtask 2.1: Conclusions

The ASTM International E10.03 Subcommittee will continue pursuing further testing protocol and standards development for fixatives and other technology categories associated with D&D, creating consensus-based standards for D&D technologies that are not only aligned with technical specifications, but also account for the safety, regulatory, and operational requirements encountered during D&D activities. Addressing existing shortfalls through standards will provide credibility, yield a significant return on investment, and allow all types of D&D technologies (robotics, fixatives, characterization, decontamination, demolition, etc.) to be developed, tested, evaluated, and compared to a set of uniformly accepted metrics.

International standards and testing protocol development plays a critical role in successful technology development and deployment programs. These standards lay the groundwork for setting the necessary conditions to successfully test, evaluate, compare, transition, and employ technologies in support of D&D activities in the highly regulated, safety conscience, risk adverse industry in which work is done. Universally accepted standards are essential in building the bridge to full field deployment of new technologies. This is particularly relevant when working at the higher ends of the TRL readiness scale and addresses many concerns on the part of all stakeholders – from researchers and developers to end users, regulatory agencies, and the public.

Subtask 2.1: References

ASTM International. (2017). *E3104-17 Standard Specification for Strippable & Removable Coatings to Mitigate Spread of Radioactive Contamination.* Retrieved from https://doi.org/10.1520/E3104-17

ASTM International. (2017). *E3105-17 Standard Specification for Permanent Coatings Used to Mitigate Spread of Radioactive Contamination.* Retrieved from https://doi.org/10.1520/E3105-17

ASTM International. (2018). *E3191-18 Standard Specification for Permanent Foaming Fixatives Used to Mitigate Spread of Radioactive Contamination.* Retrieved from https://doi.org/10.1520/E3191-18

ASTM International. (2019). *E3190-19 Standard Practice for Preparation of Fixed Radiological/Surrogate Contamination on Porous Test Coupon Surfaces for Evaluation of Decontamination Techniques.* Retrieved from https://doi.org/10.1520/E3190-19

ASTM International. (2021). *E3283-21 Standard Practice for Preparation of Loose Radiological/Surrogate Contamination on Nonporous Test Coupon Surfaces for Evaluation of Decontamination Techniques.* Retrieved from https://doi.org/10.1520/E3283-21

Subtask 2.2: Applications of Intumescent Foams and Other Fire-Retardant Materials to Mitigate Contaminant Release during Nuclear Pipe Dismantling and other D&D Activities

Subtask 2.2: Introduction

In support of the DOE-FIU Cooperative Agreement under Project 3 (Waste and D&D Engineering and Technology Development), Task 2 (D&D Support for Technology Innovation, Development, Evaluation and Deployment), the FIU Applied Research Center (ARC) focused its research activities on identifying, testing and evaluating commercial-off-the-shelf (COTS) intumescent material technologies as fire resistant fixative solutions that have a high potential to: 1) successfully address postulated contingency scenarios outlined in Basis for Interim Operations (BIO) / Safety Basis documents across the complex; and, 2) demonstrate a high probability of transitioning to an operational test and evaluation in a radioactive environment on site. This approach resulted in one intumescent coating technology being deployed in the Entry Hood to Process Cell 1 and Process Cell 7 at the SRS 235-F PUFF Facility in September /October of 2018. It has also led to the identification of another COTS intumescent foam technology that has demonstrated initial promise during proof-of-concept experiments this year in addressing an operational requirement for a rigid, fire-resistant fixative technology to immobilize and/or isolate residual contamination within a 3-dimensional void space of various volumes at sites across the complex.

An operational concept has been developed and proposed using the intumescent foam technology as an internal barrier, or “plug”, prior to cutting contaminated pipework during dismantling and demolition operations on nuclear sites. Phase I of this research activity involved down-selecting a potential intumescent foam against some initial operational parameters outlined in ASTM E3191-18, Standard Specification for Permanent Foam Fixatives, specifically developed by the ASTM International E10.03 Subcommittee to support this broader activity. These included: 1) the ability to immobilize contamination and fill 3D spaces; 2) fire resistance to extreme temperatures and thermal stressors; 3) ability to withstand certain environmental factors such as water; 4) mechanical properties such as rigidity and adhesion to ensure the material can act as a “plug” in piping and not be adversely affected when exposed to expected impact stressors; and, 5) confirmation of temperature profiles related to curing and uniform application of the material. Based on the initial findings and through extensive discussions with SRNL and other stakeholders across DOE EM, a COTS intumescent polyurethane foam (naming convention "I-H") has been identified and down-selected as a technology that warrants further investigation. The research plan for the next phase is to develop, in close collaboration with SRNL and site personnel, an operationally-focused test plan designed to directly evaluate the technology in terms of immediate, high priority requirements from safety basis personnel to conduct an operational test and evaluation on a DOE EM site by 2021. This approach mirrors the highly successful phased test and evaluation model employed by ARC and SRNL for the intumescent coating technology deployed in support of the SRS 235-F PUFF Facility as highlighted in the December 2018 Defense Nuclear Facility Safety Board (DNFSB) report and SRNL promotional video on the activity.

Subtask 2.2: Objectives

This research activity involved down-selecting a potential commercial-off-the-shelf (COTS) intumescent foam against some initial operational parameters outlined in ASTM E3191-18, Standard Specification for Permanent Foam Fixatives. Mechanical testing included overall "Plug Strength" to determine the force required to cause the intumescent foam and other specialized concretes/mortars to fail (delaminate or a combination of failures) when inside 304-stainless steel pipes.

Subtask 2.2: Methodology

The COTS intumescent foam selected for evaluation is the I-H foam. This product is a two-component polyurethane foam that expands up to six times in volume upon application and cures in approximately one minute. The volume of foam produced per cartridge is up to 110 in^3. Per the application instructions, the first five pumps of the dispenser (or until the foam in the mixer nozzle has a consistent red color) will be discarded because this initial portion is unevenly mixed. FIU also assessed the viability of a fire barrier mortar, as an alternative to the I-H foam, as a fire resistant "plug". The mortar's self-leveling consistency (two parts mortar to every one part water) was selected for testing for ease of application.

Mechanical properties tested included Plug Strength, baseline and when exposed to stressors. Plug strength is defined as, the force level at which failure occurs in which the fixative no longer acts as a plug, in units of pounds force (lbf), in a push-out test with a specific test specimen geometry and size. The stressors involved drop test, water submersion, and extreme heat conditions. Drop testing was performed at heights of 4, 8, and 12 ft. Water submersion was accomplished at a water depth of 3 ft. and submerged for 8, 12, and 24 hrs. Thermal conditions were evaluated by exposing samples to open flames from a propane torch at temperatures of at least 1475°F for 30 minutes. These testing protocols comply with Normal Conditions of Transport and Hypothetical accident conditions described in the United States Nuclear Regulatory Commission (NRC) 10 CFR 71.83 standard for hypothetical accident conditions for packaging and SRNL's Model 9977 Safety Analysis for Packaging. All mechanical properties tests were conducted using the MTS Criterion Series 43 Tensile Tester, which has a 40kN rated force capacity.

A view of how the foaming fixative is evaluated for plug strength in 304-stainless steel pipes is shown in Figure 8. An MTS 43 Criterion tensile tester was used with compression plates. A rate of 0.2 inches per minute was used during MTS testing. This procedure is not standardized, but followed some protocols described in ASTM D1621 “Standard Test Method for Compressive Properties of Rigid Cellular Plastics (Methods)”.

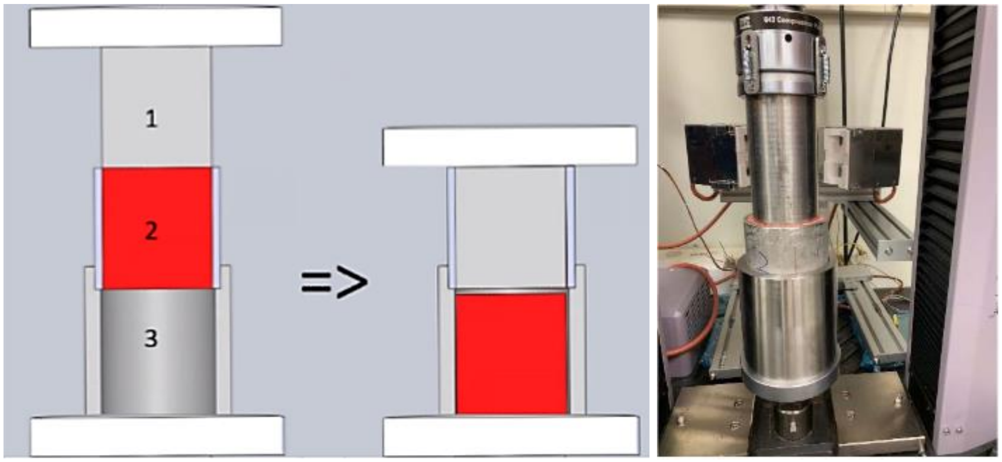

Figure 8. Plug strength test schematic (left) and plug strength testing for pipe samples using the “plunger – bucket” method on an MTS testing device (right).

Subtask 2.2: Results and Discussion

<u>Fire Barrier Mortar (FBM)</u>

The initial tests were performed using 2” pipe samples to characterize the “plug strength” of the mortar using both mixtures of a trowelable consistency (three parts mortar to every one part water) and a self-leveling consistency (two parts mortar to every one part water). FBM mixed to a trowelable consistency was difficult to apply and left large gaps that could allow contamination to be released.

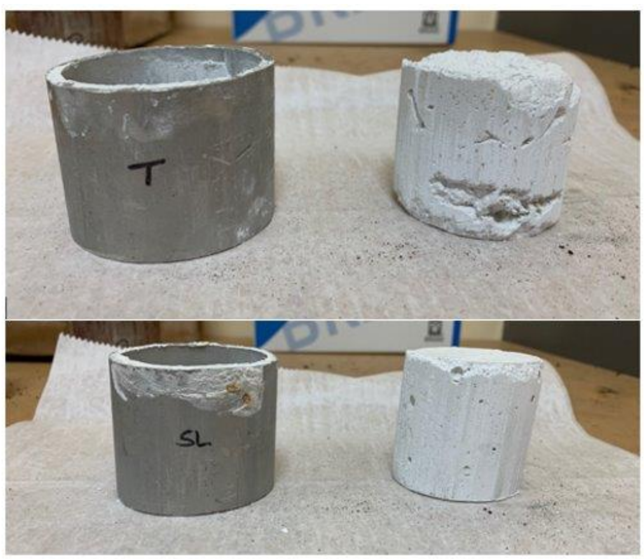

Figure 9. Trowelable consistency Fire Barrier Mortar sample (top) and self-leveling consistency sample (bottom) after plug strength test.

The mortar showed promising results during the “plug” test, withstanding a maximum load of 2,659.7 lbf. The 2” I-H foam only withstood an average maximum load of 1,302.24 lbf. Both mortar samples and especially the self-leveling mixture show more adhesive failure than was observed from I-H foam, indicated by the way the mortar stays intact when pressed out and the lack of mortar that remains on the pipe walls.

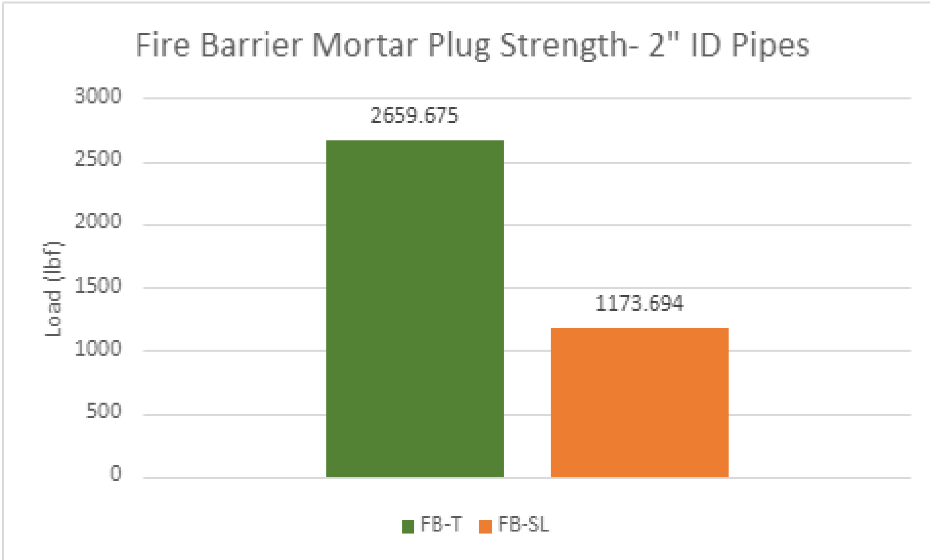

Figure 10. Maximum load before failure for Fire Barrier Mortar samples.

Small pipe samples of about 6.3 in^3 (2-inch diameter, 2-inch length) were used for the FBM samples to compare to previous foam testing. The baseline plug-strength testing showed that FBM withstood an average maximum failure of 1,892.9 lbf/in². The samples that were subjected to free drop withstood a greater load before failure. This could be due to inconsistencies in the application or the smaller data set. It is also important to note that each sample failed due to complete adhesion failure as opposed to the cohesion failure found in the I-H foam. The water immersion had very inconsistent plug strength results as well. This could also be attributed to the mixing and application process.

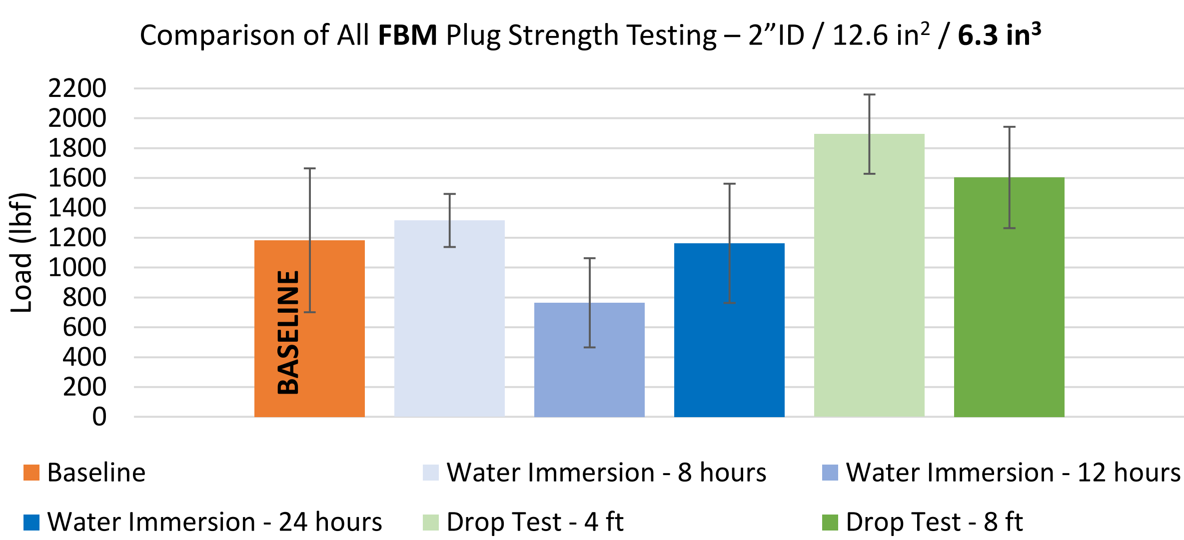

Figure 11. Average maximum failure load for 2" inner diameter x 2" length FBM baseline and stressor samples.

FBM is advertised to be firestop tested for up to 3 hours in accordance with ASTM E 814 (UL 1479). Initially, the flame test showed minimal degradation of the material and no smoke or flame propagation. At the conclusion of the test, there was complete adhesion failure with the material separating from the pipe samples. This is perhaps due to the expansion and contraction of the material or stainless-steel pipe, but further investigation is needed. Other considerations include user error and material incompatibility. As a result of the direct flame test, the plug strength was not tested because these samples completely delaminated from the pipe.

Figure 12. FBM samples during and after direct flame testing.

Large pipe samples of about 100 in^3 (3-inch diameter, 14-inch length) were used for further characterization and to compare with a full application of the I-H foam cartridge. However, difficulties arose with these larger samples under the same stressor conditions. One of the FBM 3" pipe water immersion samples showed to have not been fully cured, even after several days, when the plug strength test was performed (Figure 13). There may be issues with the application not resulting in proper initial curing. If fully cured, the mortar should withstand the effects of water and not revert to an uncured state.

Figure 13. FBM 3" pipe sample that was immersed in water for 8 hours and may have not been fully cured internally.

Another water immersion sample that was immersed for 12 hours was able to withstand 12,777 lbf before the bucket support piece failed, shown in Figure 14. The 3D printed bucket piece failed due to excess force applied to the support lip.

Figure 14. 3D printed bucket piece failed during testing of the large FBM pipe samples.

Overall, there were many plug strength inconsistencies and issues with the FBM when it is applied in larger quantities. For this reason, FBM was deemed incompatible for further testing as a potential fixative for use in 3D void spaces.

<u>I-H Foam</u>

The results for the I-H foam for 2-inch diameter samples was previously reported last year. This performance year, large pipe samples of about 100 in^3 (3-inch diameter, 14-inch length) were used for the I-H foam to further characterize a full application of the foam cartridge.

For the thermal stressor test, the same protocols were used where propane torches were directed at the exposed pipe ends. Intumescing was observed but it seemed to protect the rest if the sample. Unintumesced foam can be seen on one sample where the foam and metal meet. Previous fire testing indicated that unintumesced foam had significantly higher strength and that a higher amount of unintumesced foam yielded higher plug strength.

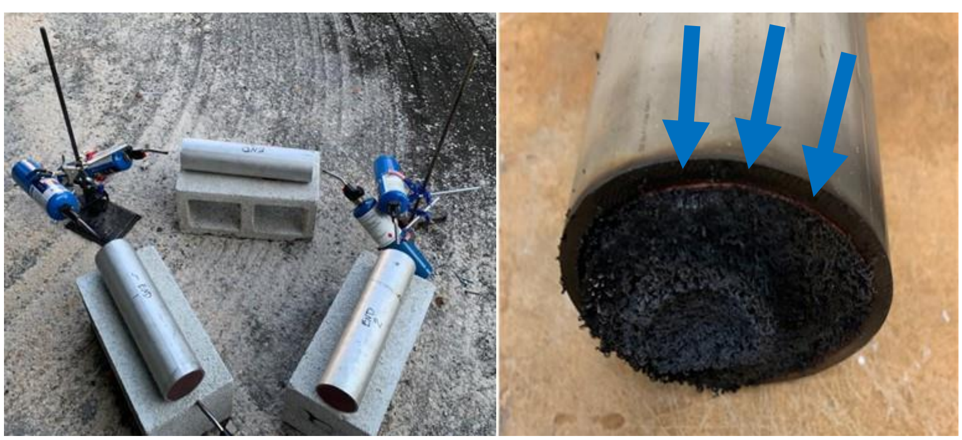

Figure 15. Direct flame testing setup with propane torches directed at the pipe ends only (left) and unintumesced portion of a sample at pipe interface (right).

In addition, propane torches were directed at the sides of the pipe samples, shown in Figure 16. All samples exhibited mild to significant smoke propagation. One sample even pushed out about 4in. of foam, which is likely due to a buildup of pressure at the center, shown in Figure 17.

Figure 16. Direct flame testing setup with propane torches directed at the sides of the pipe near the center.

Figure 17. Sample exhibiting significant smoke propagation (left) and sample pushed out about 4in. of foam (right).

Overall, most stressors had minimal impact to plug strength of the I-H foam. Baseline samples had an average plug strength of 7447 lbf and the water immersion samples performed relatively well. The larger pipe samples performed better under direct flame testing than the previous 2-inch samples. The “exposed ends” samples performed very well, with an average plug strength of 5705.5 lbf, since the intumescent char thermally protected the rest of the pipe sample. On the other hand, the “center” samples performed significantly less, with an average plug strength of 1679.7 lbf. This was attributed to intumescing in the middle and a large buildup of pressure at the center.

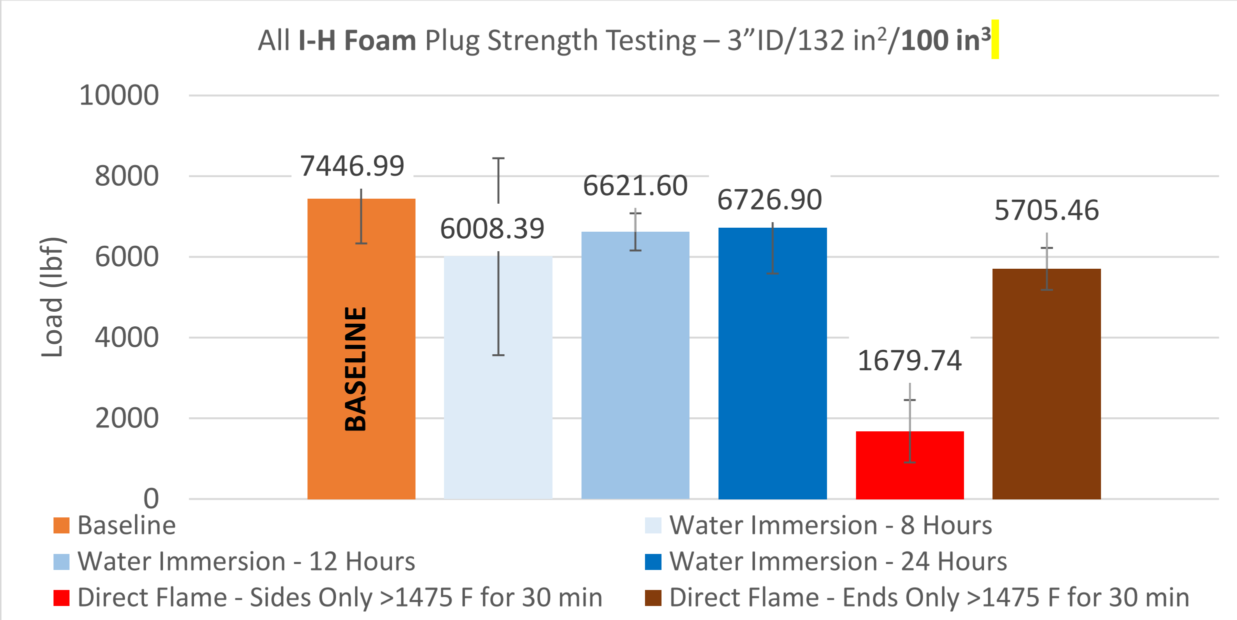

Figure 18. Average maximum failure load for 3" inner diameter x 14" length I-H foam baseline and stressor samples.

Subtask 2.2: Conclusions

FIU in collaboration with SRNL and the F/H Lab Deactivation Site Team have begun discussions on a Cold Demo Test Plan for this activity. The general test objectives will include: 1) confirm curing temperatures of the I-H foam; 2) confirm the "plug strength" of the I-H Foam in Hastelloy pipes; 3) confirm the adhesion capabilities of the I-H Foam in Hastelloy pipes under moisture conditions; 4) replicate the operational conditions where plugging the pipes will occur at F/H labs; 5) verify application of the I-H Foam can occur utilizing an approved hot tap method; 6) cutting demonstration of the pipes; and 7) basic life cycle analysis of the I-H plug. There is a desire to conduct an onsite hot demo o/a FY'23/24 contingent on the results of the cold demo.

Subtask 2.2: References

A. Materials, "C1892: Nominal Joint Strength of End-Plug Joints in Advanced Ceramic Tubes at Ambient and Elevated Temperatures".

ASTM International. (2016). *D1621-16 Standard Test Method for Compressive Properties of Rigid Cellular Plastics.* Retrieved from https://doi.org/10.1520/D1621-16

ASTM International. (2017). *D1623-17 Standard Test Method for Tensile and Tensile Adhesion Properties of Rigid Cellular Plastics.* Retrieved from https://doi.org/10.1520/D1623-17

ASTM International. (2018). *E3191-18 Standard Specification for Permanent Foaming Fixatives Used to Mitigate Spread of Radioactive Contamination.* Retrieved from https://doi.org/10.1520/E3191-18

Extech Instruments. (2016). *Product Datasheet SDL200.* Retrieved from Extech: http://www.extech.com/resources/SDL200_DS-en.pdf

FLIR. (2019). *Electrical/Mechanical Applications FLIR EXX-Series.* Retrieved from https://www.flir.com/globalassets/imported-assets/document/17-3307-ins-e53-_-exx-series-datasheet-mfg-web.pdf

Hilti. (2015). *Hilti CP 620 Instruction for use.* Retrieved from Hilti: https://www.hilti.com/medias/sys_master/documents/h4a/9158089048094/Instruction-for-use-INT-CP-620-Instruction-for-use-PUB-5188045-000.pdf

Hilti. (2016). *Hilti Firestop Foam solid CFS-F SOL; CP 620 Safety information for 2-Component-Products.* Retrieved from Hilti: https://www.hilti.com/medias/sys_master/documents/hfc/9178915405854/Documentation-ASSET-DOC-APPROVAL-0564.pdf

Lagos, L., Sinicrope, J., Shoffner, P., Komninakis, M., Simoes-Ponce, T., Nuñez, J., & Rendon, J. (2019). *Testing and Evaluating Intumescent Foams in Operational Scenarios - Test Plan.* Miami: Applied Research Center - Florida International University.

Lagos, L., Sinicrope, J., Shoffner, P., Viera, J., Simoes-Ponce, T., & Nuñez, J. (2018). *Testing and Evaluating Radiological Shielding Foams Resistance to Thermal Stressors - Test Plan.* Miami: Applied Research Center - Florida International University.

Klempner, D., & Sendijarevic, V. "Polymeric foams and foam technology," Hanser, 2004.

MTS Criterion® Series 40. (2014). Retrieved from Product Information: https://engineering.jhu.edu/labs/wp-content/uploads/sites/76/2016/04/MTS-Criterion-40-Product-User-Manual.pdf

Mahmood, N. "Investigations on the adhesion and interfacial properties of polyurethane foam/thermoplastic materials," 2007. [Online]. Available: https://www.academia.edu/6047100/Investigations_on_the_adhesion_and_interfacial_properties_of_polyurethane_foam_thermoplastic_materials.

Marinzuli, G., Surace, R., & Ludovico, A. "A preliminary study on adhesion on steel cylinder filled with aluminum foam," 213.

Nicholson, D., Peters, B., Washington, D., & Wilson, J. (2016). *Fabrication and Evaluation of Radiation Hardened Polyurethane Foams for D&D Activities (SRNL-L3100-2016-00231).* Savannah River National Laboratory.

Subtask 2.3: Support to SRNL and SRS 235-F to Complete Final Data Collection and Technical Report for Onsite Hot Demonstration of Intumescent Fixative at SRS 235-F PUFF Facility

Subtask 2.3: Introduction

FIU has supported SRNL with follow up activities for the intumescent coating fixative hot demonstration at SRS. The hot field test involved the use of a selected intumescent coating within Process Cell 7 and a contaminated entry hood to Process Cell 1 of the Plutonium Fuel Form Facility (PuFF) at SRS Building 235-F. The objective of this research was to select and validate the operational performance of fire resilient fixative coating material(s) for residual surface contamination after gross decontamination is completed in a hot, radioactive environment in support of the 235-F Risk Reduction Project.

Based on discussions with SRNL, there was funding to support the final data collection related to thickness measurements of the intumescent fixative coating in the SRS 235-F Process Cells where it was applied, as outlined in the approved Test Plan titled, “Incombustible Fixative and ACE 2.0 Test Plan: Radiological Hot Field Test of Intumescent Coatings and Electrostatic Precipitators”, SRNL-TR-2018-00074, dated July 23, 2018. These measurements, combined with data collected on control coupons by FIU over the past two years, will be analyzed and incorporated into a full Technical Report authored by SRNL and FIU on the research activity and distributed to the DOE EM community.

Subtask 2.3: Objectives

The objective of this research activity was to assist with the completion of a comprehensive, collaborative SRNL-FIU close out report on the Incombustible Fixative Research Activity and Hot Demonstration.

Subtask 2.3: Methodology

The final report outline for the SRNL Hot Demo was approved and an associated POAM has been developed for the close-out activities. The outline included the proof-of-concept, down-selection process, cold demonstration, hot demonstration, results, challenges, and lessons learned.

Subtask 2.3: Results and Discussion

On December 3, 2020, The SRS 235-F Risk Reduction team went back into the entry hood of Process Cell #1 and took the final thickness measurements of the FD Intumescent Fixative. This provided SRNL and FIU with the needed data points to press forward with the collaborative final report on the Intumescent Fixative research activity. Some photos and measurements of the entry hood in 235-F are included in Figure 19. A few things to note:

- The measurements this time are thinner for the most part than the original application thicknesses. Most of this is attributed to continued curing, running of the material, or the removal of material activities that took place after the application.
- Setting of equipment due to lack of space caused a number of depressions during the curing time that were recorded as thicknesses. This is a good lesson learned that the material stays pliable through its curing process.
- Removal of plastic coverings (back wall around square door) were successfully achieved but caused some delamination of the FD where the plastic was still underneath. Lesson learned: better to cut the plastic to size to limit this type of delamination.
- Absorbent required for the water to purge the sprayer caused some of the absorbent to exit the bag and deposit on the surface, resulting in cracking fissures. This is also apparent in the Cell 7 pictures in front of the two-glove window where absorbent was also spilled.
- Rad survey data that were taken prior to thickness measurement activities is currently being evaluated.

Figure 19. Cracking fissures due to absorbent spill (left) and sagging on the vertical wall (right).

FIU took another measurement on the control coupons for comparison to the results from the SRS hot demonstration. These control coupons were coated with the same selected intumescent coating being used at SRS and are being aged at FIU under cold (non-radioactive) conditions similar to the environmental conditions at SRS. Comparison of the control coupon results will support the hot demonstration objective to determine the mechanisms of failure that the material may experience due to long-term alpha/gamma radiation exposure. One control coupon is being maintained in ARC's indoor laboratory under ideal conditions at ~72ºF and 30% humidity. The second is being maintained outside in ARC's hot cell testbed at Miami's ambient high temperatures and humidity. Weather conditions were also being monitored and a monthly average temperature and humidity was documented.

The data collected by FIU is being evaluated for changes to the baseline data collected in December 2018. If a monthly measurement falls within the min-max range established, then that provides evidence that there has been no significant degradation of the coating or change in thickness. If a monthly reading falls outside of the min-max range, some amount of degradation or change in thickness has occurred. The following tables provide a snapshot of the thickness measurements for the two 304-stainless steel control coupons coated in intumescent fixative. All the thickness measurements across all points on the 12"x12" coupons remained within tolerances of the established baseline range, indicating that there has been no significant degradation in coating thickness.

Table 2. Monthly Measurements of Control Coupon 1 (indoors) at FIU

Control Coupon 1 - Indoors								
	Baseline		Monthly Measurements - 2019			2020		
Point	Minimum Average Tolerance Range (mm)	Maximum Average Tolerance Range (mm)	October	November	December	July	December	Standard Deviation
1	4.16	4.44	4.24	4.25	4.24	4.33	4.34	0.032
2	4.80	5.12	4.89	4.90	4.89	4.85	4.97	0.033
3	-	-	-	-	-	-	-	-
4	4.29	4.57	4.46	4.46	4.44	4.44	4.48	0.033
5	3.92	4.19	4.03	4.00	4.01	4.03	4.08	0.021
6	4.19	4.47	4.36	4.32	4.32	4.42	4.41	0.036
7	4.12	4.69	4.24	4.26	4.21	4.34	4.39	0.055
8	3.79	4.04	3.92	3.92	3.91	3.97	3.90	0.021
9	4.20	4.48	4.39	4.35	4.38	4.33	4.25	0.037
10	3.89	4.15	4.04	4.01	4.01	4.02	4.05	0.016
11	3.28	3.51	3.41	3.40	3.43	3.41	3.41	0.017
12	4.05	4.32	4.20	4.17	4.17	4.17	4.19	0.016
13	3.55	3.79	3.66	3.65	3.67	3.68	3.69	0.018

Table 3. Monthly Measurements of Control Coupon 2 (outdoors) at FIU

Control Coupon 2 - Outdoors								
	Baseline		Monthly Measurements - 2019			2020		
Point	Minimum Average Tolerance Range (mm)	Maximum Average Tolerance Range (mm)	October	November	December	July	December	Standard Deviation
1	3.23	3.45	3.37	3.38	3.37	3.38	3.43	0.023
2	3.39	3.62	3.51	3.52	3.51	3.53	3.55	0.025
3	3.03	3.24	3.10	3.13	3.11	3.10	3.22	0.031
4	3.92	4.19	4.08	4.10	4.08	4.09	4.09	0.032
5	3.75	4.00	3.89	3.90	3.89	3.90	3.95	0.031

6	4.39	4.68	4.54	4.57	4.52	4.60	4.56	0.030
7	4.19	4.47	4.31	4.33	4.30	4.37	4.34	0.028
8	3.67	3.92	3.75	3.76	3.74	3.76	3.74	0.019
9	3.59	3.83	3.69	3.72	3.70	3.69	3.71	0.026
10	3.33	3.55	3.41	3.42	3.41	3.40	3.42	0.022
11	3.25	3.47	3.36	3.38	3.38	3.34	3.35	0.019
12	3.32	3.55	3.43	3.42	3.44	3.43	3.41	0.016
13	3.01	3.22	3.12	3.12	3.15	3.06	3.07	0.028

Subtask 2.3: Conclusions

The final technical report, titled "A Novel Approach to Mitigating the Potential Release of Radioisotopes under Fire Conditions - Enhancing Fire Resiliency of Radiological Contamination Fixatives During Deactivation & Decommissioning Activities", was completed and distributed to DOE. The report was also posted to OSTI by SRNL (https://www.osti.gov/servlets/purl/1772363). This subtask has been reported to DOE as complete.

Subtask 2.3: References

Lagos, L., Sinicrope, J., Shoffner, P., Awwad, A., & Rivera, J. (2015). *Enhancing Operational Performance of Fixatives and Coatings for D&D Activities: Phase I - Baselining and Proof of Concept - Test Plan.* Miami: Applied Research Center - Florida International University.

Sinicrope, J., Shoffner, P., Washington, A., Lagos, L. A Novel Approach to Enhancing Fire Resiliency in D&D: Adapting Intumescent Coatings as Fixatives for D&D Activities to Mitigate the Release of Radioisotopes in Fire and Extreme Heat Conditions, Waste Management Symposia, Phoenix, AZ, March 5-9, 2016.

Lagos, L., Sinicrope, J., Shoffner, P., Viera, J., Simoes-Ponce, T., & Nuñez, J. (2018). *Potential Applications of Intumescent Coatings to Address Safety Basis Requirement - Technical Progress Report.* Miami: Applied Research Center - Florida International University.

Nicholson, J., Siegfried, M., *Incombustible Fixative and ACE 2.0 Test Plan: Radiological Hot Field Test of Intumescent Coatings and Electrostatic Precipitators*, Savannah River National Laboratory, July 2018.

Groden, N.D., S. Taylor, M. Komninakis, J. Sinicrope, J.C. Nicholson. A Novel Approach to Mitigating the Potential Release of Radioisotopes Under Fire Conditions - Enhancing Fire Resiliency of Radiological Contamination Fixatives During Deactivation & Decommissioning Activities (SRNL-STI-2021-00115), March 2021.

Subtask 2.4: Certifying Fixative Technology Performance when Exposed to a Variety of Stressors Postulated in Contingency Scenarios Highlighted in Safety Basis Document

Subtask 2.4: Introduction

Under this subtask, FIU is evaluating fixative performance when exposed to various stressors (i.e. impact, environmental such as water immersion, thermal/fire, etc.) associated with open-air demolition activities and safety basis analysis in response to high priority requirements identified across the DOE complex. This research effort has the added benefit of potentially providing essential data points on the positive effects of fixative technologies on mitigating airborne release fractions, respirable fractions, and resuspension rates used in safety basis calculations and the Source Term Formula outlined in DOE-HDBK-3010. The results from this initiative will be shared with the ASTM International E10.03 Subcommittee to begin formalizing the development and promulgation of a new series of testing standards for the DOE EM and international D&D communities.

FIU has also developed an approved experimental design to quantitatively ascertain the effects of fixative technologies in immobilizing residual contamination under ideal conditions, as well as exposure to certain impact stressors. The experimental design was previously published and uploaded as a Technical Progress Report on OSTI and KMIT. The data obtained during the experimental phase of this activity will be used to support the update of the DOE-HDBK-3010.

Subtask 2.4: Objectives

1. **Develop and validate experimental design for the quantification of contamination release during impact stress.**
   This objective focuses on the experimental methodology for impact stress and includes four main aspects: surrogate contaminant, impact test chamber, collection of released particulates, and analysis.
2. **Reevaluate ARF coefficients for powder contaminants under impact stress.**
   This approach will either confirm or dispute the original ARFs for powder contamination as determined in the DOE-HDBK-3010. Since there have been new technological advances in analytical techniques, it is possible that the coefficients in the present version of the handbook are outdated and do not accurately reflect the airborne release.
3. **Determine ARF coefficients for fixative materials under impact stress.**
   This objective focuses on investigating the ARFs for fixatives applied over powder contamination under impact. Initially, two polymer fixatives will be used as a starting point to provide data to substantiate the Fixative State for this stressor. Based on previous research conducted, the use of fixatives will produce much lower ARFs.

Subtask 2.4: Methodology

Throughout numerous DOE nuclear facilities, there are many different types of substrates to which the fixatives may be applied. However, these initial experiments only consider non-porous substrates (stainless steel coupons). All testing is performed on: (1) coupons without a fixative as a baseline and to confirm the original data for ARFs for powder contaminants under impact and; (2) two fixatives (FD and PBS) as a starting point to provide data to substantiate the fixative/polymer state under impact. There are four main aspects to this experimental methodology: surrogate contaminant, impact test chamber, collection of released particulates, and analysis.

<u>Surrogate Contaminant and Controlled Contamination of Test Coupons</u>

Cesium chloride (CsCl) is the surrogate contaminant used as it is a non-radioactive soluble powder and contains a unique chemical element that will be detectable in the analysis component. It is essential that the coupons are weighed before and after contaminant application in order to quantify the initial amount of contamination prior to any stressor for proper release measurements. Another main aspect is to be able to uniformly contaminate the test coupons for all experiments. Previous work and existing standards, such as ASTM E3283-21 “Standard Practice for Preparation of Loose Radiological/Surrogate Contamination on Nonporous Test Coupon Surfaces for Evaluation of Decontamination Techniques”, are being leveraged for this design.

A small known quantity of CsCl was used to create a solution in deionized (DI) water. The contaminant solution was mixed homogenously and then applied to 304-stainless steel coupons at different points. 10 µL drops of contaminant solution were stippled in a pattern towards the center of the coupon, per ASTM E3283, which created a uniform distribution and reduced the risk of run-off at the edge of the coupon. The coupons were undisturbed while the solvent was allowed to evaporate. After evaporation, the coupons are weighed to initially quantify the amount of contaminant present. The fixative could then be applied and cured to the manufacturer’s requirements. The coating thickness confirmed using the Defelsko PosiTector 6000. The Defelsko PosiTest LPD pin-hole detector is used, where appropriate, to confirm that there are no small cracks/holes in the coating application before all testing.

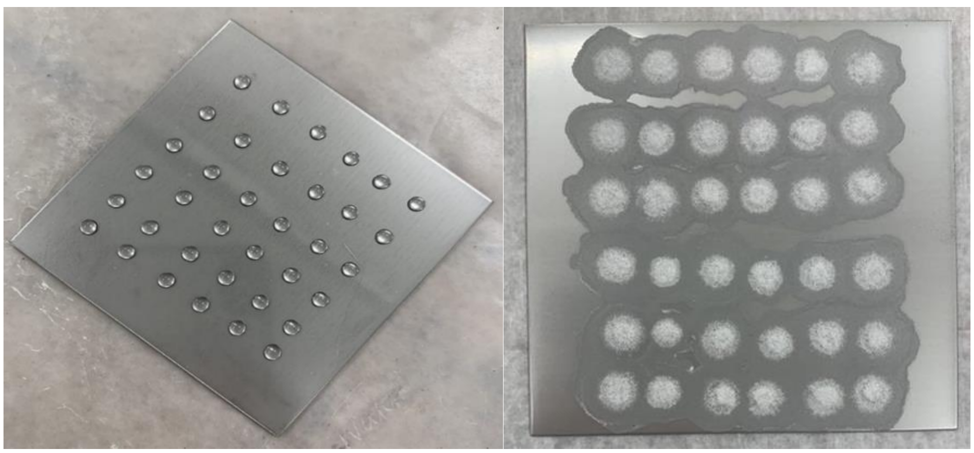

Figure 20. Stippled contaminant solution on 304-SS coupon (left) and after solvent evaporation (right).

<u>Impact Stressor</u>

BYK-Gardner PF-5546 Extra Heavy-Duty Impact Tester has a maximum force of 320 in-lb and is used to evaluate impact resistance and determine the exact point of failure and/or establish pass/fail specifications. It specifically complies with ASTM D2794, “Standard Test Method for Resistance of Organic Coatings to the Effects of Impact”. While this method was not originally designed to test for contamination release, it establishes a standard method to test a coating’s response to rapid deformation. The coupons are required to have the following dimensions: 3.0” length, 3.0” height; and 0.024” width. Additionally, an acrylic housing assembly was placed around the device which will allow for artificially contaminated coupons to be tested for release fractions.

Figure 21. BYK-Gardner PF-5546 Extra Heavy-Duty Impact Tester.

Contamination Release Collection

In order to quantify a total release, effective collection methods must be used to ensure accuracy of the data. Collection of released contamination includes airborne and any particulates that may have resettled on the stressor apparatus or test chamber surfaces. MCE (mixed cellulose ester) filter cassettes and an air-sampling pump were used to collect any suspended airborne particulates. Any contamination that has settled on the walls of the test chamber or stress apparatus can be collected using sampling wipes. Then the filters and wipes are dissolved in an acidic medium for the analysis process.

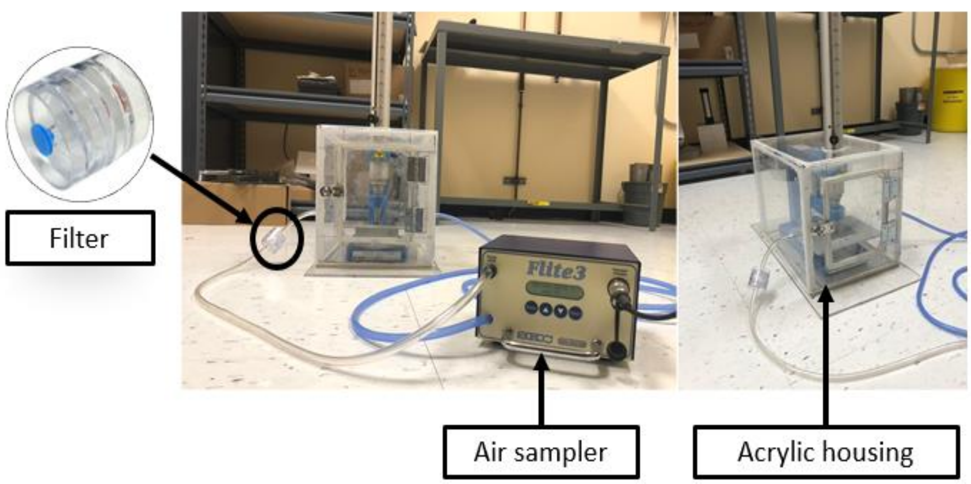

Figure 22. Impact tester with acrylic impact housing and Flite 3 901-3011 air sampler setup.

Analysis

After collection of the released contaminant, it can be analyzed using mass spectrometry. The surrogate contamination has a unique signature that can be detected using ICP-MS. Mass spectroscopy detects charged particle impacts following a deflection by a magnetic field that separates ions by mass/charge ratios. Carefully tracked dilutions or dissolutions are required in order to correctly determine the amount of collected contaminant. These analysis methods will detect only the specified element in the surrogate (Cesium), which is imperative in certifying and quantifying fixative performance.

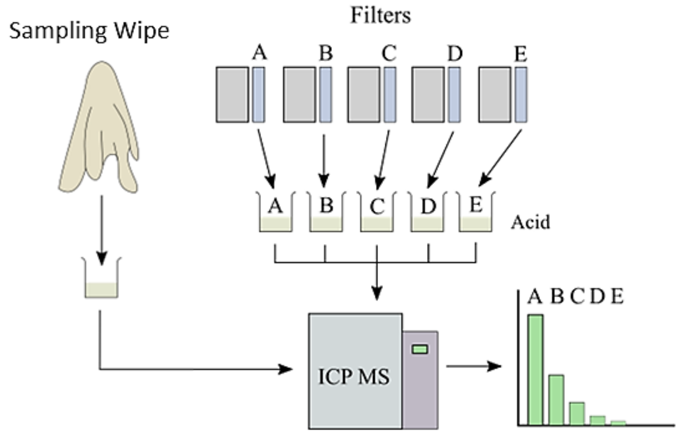

Figure 23. Collection and analysis process.

Subtask 2.4: Results and Discussion

ICP-MS analysis on baseline samples, powder contamination only, were tested initially at maximum impact of 320 in-lb and 160 in-lb. The results are displayed in Table 4. When comparing the ICP measurements to the original mass of cesium chloride deposited onto the coupon, it was seen that several samples had a release greater than its original mass and/or the mass after impact. This suggests that there may be some carryover from experiment to experiment, in either the impact apparatus, ICP, or another entity. Other samples had a very low capture rate in the ICP analysis.

These findings were explored since the mass recorded before and after impact indicates the amount of cesium chloride released that should correlate with the ICP results. Blank filters and filters that sampled the air in the labs in case of outside contamination were tested to determine the cause of carryover cesium. The results indicated that the cesium found in the air sampled in the labs were negligible. Therefore, it can be concluded that the source of the cross contamination between experiments is the impact apparatus. More methodical cleaning measures between samples and/or periodical changing of the sampling tubes were implemented in the re-test.

Baseline testing was re-conducted using force levels of 320 in-lb (maximum) and 160 in-lb, following the implementation of additional methods to reduce cross-contamination. These initial results for powder contamination (Table 4) produced an average ARF of 3.59e-4, which is similar to the ARF value presented in the DOE-HDBK-3010, 3e-4.

Table 4. ICP Analysis and the Associated Airborne Release Fractions for Baseline Powder Contamination – Retested

Samples	Impact (in-lb)	CsCl on Coupon (g)	ICP Samples	ICP-MS CsCl (g)	ICP Total Released (g)	Airborne Release Fraction
Baseline 13	320	0.2172	Baseline 13 Baseline 13 Filter	0.001974569 1.20387E-07	0.00197	6.10E-05
Baseline 14	320	0.2135	Baseline 14 Baseline 14 Filter	0.00417 3.0126E-06	0.00417	7.22E-04
Baseline 15	320	0.2159	Baseline 15 Baseline 15 Filter	0.004720123 4.4517E-06	0.00472	9.42E-04
Baseline 320 Average						**5.75E-04**
Baseline 16	160	0.2158	Baseline 16 Baseline 16 Filter	0.003118709 4.132E-08	0.00312	1.32E-05
Baseline 17	160	0.2159	Baseline 17 Baseline 17 Filter	0.006406886 5.66457E-08	0.00641	8.84E-06
Baseline 18	160	0.2211	Baseline 18 Baseline 18 Filter	0.002606382 1.05625E-06	0.00261	4.05E-04
Baseline 160 Average						**1.42E-04**
OVERALL BASELINE AVERAGE						**3.59E-04**

Initial testing on the fixatives began using maximum impact of 320 in-lb and 160 in-lb. The results are displayed in Table 5 and Table 6 for FD and PBS, respectively. FD had a higher percentage of Cs released even though there were no obvious signs of cracking or tears in the coating after impact, like that seen in PBS. Overall, both fixatives showed a significant reduction in the ARFs for powder contaminants. The initial data seems to support that there is a different ARF coefficient that should be implemented for fixatives.

Table 5. ICP Analysis and the Associated Airborne Release Fractions for FD coating

Samples	Impact (in-lb)	CsCl on Coupon (g)	ICP Samples	ICP-MS CsCl (g)	ICP Total Released (g)	Percent Released	Airborne Release Fraction
FD-1	320	0.3537	FD-1 FD-1 Filter	0.0025589 1.01E-07	0.00256	0.72%	2.86E-07
FD-2	320	0.3557	FD-2 FD-2 Filter	0.0038395 2.551E-07	0.00384	1.08%	7.17E-07
FD-3	320	0.3543	FD-3 FD-3 Filter	0.0008712 3.209E-07	0.00087	0.25%	9.06E-07
FD-7	320	0.2875	FD-7 FD-7 Filter	0.0024368 2.151E-07	0.00244	0.85%	7.48E-07
FD-8	320	0.2877	FD-8 FD-8 Filter	0.0007196 6.48E-08	0.00072	0.25%	2.25E-07
FD-9	320	0.2882	FD-9 FD-9-filter	0.0009742 1.298E-07	0.00097	0.34%	4.50E-07
FD 320 Average							**5.55E-07**
FD-4	160	0.3351	FD-4 FD-4 Filter	0.0003196 1.551E-08	0.00032	0.10%	4.63E-08
FD-5	160	0.3555	FD-5 FD-5 Filter	0.0002015 1.322E-08	0.00020	0.06%	3.72E-08
FD-6	160	0.3585	FD-6 FD-6 Filter	0.0002416 1.025E-08	0.00024	0.07%	2.86E-08
FD-10	160	0.3002	FD-10 FD-10 Filter	0.0009919 8.117E-09	0.00099	0.33%	2.70E-08
FD-11	160	0.2916	FD-11 FD-11-filter	0.001015 1.1E-08	0.00102	0.35%	3.77E-08
FD-12	160	0.2832	FD-12 FD-12 Filter	0.000268 6.417E-09	0.00027	0.09%	2.27E-08
FD 160 Average							**3.33E-08**
OVERALL FD AVERAGE							**2.94E-07**

Table 6. ICP Analysis and the Associated Airborne Release Fractions for PBS coating

Samples	Impact (in-lb)	CsCl on Coupon (g)	ICP Samples	ICP-MS CsCl (g)	ICP Total Released (g)	Percent Released	Airborne Release Fraction
BPBS-1	320	0.2914	BPBS-1 BPBS-1 Filter	0.0003035 1.0033E-07	0.00030	0.10%	3.44E-07
BPBS-2	320	0.2917	BPBS-2 BPBS-2-filter	0.0001134 2.7541E-07	0.00011	0.04%	9.44E-07
BPBS-3	320	0.2894	BPBS-3 BPBS-3 Filter	0.00011459 1.4847E-07	0.00011	0.04%	5.13E-07
BPBS 320 Average							**6.00E-07**
BPBS-4	160	0.2883	BPBS-4 BPBS-4-filter	0.00017 1.8204E-07	0.00017	0.06%	6.31E-07
BPBS-5	160	0.2920	BPBS-5 BPBS-5 filter	0.00016141 6.1556E-08	0.00016	0.06%	2.11E-07
BPBS-6	160	0.2861	BPBS-6 BPBS-6-filter	0.00061364 3.2314E-08	0.00061	0.21%	1.13E-07
BPBS 160 Average							**3.18E-07**
OVERALL BPBS AVERAGE							**4.59E-07**

Subtask 2.4: Conclusions

The preliminary data collected during this research supports the original ARF for powder contaminants in the DOE-HDBK-3010 and the idea of a fixative/polymer state. These initial results for fixatives support an ARF that is less than that of a liquid contaminant, as shown in Figure 24.

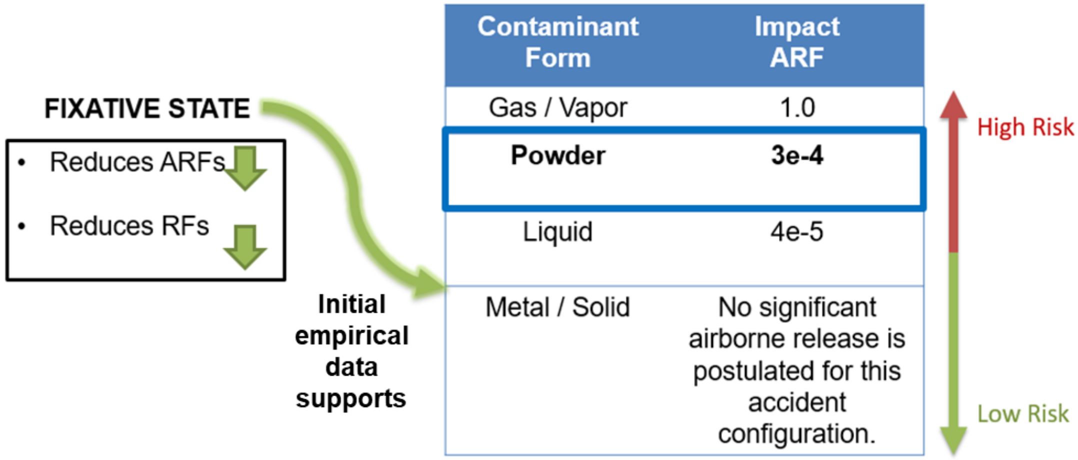

Figure 24. DOE-HDBK-3010 ARF coefficients for various contaminant forms under impact stress. Initial data indicates a fixative state with an ARF less than a liquid contaminant.

FIU will continue collaboration with SRNL and other sites to leverage ASTM practices and principals to further define operational parameters. FIU will proceed with additional testing required to quantify release and the performance of fixative technologies and reconfirm powder contaminant airborne release fractions to support and update the DOE-HDBK-3010. Additional impact forces will be evaluated to solidify the initial findings. Various substrate types and/or thicknesses will be considered for future testing.

Subtask 2.4: References

U.S. Department of Energy, "Airborne Release Fractions/Rates and Respirable Fractions for Nonreactor Nuclear Facilities (DOE-HDBK-3010-94)," December 1994. [Online]. Available: https://www.nrc.gov/docs/ML1307/ML13078A031.pdf.

ASTM International, "E3283-21 Standard Practice for Preparation of Loose Radiological/Surrogate Contamination on Nonporous Test Coupon Surfaces for Evaluation of Decontamination Techniques," 2021. Available: https://doi.org/10.1520/E3283-21.

SKC Inc., "Flite 3 High Flow Air Sampler Product Data Sheet," [Online]. Available: https://www.skcinc.com/catalog/pdf/instructions/1806.pdf.

ASTM International, "D522/D522M-17 Standard Test Methods for Mandrel Bend Test of Attached Organic Coatings," 2017. Available: https://doi.org/10.1520/D0522_D0522M-17.

ASTM International, "D2794-93(2019) Standard Test Method for Resistance of Organic Coatings to the Effects of Rapid Deformation (Impact)," 2019. Available: https://doi.org/10.1520/D2794-93R19.

3M, "3M Fire Protection Products 3M™ FireDam™ Spray 200". Available: https://multimedia.3m.com/mws/media/373702O/3m-firedam-spray-200-flyer.pdf.

3M, "3M™ FireDam™ Spray 200 Product Data Sheet". Available: https://multimedia.3m.com/mws/media/373703O/3m-firedam-spray-200-flyer-technical-data-sheet.pdf.

BHI Energy, "Specialty Coatings". Available: https://www.bhienergy.com/services/power-services/technologies/specialty-coatings/.

Bartlett Nuclear, Inc. , "Product Data Sheet Polymeric Barrier System (PBS)". Available: https://www.dndkm.org/DOEKMDocuments/GetMedia/Technology/1620-PBS%20Data%20Sheet.pdf.

BHI Energy, "Material Safety Data Sheet Polymeric Barrier System (PBS)". Available: http://www.bhienergy.com/assets/PBS-MSDS-2015Revised-3-15.pdf.

3M, "Safety Data Sheet 3M FireDam Spray 200 - Red," 13 April 2020. Available: https://multimedia.3m.com/mws/mediawebserver?mwsId=SSSSSuUn_zu8l00xM82vn8tUOv70k17zHvu9lxtD7SSSSSS--.

R. Demmer, D. Fox, S. Reese, A. Banford and J. Dodds, "Fixatives Used for Decommissioning and Maintenance of Radiological Facilities – 17537," in *Waste Management Symposia*, Phoenix, AZ, 2017.

J. Hubbard, T. Boyle, E. Zepper, A. Brown and T. Settecerri, "Airborne Release Fractions from Surrogate Nuclear Waste Fires Containing Lanthanide Nitrates and Depleted Uranium Nitrate in 30% Tributyl Phosphate in Kerosene," *Nuclear Technology*, vol. 207, no. 1, pp. 103-118, 2020.

ASTM International, "D7091-13 Standard Practice for Nondestructive Measurement of Dry Film Thickness of Nonmagnetic Coatings Applied to Ferrous Metals and Nonmagnetic, Nonconductive Coatings Applied to Non-Ferrous Metals," 2013. Available: https://doi.org/10.1520/D7091-13.

ASTM International, "E3190-19 Standard Practice for Preparation of Fixed Radiological/Surrogate Contamination on Porous Test Coupon Surfaces for Evaluation of Decontamination Techniques," 2019. Available: https://doi.org/10.1520/E3190-19.

Subtask 2.5: Multi-functional 3D Polymer Framework for Mercury Abatement (NEW)

Subtask 2.5: Introduction

Mercury (Hg) is a global pollutant that affects human and ecosystem health. Mercury element is naturally generated but has been mobilized and concentrated by humans into aquatic and terrestrial ecosystems through mining, electricity generation, and industrial production. The annual global Hg emission is 6500-8200 million grams (Mg) in the forms of Hg(0), Hg(I), Hg(II), and other organic derivatives of Hg. Hg(II), the oxidized form of Hg, is one of the major water-soluble forms that can be easily deposited locally and results in regional ecological system contamination. The development of new generation mercury abatement technologies containing high fixative efficiency, low environmental toxicity, high selectivity, low cost, and high recyclability has been of great interest.

The development of innovative, new generation mercury abatement technologies containing high fixative efficiency, low environmental toxicity, high selectivity, low cost, and high recyclability is of great interest to DOE-EM. During Year 1, FIU investigated the feasibility of using a 3D polymeric filtration/absorption matrix containing self-assembled and functionalized polymer micro-ribbons (MRs) for Hg(II) abatement in aqueous systems. FIU also developed methods for functionalization of PDMS-MRs surfaces for mercury abatement.

Subtask 2.5: Objectives

The objectives for this subtask include: to synthesize, functionalize, characterize, and test the 3D polymeric matrix at the lab-scale to prove the concept of this novel Hg abatement strategy. A multi-step approach will be followed:

- Synthesize the polymer MRs on glass substrates. Optimize the synthesis conditions to obtain the polymer MR, the most suitable for Hg(II) abatement in aqueous systems. Explore the possibility of synthesizing the polymer MRs on stainless steel substrates for potential large-scale synthesis.
- Enable functionalization for Hg(II) abatement at the polymer MRs surfaces using two different strategies: grafting functional groups at polymer MR surfaces (Approach A) and embedding functional nano/microparticles in the polymer MR backbones (Approach B). The approach yielding a better functionalization result will be chosen for further processing.
- Characterize the polymer MRs using spectroscopies and microscopies to evaluate the polymer MRs properties including functionality, porosity, and mechanical properties.
- Test the Hg(II) absorbability of the functionalized 3D polymeric matrix. Compare it to that of the unfunctionalized 3D polymeric matrix. Study the effects of environmental parameters, for example, temperature, and pH, on the Hg(II) absorbability of the functionalized 3D polymeric matrix.

Subtask 2.5: Methodology

The lab-scale fabrication conditions for PDMS micro-ribbons (MRs) formation on glass slides were explored. Specifically, the effects of PDMS film thickness and heating temperature on PDMS MRs formation were studied. The results are shown in Table 7.

Table 7. PDMS Film Coated Glass Slides after Cooling with Different Starting Film Thicknesses and Heating Temperatures

	4000 RPM, 30s	4500 RPM, 30s	5000RPM, 30s
450°C, 4 min	 Unpatterned cracks were formed during cooling. Thick and less curled MRs were formed during cooling.	 Unpatterned cracks were formed during cooling. Thick and less curled MRs were formed during cooling.	 Patterned cracks were formed. Long and curled MRs were formed.
460°C, 4 min	 Unpatterned cracks were formed during cooling. Thick and less curled MRs were formed during cooling.	 Patterned cracks were formed. The MRs were curled but short at length.	 Patterned cracks were formed. Long and curled MRs were formed.
470°C, 4 min	 Unpatterned cracks were formed during cooling. Thick and less curled MRs were formed during cooling.	 Massive fine cracks were formed during heating. No MRs formed.	 Massive fine cracks were formed during heating. No MRs formed.

It was concluded that the PDMS MRs with proper shape, number, and length will be formed under these conditions: spin-coating speed of 5000 RPM for 30s, followed by 4 min heating at 450°C. The close view of the formed PDMS MRs are shown in Figure 25.

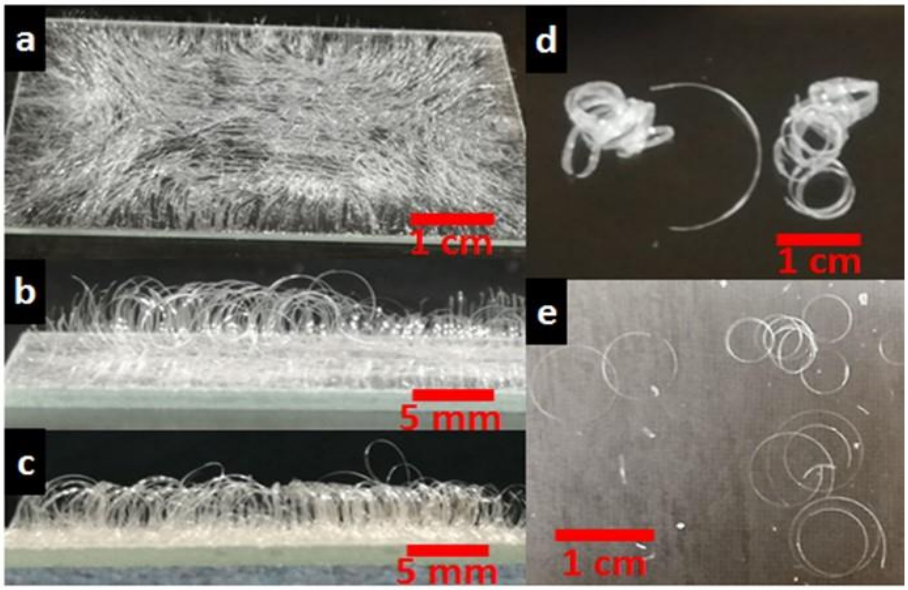

Figure 25. Close-up views of PDMS MRs: (a) Top view of the PDMS MRs formed on a glass slide; (b and c) Side view of the PDMS MRs formed on a glass slide; (d) The entangled PDMS MRs; (e) Spiral shaped PDMS MRs.

Subtask 2.5: Results and Discussion

FIU massively improved fabrication of the PDMS MRs following the optimized fabricating conditions summarized previously. During the fabrication, PDMS MRs with larger length, smaller width, and highly curled shaped were preferred and produced in a large amount. The fabricated PDMS MRs were stored in glass vials for further cleaning, surface functionalization, and characterizations.

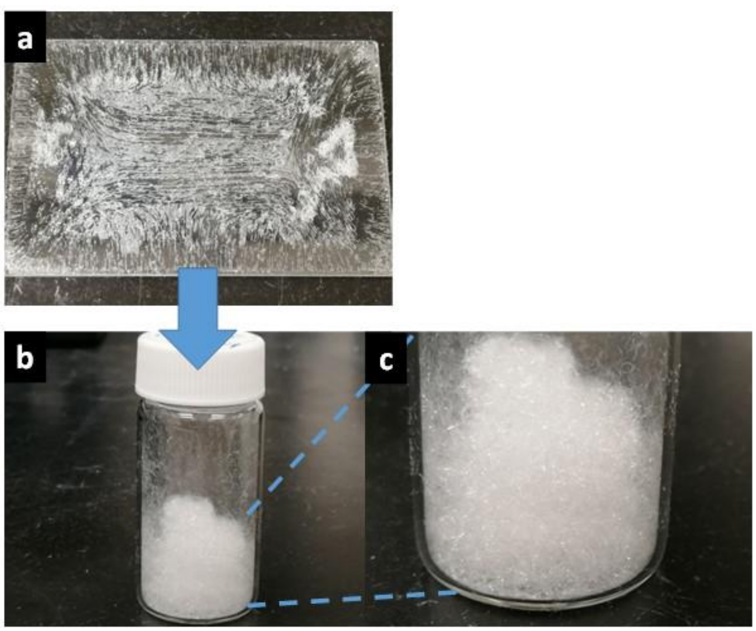

Figure 26. PDMS MRs fabricated on a glass slide under optimized conditions (a) and collected in a glass vial (b). A magnified view of the collected PDMS MRs is shown in (c).

Next, the self-assembly of PDMS MRs in water and water-oil mixtures were tested. The results indicated that the PDMS MRs tend to self-assemble via physical entanglement to minimize the contact between their hydrophobic surfaces and the water. This entanglement is strong and will recover after being untangled by water turbulence (stirring). The entangled network can collect the oil molecules mixed in the water and rapidly form an oil-MRs phase isolated from the water phase.

Figure 27. 0.5g of PDMS MRs added to 200 mL of water. The entangled MRs were pushed into the water using a spatula. The MRs formed a hydrophobic network and disliked getting wetted by water.

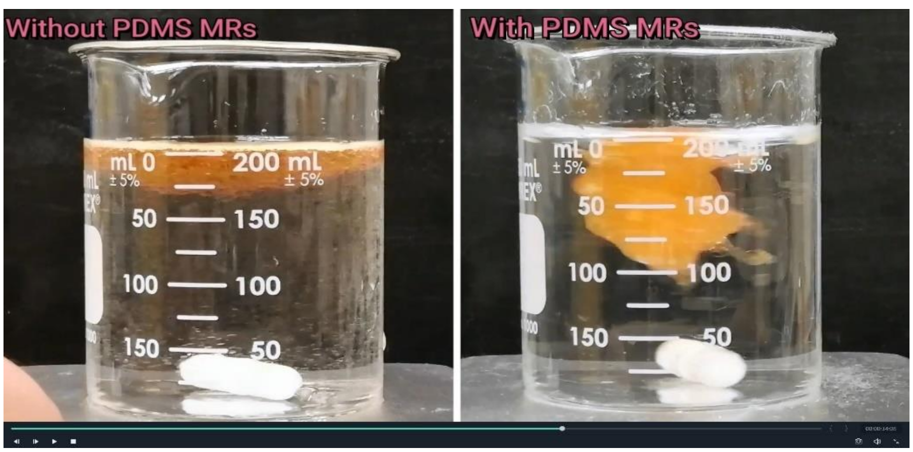

Figure 28. Oil-water separation in a system containing 10 mL silicon bath oil and 200 mL of water using 0.5g PDMS MRs. Emulsions were observed after stirring without PDMS MRs. However, the isolated oil-MRs phase was formed during stirring and was stabilized within a few seconds after stirring when PDMS MRs were added to the oil-water mixture.

The possibilities of PDMS-MRs surface functionalization to enable the Hg abatement ability of PDMS-MRs were then investigated. The reusability of PDMS-MRs after oil/water separation was studied. The effect of different extracting solvent on oil elution and PDMS-MRs regeneration was also explored. An optimized result was obtained using toluene as the elution solvent. More than 70% of the PDMS-MRs (originally ~0.5 g) after oil/water separation of a mixture containing 30 mL silicone bath oil and 200 mL water were successfully regenerated. About 25 mL silicone bath oil was recovered after separation.

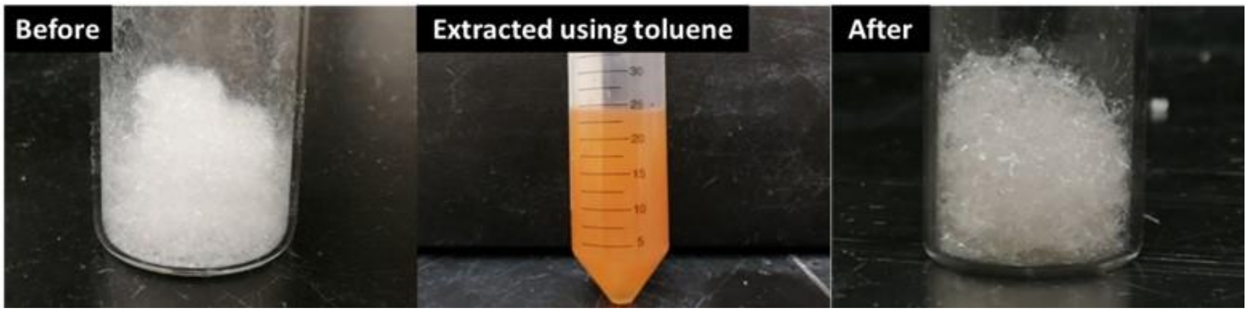

Figure 29. The PDMS-MRs before (left) and after (right) oil/water separation. The middle image shows ~ 25 mL oil bath where oil separated from the mixture.

Methods for functionalization at PDMS-MRs surfaces for mercury abatement were developed. (3-Mercaptopropyl)-trimethoxysilane (MPTMS) was selected as the sulfur source and a self-assembled monolayer (SAM) silanization was performed to functionalize PDMS-MRs surfaces. The effects of solvent, MPTMS concentration, reaction temperature, reaction time, and cleaning procedure need to be considered for PDMS-MRs surface silanization quality. The PDMS-MRs surfaces were successfully functionalized using this optimized method.

FIU focused on fabricating PDMS-MRs for the mercury abatement ability test. Two sample groups were made having non-silanized PDMS-MRs and silanized PDMS-MRs with ~ 3g samples for each group. The sample in the silanized PDMS-MRs group was prepared using the method developed in March. The non-silanized group was used as a control group to evaluate the quality and mercury abatement functionality of the silane monolayer graft at PDMS-MRs surfaces. A series of experiments were also developed to study the effect of different variations, for example, the environmental pH, environmental temperature, soaking time, mercury concentration, and the amount of PDMS-MRs on the mercury abatement performance of PDMS-MRs. The results were compare to some commercially available mercury abatement materials to evaluate the mercury abatement ability of PDMS-MRs.

Furthermore, the surface functionalization of oPDMS-MRs was completed using (3-Mercaptopropyl)-trimethoxysilane (MPTMS). Samples were prepared for testing mercury absorbing kinetic of oPDMS-MRs (Table 8 and Table 9) to figure out the optimized oPDMS-MRs amount for mercury abatement.

Table 8. oPDMS-MRs Dose 1:1000

oPDMS-MRs (mg)	*Hg solution 10 ppm (mL)*	*Distilled water (mL)*	*Total volume (mL)*	*Hg level (ppm)*	*Soaking time (min)*	*oPDMS-MRs dose (w/w)*
10	0.5	9.5	10	0.5	1	1:1000
10	0.5	9.5	10	0.5	5	1:1000
10	0.5	9.5	10	0.5	10	1:1000
10	0.5	9.5	10	0.5	30	1:1000
10	0.5	9.5	10	0.5	60	1:1000
10	0.5	9.5	10	0.5	180	1:1000
10	*0.5*	*9.5*	*10*	*0.5*	*360*	*1:1000*

Table 9. oPDMS-MRs Dose 1:200

oPDMS-MRs (mg)	*Hg solution 10 ppm (mL)*	*Distilled water (mL)*	*Total volume (mL)*	*Hg level (ppm)*	*Soaking time (min)*	*oPDMS-MRs dose (w/w)*
50	0.5	9.5	10	0.5	1	1:200
50	0.5	9.5	10	0.5	5	1:200
50	0.5	9.5	10	0.5	10	1:200
50	0.5	9.5	10	0.5	30	1:200
50	0.5	9.5	10	0.5	60	1:200
50	0.5	9.5	10	0.5	180	1:200
50	*0.5*	*9.5*	*10*	*0.5*	*360*	*1:200*

The mercury concentration in the elutions were analyzed using a Direct Mercury Analyzer (DMA). The results are shown in Figure 30. The total mercury abatement ratios for the samples containing 10 and 50 mg PDMS-MRs at 60 h were 51% and 61.5% respectively. The efficiency for mercury removal of PDMS-MRs at 60 h was ~0.11mg/g and 0.12 mg/g respectively. The low mercury abatement rate and efficiency were attributed to two reasons: 1) the high hydrophobicity of PDMS-MRs which resulted in the low absorbance rate of mercury at PDMS-MRs surface-solution interfaces; 2) the low thio-silane functionalization efficiency at PDMS-MRs surfaces due to the low -OH density. It should be noted that the mercury abatement using thio-silane functionalized PDMS-MRs did not reach the absorbing equilibrium at 60 h. Therefore, a longer absorbing time is required.

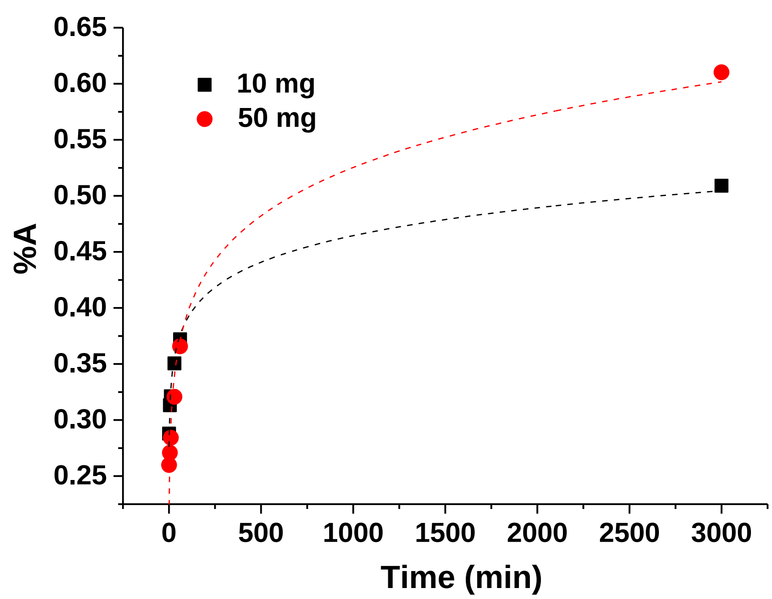

Figure 30. DMA results for mercury abatement rate of PDMS-MRs.

The research continued on improving the surface hydrophilicity of PDMS-MRs for two purposes: (1) to increase water and PDMS-MRs surface contact to allow more efficient transfer of mercury from the solution to the PDMS-MRs; and (2) to enhance the functionalization of thio-silane at the

PDMS-MRs surfaces. The PDMS-MRs were thermally oxidized by heating the MRs at different temperatures for varying times in atmospheric air, as shown in Table 10.

Table 10. Recipe of PDMS-MRs Thermal Oxidation

Heating temperature (ºC)	300	300	330	330	350	350	350	350	350
Heating time (h)	24	60	2	3	3	6	24	48	60

After thermal oxidation, the PDMS MRs showed different extents of enhancement in hydrophilicity. Their hydrophilicities were evaluated by immersing the heated PDMS-MRs in distilled water. Some of the pictures are shown in Figure 31. It clearly shows that the hydrophilicity of PDMS-MRs increased as the heating temperature and the heating time increased.

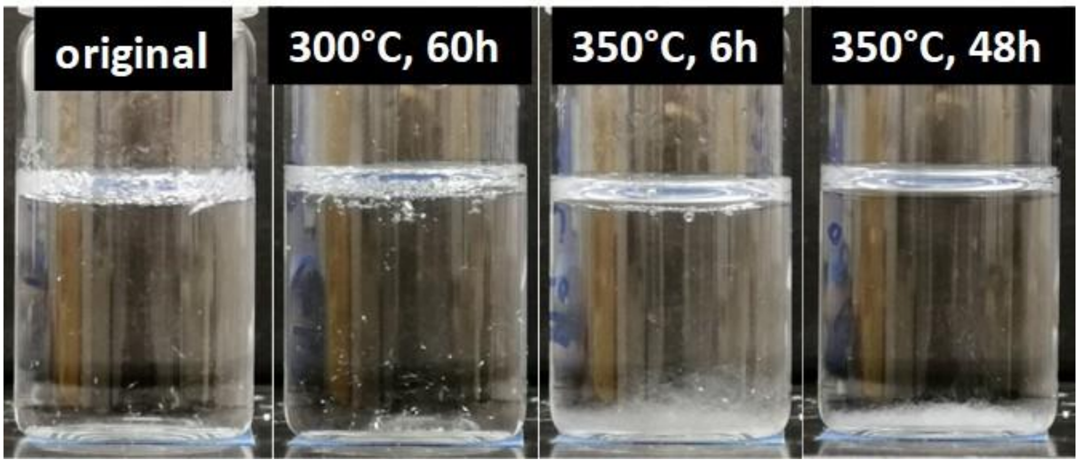

Figure 31. Thermally oxidized PDMS-MRs in water. The oxidation degree increases from left to right.

The thermally oxidized PDMS-MRs were functionalized and evaluated for its performance in mercury abatement. The PDMS-MRs thermally oxidized at 350°C for 24h were functionalized using (3-Mercaptopropyl)-trimethoxysilane (MPTMS). A mass of 5 mg of the functionalized PDMS-MRs was added to each vial containing 5 mL of ~0.3 ppm $Hg(NO_3)_2$ water solution. The mixed samples were shaken for different lengths of time. The mercury concentrations after removing the PDMS-MRs were tested. The results are shown in Table 11.

Table 11. Mercury Abatement using Thermally Oxidized and Functionalized PDMS-MRs

Sample Name	Original Hg Concentration (ppm)	Mass of PDMS-MRs (mg)	Shaking Time (min)	Final Hg Concentration (ppm)	Change (%)
1	0.306	5	5	0.633	+107
2	0.306	5	10	0.631	+106
3	0.306	5	30	0.586	+91
4	0.306	5	60	0.591	+93
background	0.306	0	NA	0.306	NA

Surprisingly, the final mercury concentrations for all the samples were about 100% higher than the final Hg concentration in the background sample. This was attributed to the small PDMS-MRs rupture pieces generated during the thermal oxidation. Those small PDMS-MRs pieces enriched the Hg and suspended in the solution. Therefore, the final Hg concentrations were significantly higher than the original concentration when a large amount of the small PDNS-MRs pieces were detected by the instrument.

The functionalization process was optimized for the PDMS-MRs by introducing multiple filtration steps to remove the small rupture pieces of the micro-ribbons. Four filtration steps were set up: (1) during the pre-cleaning of PDMS-MRs; (2) after self-assembly of the MPTMS molecules at the PDMS-MRs surfaces; (3) after polymerization catalyzation in the acidic solution; and (4) during the final cleaning of PDMS-MRs. For each filtration step, 2g of PDM-MRs were repeatedly rinsed, using 10 mL ethanol, passing through the nylon mesh (~ 150 µm pore size) three times. The functionalized and filtrated PDMS-MRs were heated to completely dry it.

In addition, mercury abatement samples were prepared containing 5 mg of the functionalized and filtrated PDMS-MRs and 5 mL ~0.5 ppm $Hg(NO_3)_2$ water solution and 0.5 ppm CH_3HgOH water solution, respectively (Table 12). Mercury abatement testing using these samples will be completed in the next series of testing.

Table 12. Mercury Abatement Samples using Filtrated and Functionalized PDMS-MRs

	Group 1		Group 2	
	0.5 ppm $Hg(NO_3)_2$	PDMS-MRs	0.5 ppm CH_3HgOH	PDMS-MRs
Background	5 mL	-	5 mL	-
5 min	5 mL	5 mg	5 mL	5 mg
10 min	5 mL	5 mg	5 mL	5 mg
30 min	5 mL	5 mg	5 mL	5 mg
60 min	5 mL	5 mg	5 mL	5 mg

Subtask 2.5: Conclusions

FIU successfully developed methods for functionalization of PDMS-MRs surfaces for mercury abatement. (3-Mercaptopropyl)-trimethoxysilane (MPTMS) was selected as the sulfur source and a self-assembled monolayer (SAM) silanization to functionalize PDMS-MRs surfaces was performed effectively. FIU also investigated the effects of solvent, MPTMS concentration, reaction temperature, reaction time, and cleaning procedure on PDMS-MRs surface silanization quality. The PDMS-MRs surfaces were successfully functionalized using this optimized method.

FIU will continue to focus on the investigation of mercury abatement performance of functionalized PDMS-MRs under different environmental conditions. Specifically, the effects of temperature, pH, ionic strength, organic compound composition in water, and repeated use of PDMS-MRs on mercury abatement performance will be evaluated including the abatement efficiency, binding strength, and abatement selectivity of functionalized PMDS-MRs. Moreover, FIU will develop a method to enable magnetic field responsibility of PDMS-MRs by embedding magnetic nanoparticles in the PDMS-MRs or at the PDMS-MRs surfaces. The effect of environmental conditions on the magnetic field responsibility of PDMS-MRs will also be investigated.

Subtask 2.5: References

R. Demmer, D. Fox, S. Reese, A. Banford and J. Dodds, "Fixatives Used for Decommissioning and Maintenance of Radiological Facilities – 17537," in *Waste Management Symposia*, Phoenix, AZ, 2017.

S. Reese and R. Demmer, "FX Hg Fogging Fixative Deployment for Mercury Vapor Suppression," in *Waste Management Symposia*, Phoenix, AZ, 2020.

D. Fox, R. Demmer and S. Reese, "Bench Scale Study of Coating Formulations for Abatement of Mercury Vapor and Recovery of Mercury Spills," February 2018. Available: doi:10.2172/1467409.

TASK 3: D&D KNOWLEDGE MANAGEMENT INFORMATION TOOL (KM-IT) (HQ, SRNL, INL, ANL)

Subtask 3.1: D&D KM-IT Enhancements

Subtask 3.1: Introduction

D&D KM-IT Enhancements includes user interface responsive design and development. This includes the redesign and development of the front end with a mobile friendly framework. Each module on the application will be modified to take advantage of all responsive design features.

Subtask 3.1: Objectives

The objective of this task is to make the D&D KM-IT application mobile friendly and to provide the visitors with a better user experience on mobile devices. It will also help with improved search results ranking as Google and other search engines algorithms are trained for responsive sites. Finally, the implementation of this enhancement will eliminate the need of a separate code base for mobile devices as a single website will be able to serve both desktop and mobile devices with optimal performance.

The Figure 32 below shows the objective of this subtask. Notice that layout of the website “responds” according to the device being used (desktop, laptop, tablet or mobile phone). The website should maintain full functionality while providing a great user experience.

Figure 32. Responsive design example across multiple devices.

Subtask 3.1: Methodology

The team put in place a plan to complete this enhancement. Since most of the development is focused on the front-end of the multi-tier application, the development took place on a development server that ran in parallel to the production application. The application uses a master page design, which includes the main navigation across the entire site. The application also uses child master pages for each module. As this is a complex design structure, the master page was the first to be modified, subsequently followed by each module’s master page accordingly. As each module was completed, it was launched on a staging server for testing on desktop and mobile devices. A screenshot of each module was shared as the team made progress on the development. Once all the modules were modified, the team moved the entire application to the staging server for final review before replacing the production application.

In January, the team moved the production application to the development server prepared during the last period. The database was also duplicated on the development environment so the development process has begun. The team conducted a code review with the DOE Fellows that will be helping with this task. The bootstrap library was also downloaded to the development environment. The team began modifying the master pages of the application and then move to modify each individual module.

In March, the team moved the production application and database to the development server, the team imported the bootstrap library to the solution and began cleaning up references to the previous skeleton structure layout. There are approximately 238 individual pages in the KM-IT application. Each of these pages have an additional code behind the page. All these pages require some form of modification to the code or front-end HTML to achieve the responsive design capability that the team is aiming for. The above pages do not include all the master pages, sitemap pages and configuration files that also need to be modified to complete this task.

The team began modifying the master pages of the application. The plan is to work on the master pages first. These pages include header and footer HTML code that is applied across the entire site including all the different modules. After these pages are done, the team will then modify the individual module master pages and finally individual pages.

The following Figure 33 and Figure 34 show a preview of the new header navigation and footer of the redesigned KM-IT application. Notice that the header is relocated to the top of the screen with a dropdown menu for the different modules. The navigation area also includes the login button and the profile status of the user along with a search textbox. When the screen is reduced, the menu adjusts accordingly to accommodate the screen size. The menu items get hidden and replaced by a mobile menu icon that the user can click to see the menu options.

Figure 33. D&D KM-IT navigation menu showing dropdown modules.

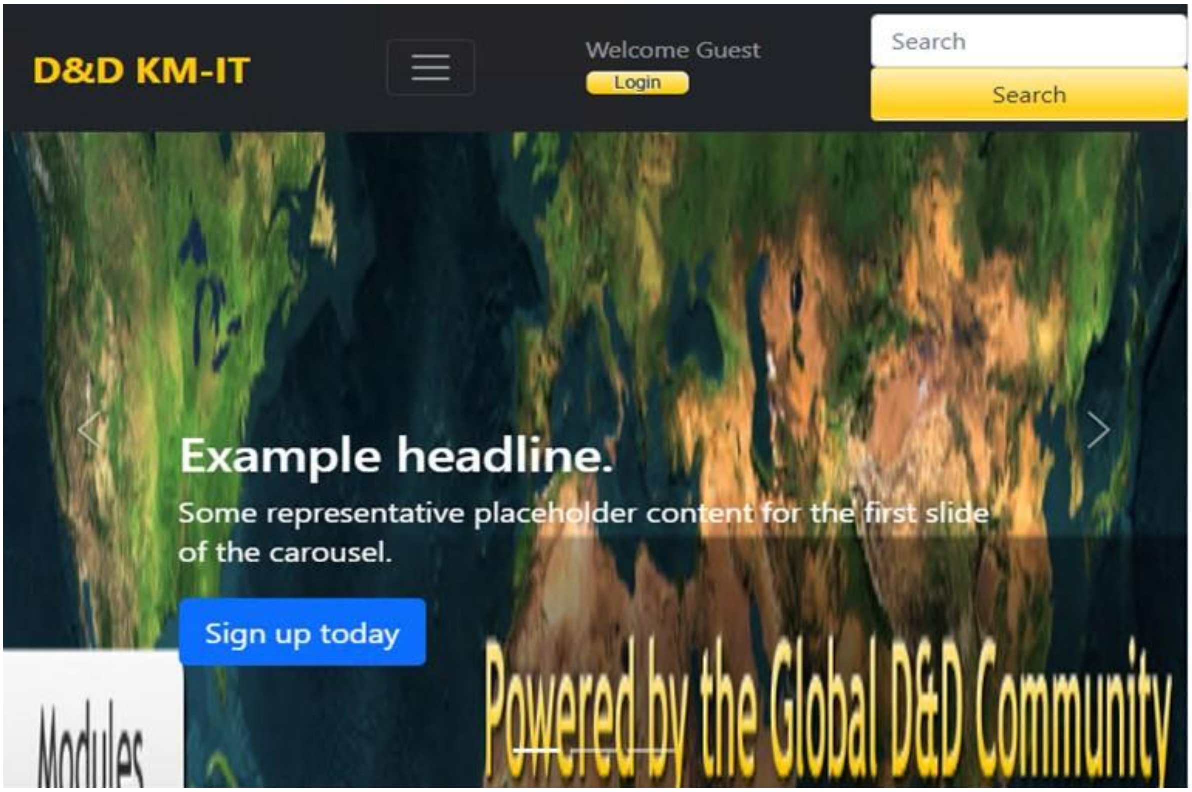

Figure 34. D&D KM-IT navigation menu adjusted for mobile devices.

Similarly, the master page footer is being updated to be mobile friendly. The images below (Figure 35 and Figure 36) show the footer for desktop and mobile devices adjusted automatically by the bootstrap framework. Notice that on the desktop, the footer is composed of three columns in a single row containing the sections: Popular Links, About, and Develop By. When the screen is reduced on a mobile device, these columns rearrange themselves and become stacked and converted to rows so that user can scroll without missing any information that can potentially go off the viewable screen area.

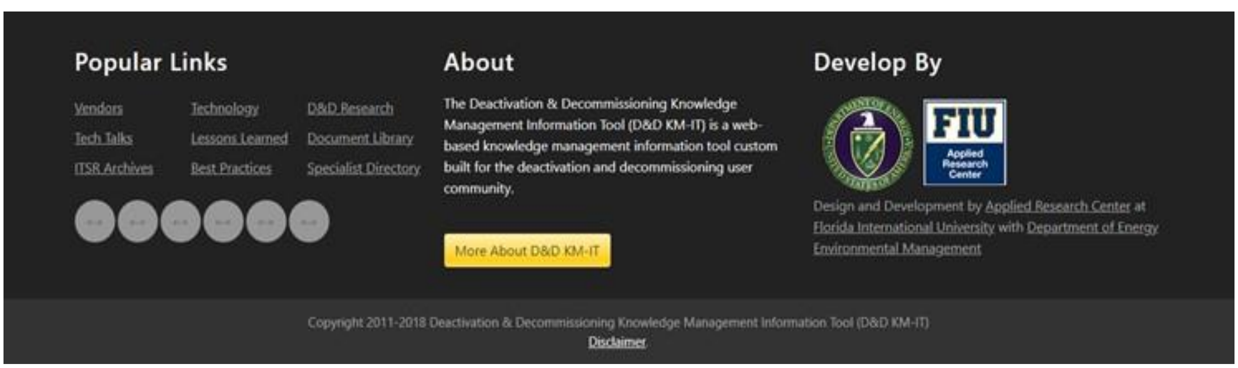

Figure 35. D&D KM-IT footer shown on desktop application.

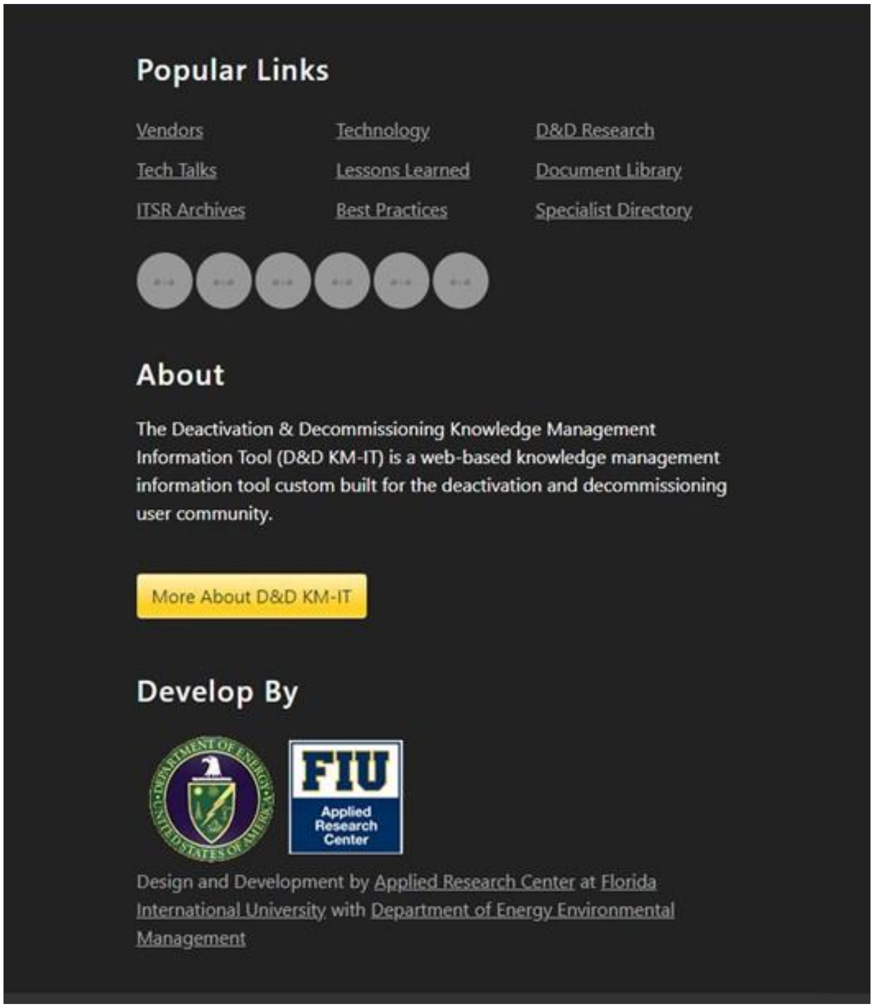

Figure 36. D&D KM-IT footer adjusted for mobile devices.

In April, the team made significant progress on the master landing page and default page of the KM-IT. The image below (Figure 37) shows a screenshot of the application homepage. Most of the content is basic placeholder information. The current version of the default site contains a top menu bar with navigation to the main root pages of the KM-IT and a dropdown module link to all the modules of the application. The team is introducing a slider just below the bar menu as well as links and a description of each module below the slider. The following section will vary, but for this version the Tech Talk is highlighted followed by additional features, industry news, and quick links. Other sections that follow include an announcement that the KM-IT is mobile friendly, the About and the Contribute sections. Finally, just above the footer, FIU kept the D&D Technologies, popular pages and problem/solution from the Hotline module. The footer contains the same information as the original KM-IT with a different layout.

Figure 37. Default page of the new KM-IT responsive design.

Figure 38 shows the landing page of the Mobile module. Similarly, to the default page, there is a menu bar at the top. Just under the menu bar there are links to the module of the system. This is followed by the menu of the module. The team kept the same layout design of content on the left and sidebar.

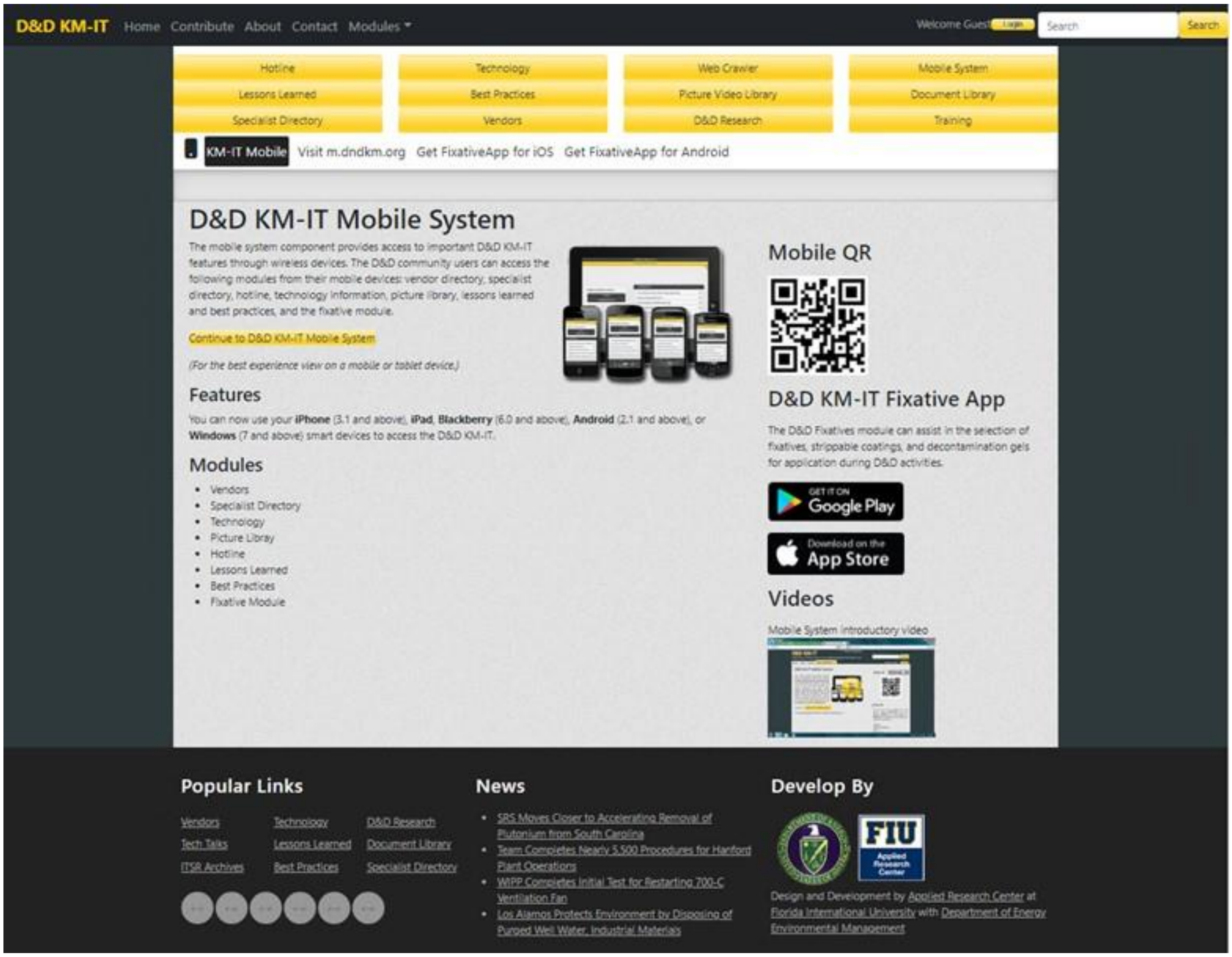

Figure 38. Landing page of the Mobile module.

DOE Fellows are contributing to this effort. Their contribution includes going through and making changes to the master pages and content pages of the different modules that are available for user access. New page layouts and functionality are implemented through the master pages by changing the menu, breadcrumb, and content areas. DOE Fellows also altered the content pages by switching the old sixteen columns grid layout to Bootstrap. Finally, they are currently focusing on making sure that the layout among all of the modules is switched over to the new one; however, once that is finished the team will move on to formatting the HTML in the content areas of every page in the modules.

In May, the team continued modifying module master pages of the application. The plan is to work on the master pages of the application and module. These pages include header and footer HTML code that is applied across the entire site including all the different modules. After these pages are done, the team will then modify the individual module master pages and finally individual pages.

The team continues to make significant progress on the master landing page and default page of the KM-IT. The following figure shows the landing page of the Mobile module. Similarly, to the default page, there is a menu bar at the top. Just under the menu bar there are links to the module of the system. This is followed by the menu of the module. The team kept the same layout design of content on the left and sidebar. A few modules were moved to the testing phase and other DOE Fellows will begin to test these modules in parallel as other members of the team continue to work on other modules. The following images (Figure 39 and Figure 40) show the module Best Practice which is currently in a testing phase. Notice that the landing page responds to a mobile device screen size by adjusting its layout. The mobile menu is activated when clicking on the mobile menu icon on the top right corner.

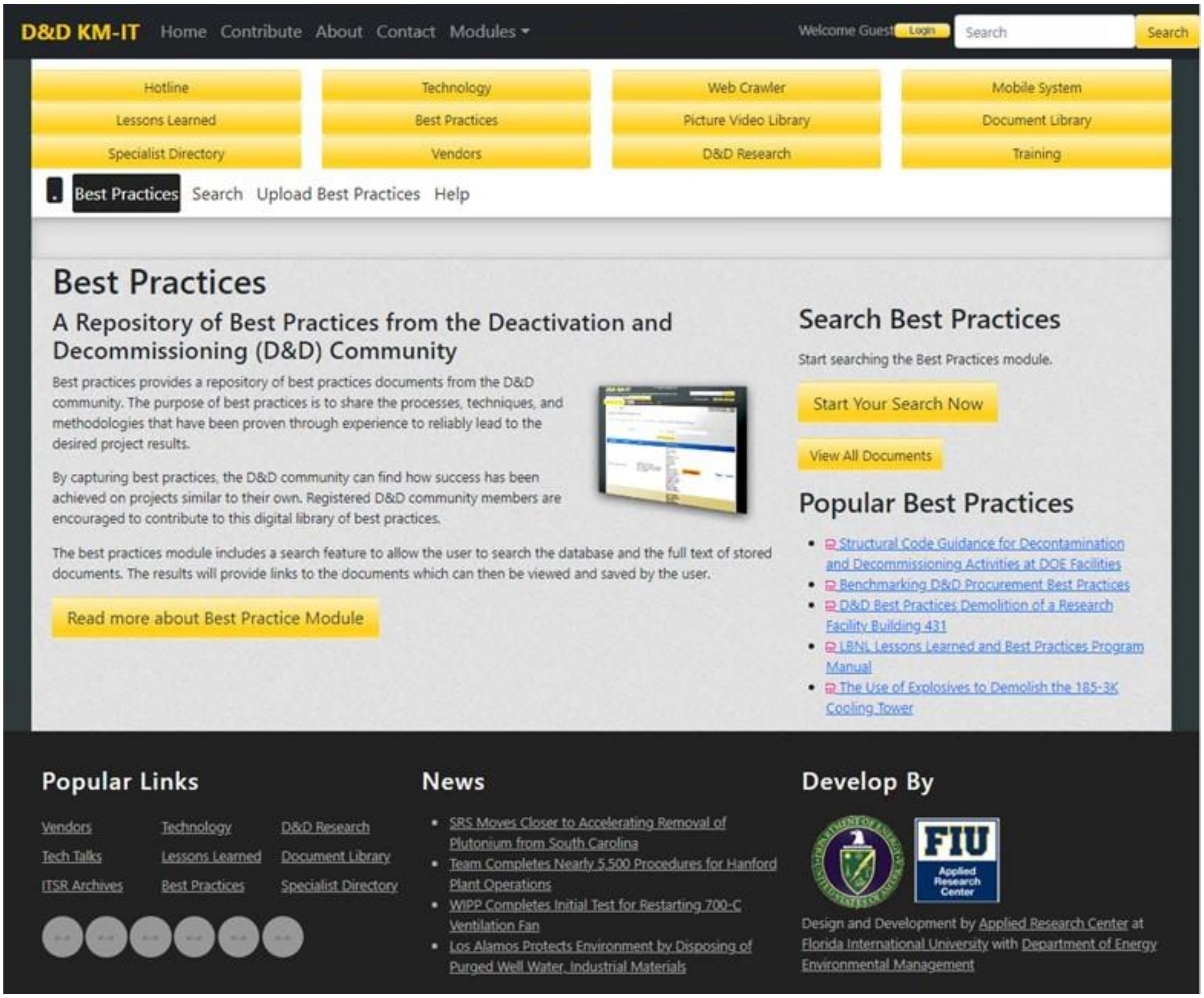

Figure 39. Best Practice module on the D&D KM-IT.

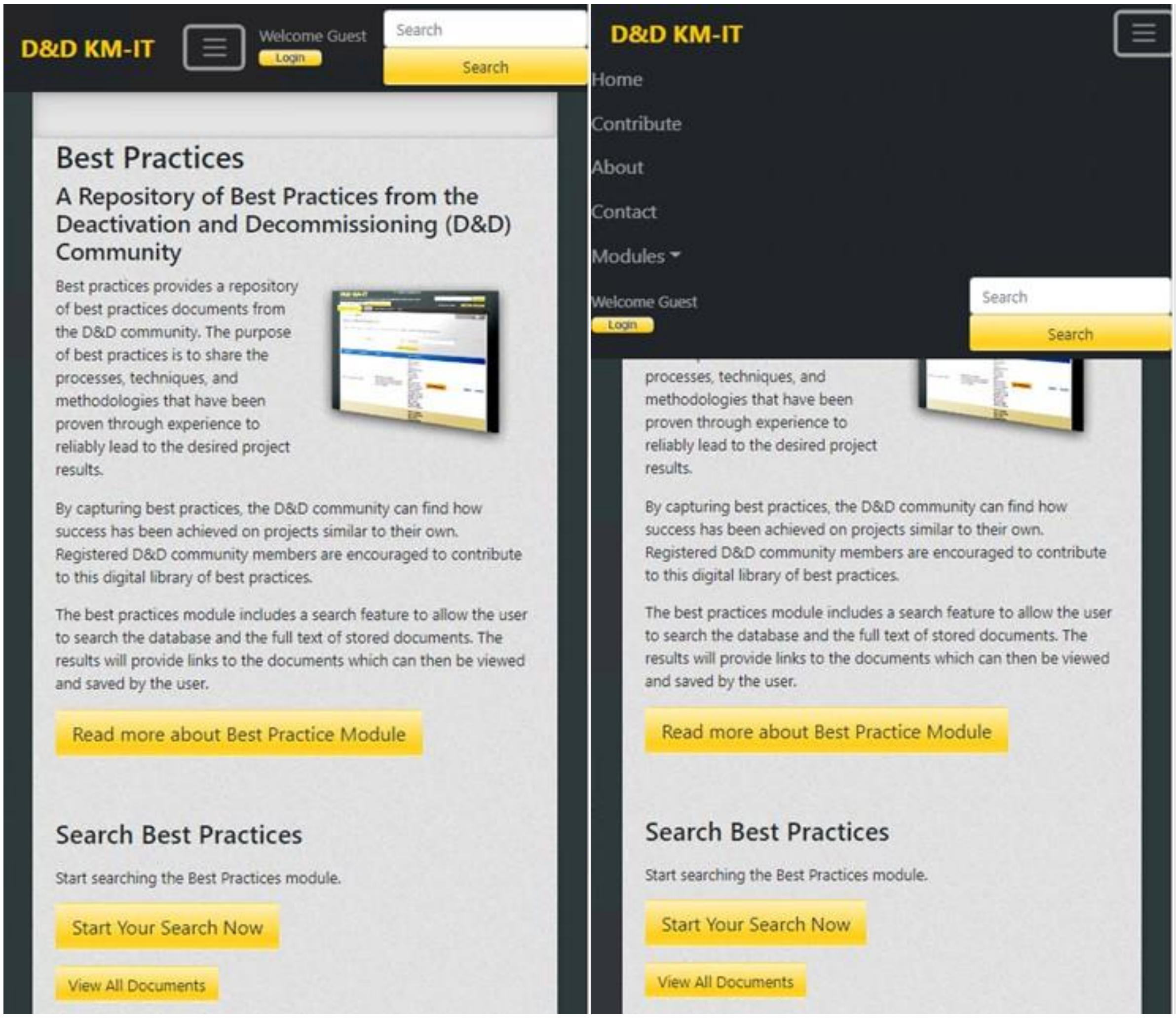

Figure 40. Best Practice module showing responsive design layout (left) and responsive design menu layout (right).

Finally, in June, the team completed updating the module master pages of the application. The focus has now shifted to working on individual content pages inside each of the modules. The team has made significant progress on the master landing page and default page of the KM-IT. As the effort progresses, functionality has been redesigned as well. For instance, the disclaimer page has been retired and instead a modal was introduced to display the disclaimer from any page on the site. This allows the user to keep the place they are browsing without leaving to a different page to display the disclaimer. Figure 41 below shows the disclaimer modal being displayed from the Best Practices module.

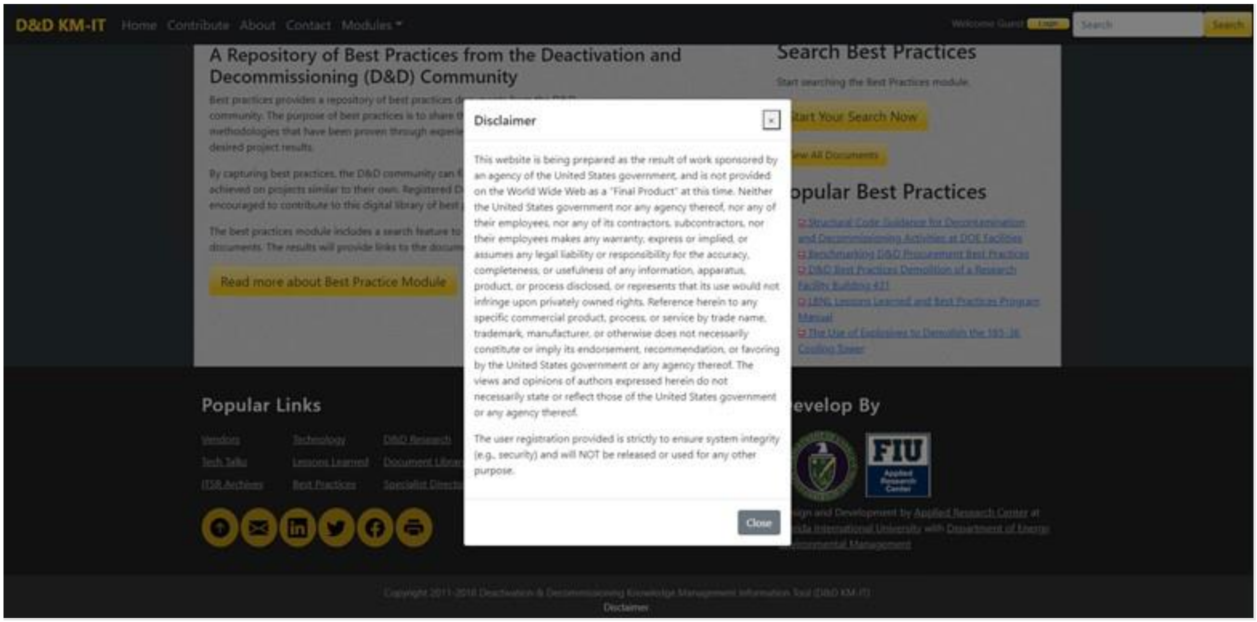

Figure 41. Disclaimer modal displayed from the Best Practices module.

Another example of functionality that was simplified is the Contribute module, which is currently retired. Instead, a single page was added to the root of the application. In addition, the login slide feature has been removed and users now go to the login page when they click on the login button. Many changes are happening across the site; for instance, the top menu was updated to include icons next to each of the module links. These icons match the module menu as you can see below for the Research Module (Figure 42).

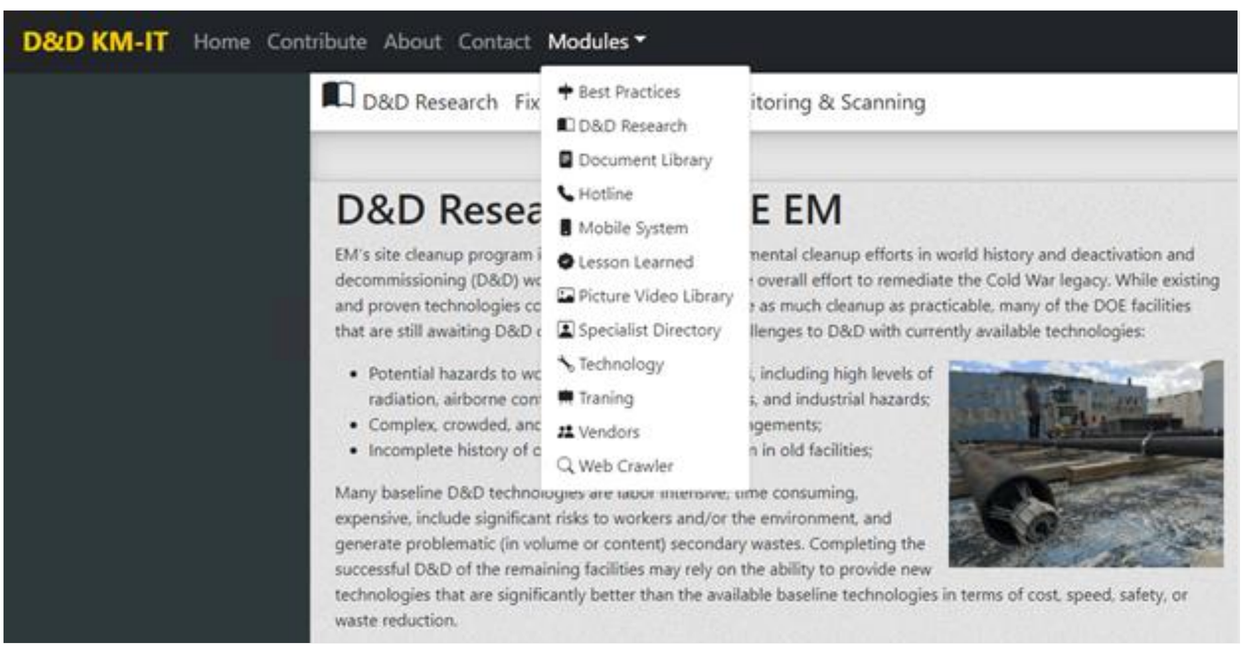

Figure 42. KM-IT menu showing an icon for each module link.

Subtask 3.1: Results and Discussion

This task involved updating the D&D KM-IT website with a responsive design. After the team completed updating the module master pages, they shifted to working on individual content pages inside each of the modules. The team continued to make progress on the master landing page and default page of the KM-IT. As each module was completed, the module was released for testing on the staging server where DOE Fellows were able to access the updated application and test the layout and functionality of the responsive design. The Figure 43 below shows the Best Practices module that has been deployed to the staging server for DOE Fellows to test.

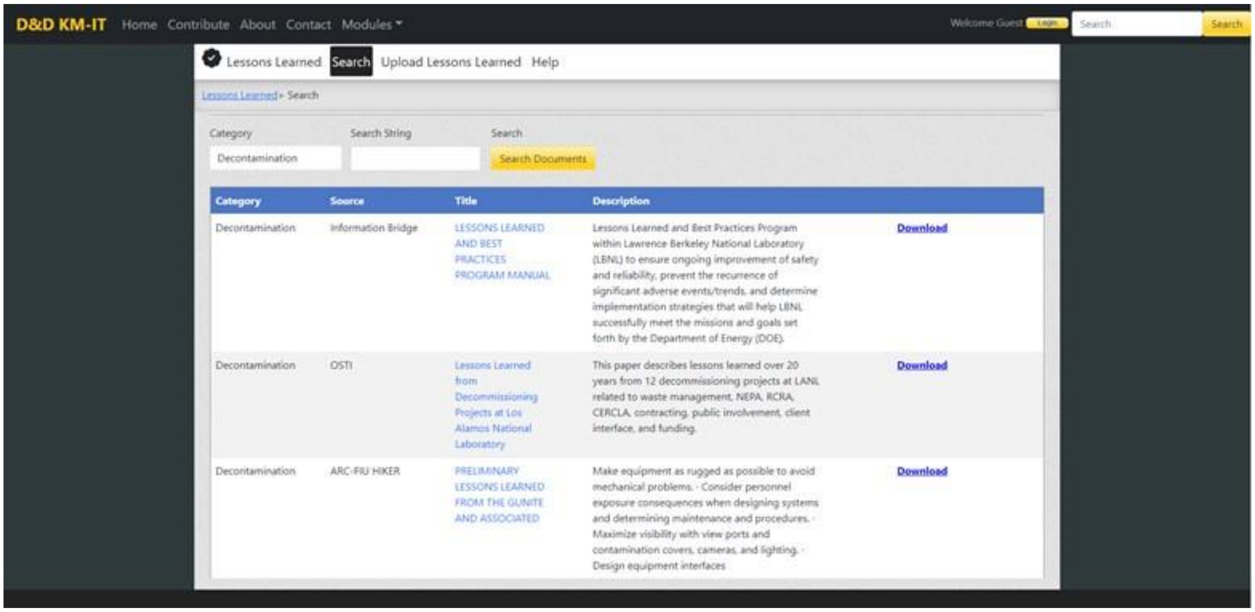

Figure 43. Best Practice module deployed to the staging server for testing.

DOE Fellows have made a substantial contribution to the past year's D&D KM-IT enhancements. Their efforts included modification of the HTML code of the master pages and content pages of the different modules. New page layouts and functionality were implemented throughout the master pages by changing the menu, breadcrumb, and content areas. DOE Fellows altered the content pages by switching the old sixteen columns grid layout to a Bootstrap design layout. The team Trello board for this project was very active (Figure 44).

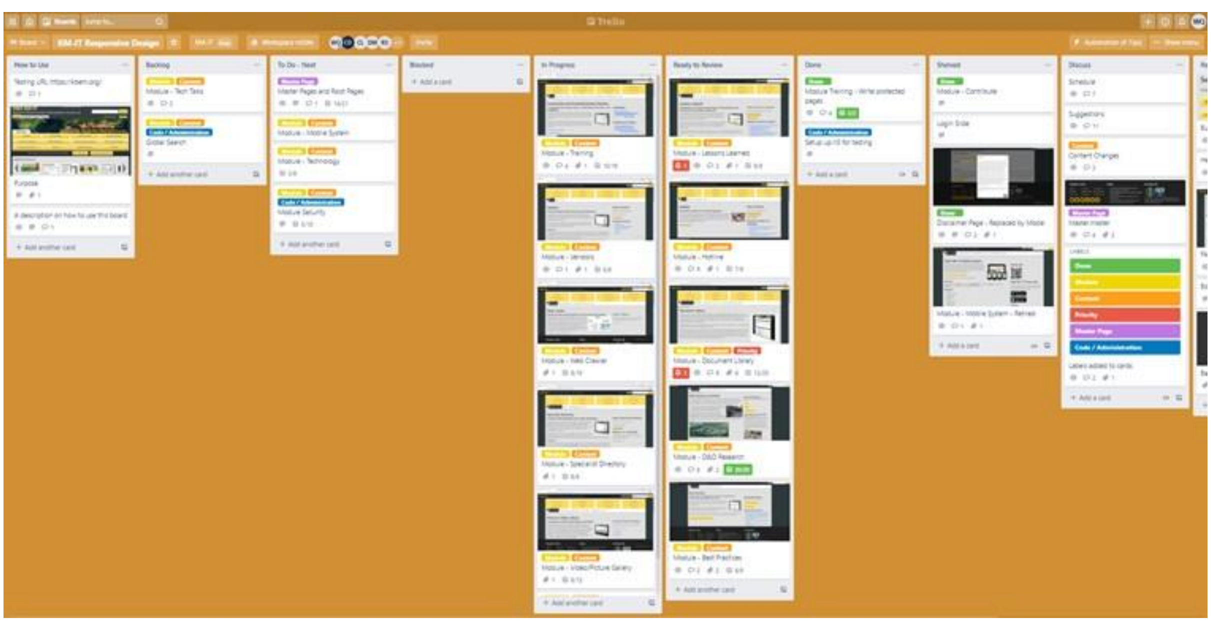

Figure 44. Trello board used to keep track of the project.

FIU successfully completed this deliverable (2020-P3-D6) D&D KM-IT - Responsive Design on August 20, 2021.

The application was deployed on the staging server for review at the following URL https://kbem.org/. The images below (Figure 45 and Figure 46) show the differences of the layouts on both desktop and mobile devices. As shown, the responsive design on the right automatically responds to the device screen size and changes its layout for a better user experience. This enhancement will eliminate the maintenance of two D&D KM-IT code bases (Desktop and mobile) to a single code base, which will be deployed at dndkm.org after review on the staging platform. Separate mobile deployment of m.dndkm.org will not be needed, leading to easy maintenance and better performance.

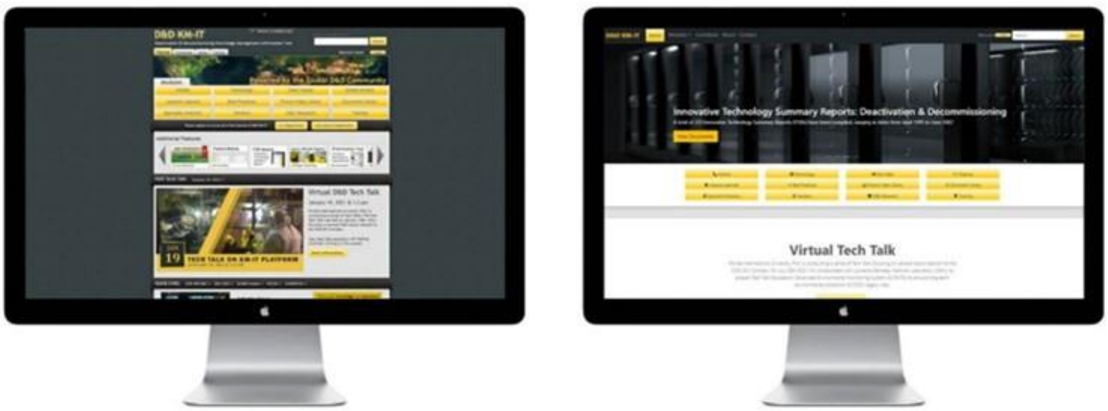

Figure 45. Before and after desktop screenshot of the D&D KM-IT application. New responsive design layout is shown on the right.

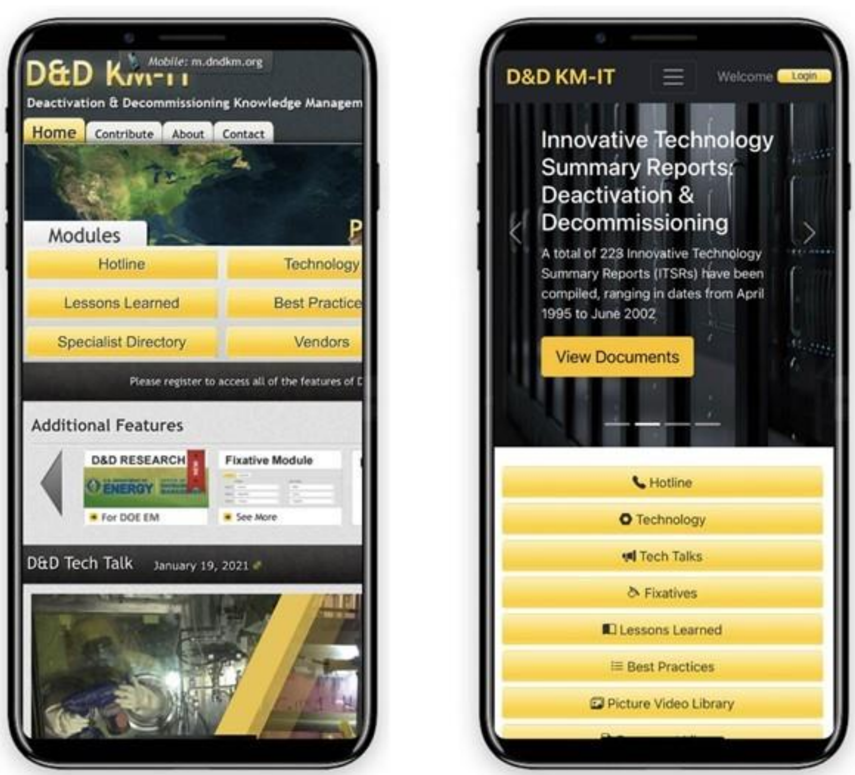

Figure 46. Before and after mobile screenshot of the D&D KM-IT application.

Subtask 3.1: Conclusions

This task achieved its objective to make the KM-IT application mobile-friendly providing a better user experience on mobile devices. In addition, the application redesign is expected to improve search results rankings like Google and other search engine algorithms prioritize websites that are mobile friendly. All the modules of the KM-IT application have been modified to take advantage of the responsive design. The team no longer needs to maintain two separate code bases (desktop and mobile) for the D&D KM-IT application. Visitors can simply visit https://kbem.org/ and the appropriate version of the website will be viewed according to their device.

Subtask 3.1: References

Deactivation and Decommissioning Knowledge Management Information Tool (D&D KM-IT), https://www.dndkm.org/, Applied Research Center, Florida International University.

Subtask 3.2: KM-IT Development – Enhance D&D Research Module for Multiple DOE EM Sites and National Laboratories

Subtask 3.2: Introduction

In this task, the FIU team focused on expanding the research module to publish the current D&D research being performed across multiple DOE EM sites, national labs, and universities. This effort started in the previous year with the development of the Research modules. This year, the team worked on expanding the content of this module with potential collaborators such as Idaho National Laboratory, Perdue University, Florida A&M University, and Los Alamos National Laboratory.

Subtask 3.2: Objectives

This task expands the content of the Research module to include D&D research being performed across multiple DOE EM sites, national labs, other universities, and internationally. The objective is for the user community to have a centralized location to review new D&D-related research in the community.

Subtask 3.2: Methodology

The FIU team engaged multiple DOE EM sites, national labs, and other universities to collaborate in sharing information to be published on the D&D KM-IT platform. This collaboration was achieved by reaching out to existing contacts at conferences and attending other scheduled meetings to discuss the possibility of collaboration. Other methods of outreach and contact involved emails, phone calls, and presentations given at different events and seminars. When an agreement was made for a collaborator's research to be shared with FIU, the team collected the information and categorized it in order for it to be added on the D&D KM-IT website. The information published included research name, description, pictures, videos, factsheets, and other research-relevant information.

Subtask 3.2: Results and Discussion

In January, FIU successfully completed the deliverable (2020-P3-D3) KM-IT Development - Enhance D&D Research Module for Multiple DOE EM Sites and National Laboratories. The team has enhanced the research module framework to publish D&D research being performed at various national labs and universities. The research framework will integrate various D&D areas like

Fixatives, Robotics, and Monitoring & Scanning. Research details captured in this framework include: Title, description (or abstract), factsheet (or paper/presentation), contact information, images, and in some cases videos. The research module can be accessed using the link https://www.dndkm.org/Research/.

FIU reached out to multiple organizations and received input from Idaho National Laboratory (INL), Argonne National Laboratory (ANL), and Savannah River National Laboratory (SRNL). D&D Research information received from these labs are published on the D&D Research module. FIU will continue to collect D&D research information being performed in the U.S. and internationally and publish it through this module on KM-IT as part of the content management efforts in future.

As mentioned above, all the research information was categorized into three main categories (Fixatives, Robotics, and Monitoring & Scanning). The screen capture below (Figure 47) shows the list of robotics research under the Robotics category.

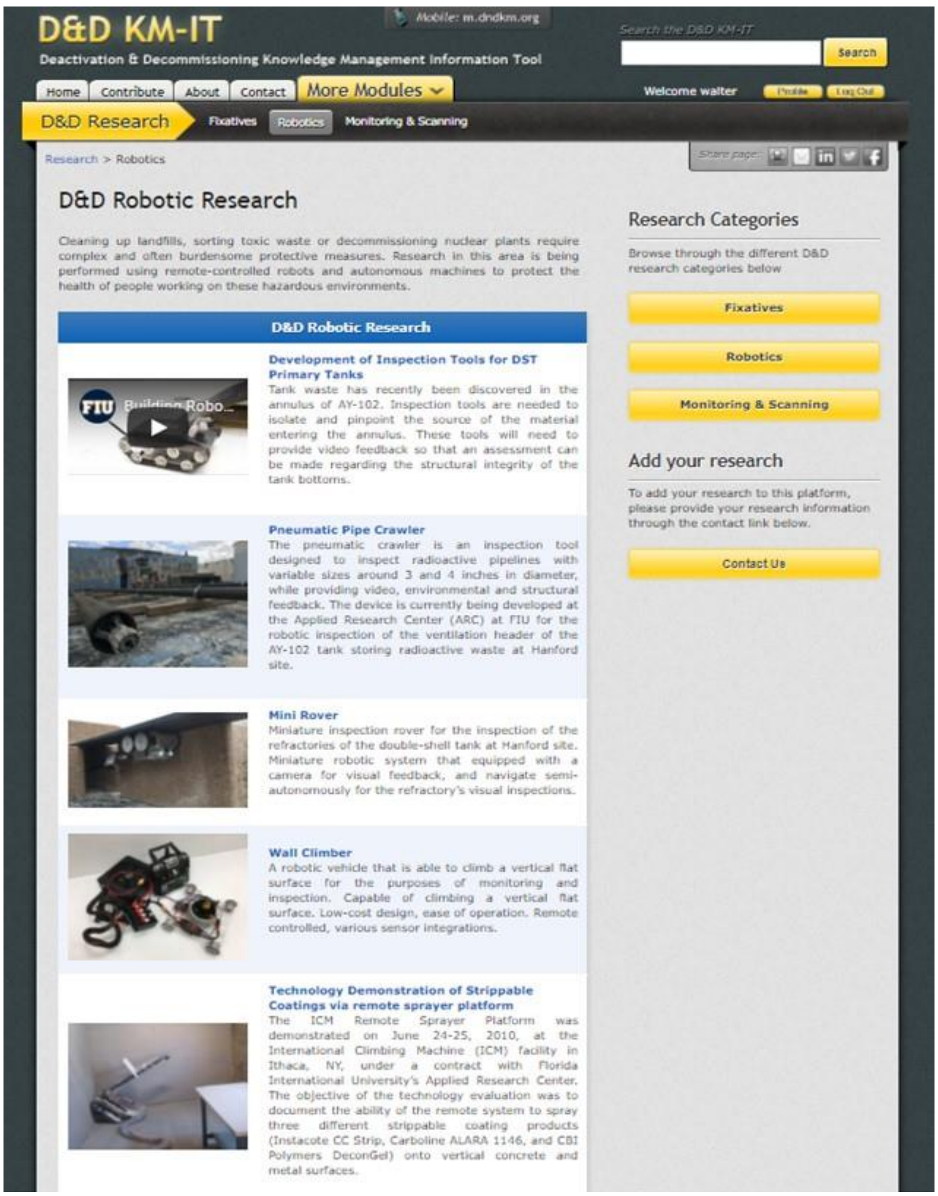

Figure 47. D&D Research on the Robotics category.

Subtask 3.2: Conclusions

FIU successfully completed the deliverable (2020-P3-D3) KM-IT Development - Enhance D&D Research Module for Multiple DOE EM Sites and National Laboratories back in January 2021. The team has enhanced the Research module framework to publish D&D research being performed at various national labs and universities. This additional content has increased the footprint of the research captured by D&D KM-IT and supports the mission of being a centralized location to review new D&D-related research in the community.

Subtask 3.2: References

Deactivation and Decommissioning Knowledge Management Information Tool (D&D KM-IT), https://www.dndkm.org/, Applied Research Center, Florida International University.

D&D Research for DOE EM, https://www.dndkm.org/Research/, Deactivation and Decommissioning Knowledge Management Information Tool (D&D KM-IT), Applied Research Center, Florida International University.

Subtask 3.3: Software Upgrades (Database and .NET Framework)

Subtask 3.3: Introduction

This subtask involves migration of the existing database to SQL Server 2019 and KM-IT modules to the .NET Framework 4.2. The D&D KM-IT is a multi-tier application and this migration will make the system more secure on both the backend (database) and front-end (user interface and middle tier). It will also improve the performance and stability of the system overall.

Subtask 3.3: Objectives

The objective of this subtask is to improve the stability of the D&D KM-IT application by performing specific upgrades to the SQL server database and the .NET framework. These upgrades will result in greater security, performance, and scalability of the application moving forward. It also brings the application up to the latest industry standards and ensure support is available for the SQL server moving forward.

Subtask 3.3: Methodology

The team began by devising a migration plan to accomplish this subtask with minimal downtime on the system. In addition, the team started with taking inventory of the hardware and software resources necessary to complete this task. This exercise ensured that any additional resources required were properly procured prior to the execution of this task. This included procuring the SQL Server 2019 license. The team proceeded by backing up the production application to the development server, followed by the installation of the SQL Server 2019 software. After the necessary updates to the software, the team proceeded to back up the existing database and imported the database to the new SQL server. The KM-IT application was configured to use the new 2019 SQL database. In addition, the application file was upgraded to the newer stable version of .NET framework 4.2. This involved using Microsoft Visual Studio and performing an application upgrade on the existing application. The application was then configured to use the new database. The staff and DOE Fellows proceeded to test the application before moving it to the production server. The image below (Figure 48) shows the SQL server version and their support date expiration. By upgrading the D&D KM-IT SQL database to SQL Server 2019, the team ensured the support for the software from Microsoft is available until 2030.

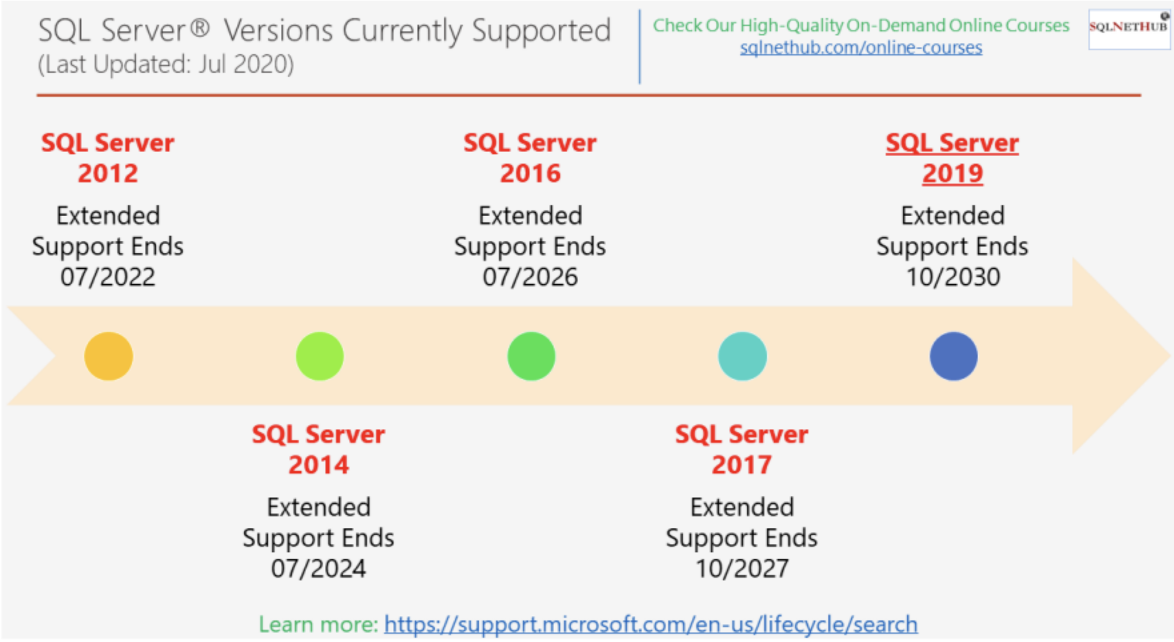

Figure 48. SQL server versions and support schedule.

Subtask 3.3: Results and Discussion

FIU has successfully completed the Milestone 2020-P3-M4, Software Upgrades - Database and .NET Framework for D&D KM-IT in February 2021. This involved migration of the SQL server database and KM-IT modules to the .NET Framework 4.2. The D&D KM-IT is a multi-tier application and this migration made the system more secure on both the backend (database) and front-end (user interface and middle tier). It will also improve the performance and stability of the overall KM-IT system while extending the support period for the SQL database server until 2030.

Subtask 3.3: Conclusions

The objectives of this subtask were met. The D&D KM-IT application stability was improved by performing specific upgrades to the SQL server database and the .NET framework. These upgrades resulted in greater security, performance and scalability of the application moving forward. It also brought the application up to the latest industry standards and ensured support is available for the SQL server moving forward

Subtask 3.3: References

Deactivation and Decommissioning Knowledge Management Information Tool (D&D KM-IT), https://www.dndkm.org/, Applied Rese arch Center, Florida International University.

Microsoft SQL Server 2019, https://www.microsoft.com/en-us/sql-server/sql-server-2019, Microsoft Inc.

Subtask 3.4: Content Management

Subtask 3.4: Introduction

Content Management includes publishing D&D technologies and QA/QC of existing content in the system. This is accomplished with the assistance of DOE Fellows who do most of the data mining across the system. Addition of vendors, lessons learned, best practices, D&D news, and conferences are also a part of content management.

Subtask 3.4: Objectives

The objective of this effort is for FIU to continue to publish additional technologies, vendors, and lessons learned on the KM-IT platform in addition to other relevant resources for the community, such as D&D related training, conferences and workshops to maintain fresh and informative content on the website.

Subtask 3.4: Methodology

FIU used factsheets, conference material (agenda, proceedings, brochures, etc.), vendor website, publication, DOE newsletters, and other sources to continue to publish additional technologies, vendors and lessons learned on the KM-IT platform. In addition, the team used other relevant resources for the community, such as D&D-related training, seminars and workshops to share information with the D&D community. The team monitored the website data analytics on the D&D KM-IT website and looked for anomalies, spikes in traffics, and other information that should be addressed. By using data analytics, the developers and team members can focus on critical issues affecting the website. It can also provide great insight about features that should be enhanced and/or added to the website based on user behavior.

Subtask 3.4: Results and Discussion

FIU continues to publish additional technologies, vendors, and lessons learned on the KM-IT platform in addition to other relevant resources for the community, such as D&D related training, conferences and workshops. There were 72 technologies published on the D&D KM-IT website. Below is the breakdown by quarter.

- First Quarter (Sep – Dec, 2020) – 13 technologies published
- First Quarter (Jan – Mar, 2021) – 23 technologies published
- First Quarter (Apr – Jun, 2021) – 17 technologies published
- First Quarter (Jul – Sep, 2021) – 19 technologies published

In addition to technologies and vendors, training and conference opportunities related to D&D were also added to the system.

Content management has allowed the D&D KM-IT to increase its content. The graph below (Figure 49) summarizes the growth over the years. As of August 2021, the system had 1,437 D&D technologies, 1,091 registered users, 997 D&D vendors, and 105 subject matter specialists.

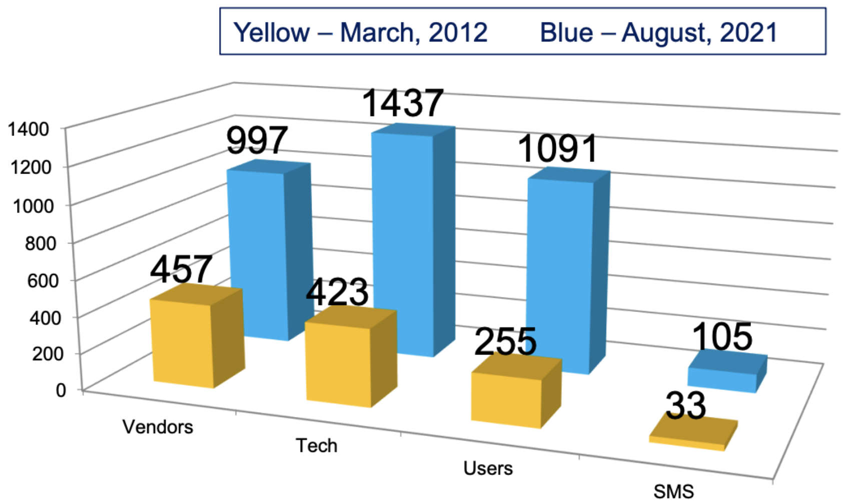

Figure 49. Number of vendors, technologies, users, and SMS as of August 2021.

As part of this task, the team also tracks web activity on the D&D KM-IT website. The following figure (Figure 50) shows the most relevant key metrics from Google Analytics (GA). Notice that by comparing 2020 vs. 2021, the system has shown substantial growth in multiple areas which include Users, New Users, Sessions, and Pageviews. Each of these areas had double percentage increases when compared to the previous year.

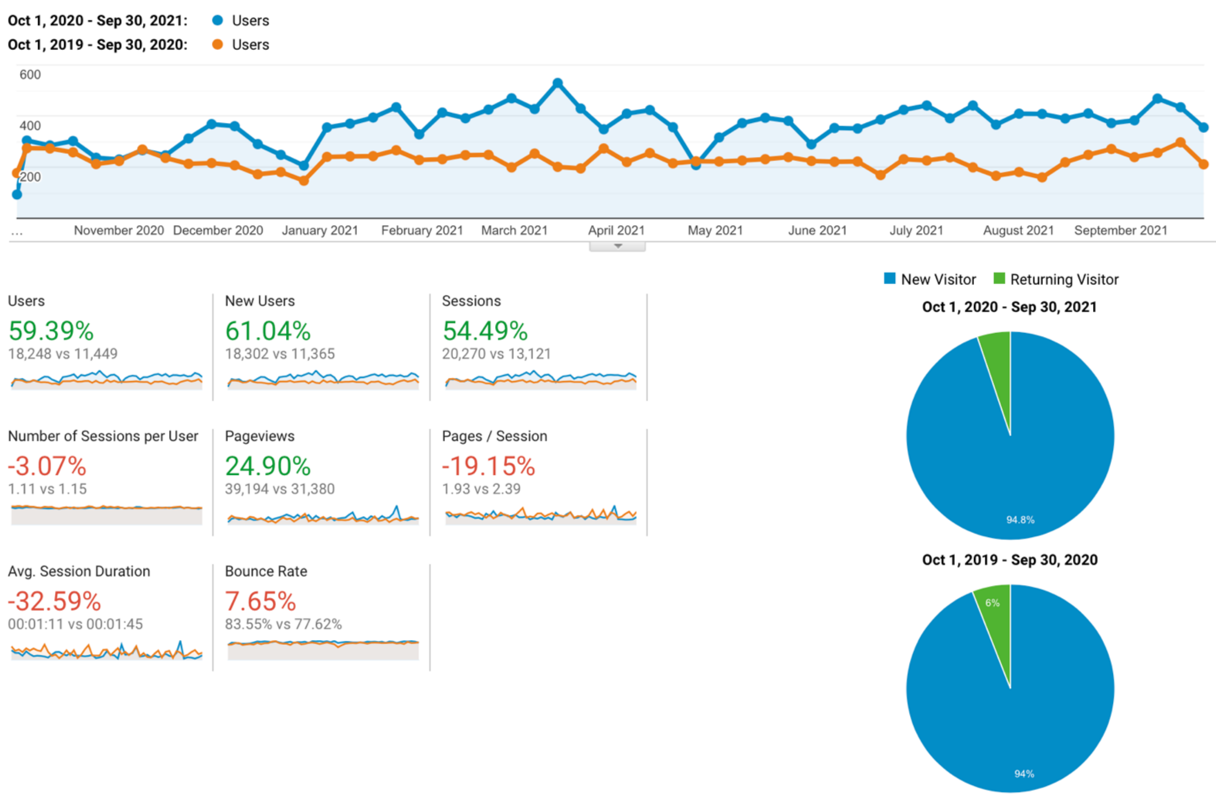

Figure 50. Google Analytics activity 2021 vs. 2021.

The GA data analytics captures some interesting information, such as the location of a user visiting the website. The map below (Figure 51) shows the changes in the amount of activity by state.

Notice the shading of each of the states. The darker color shows more activity, so from this image one can conclude that the top five states that visited the website were Illinois, California, Virginia, Texas, and Florida.

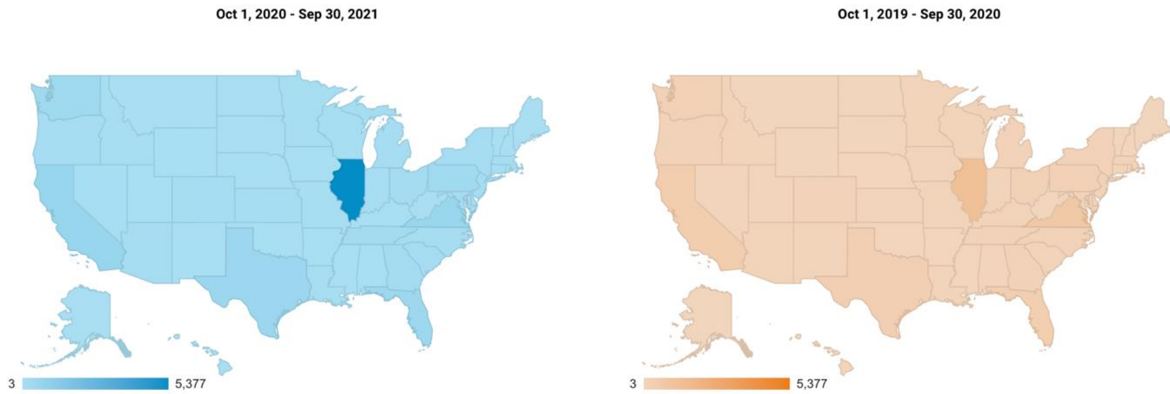

Figure 51. D&D KM-IT activity by state (2020 vs. 2021).

Other information captured by GA is the type of devices used by the visitors, operating system, mobile devices, and even browsers. Below are some comparisons of each of these metrics to the previous period (Figure 52).

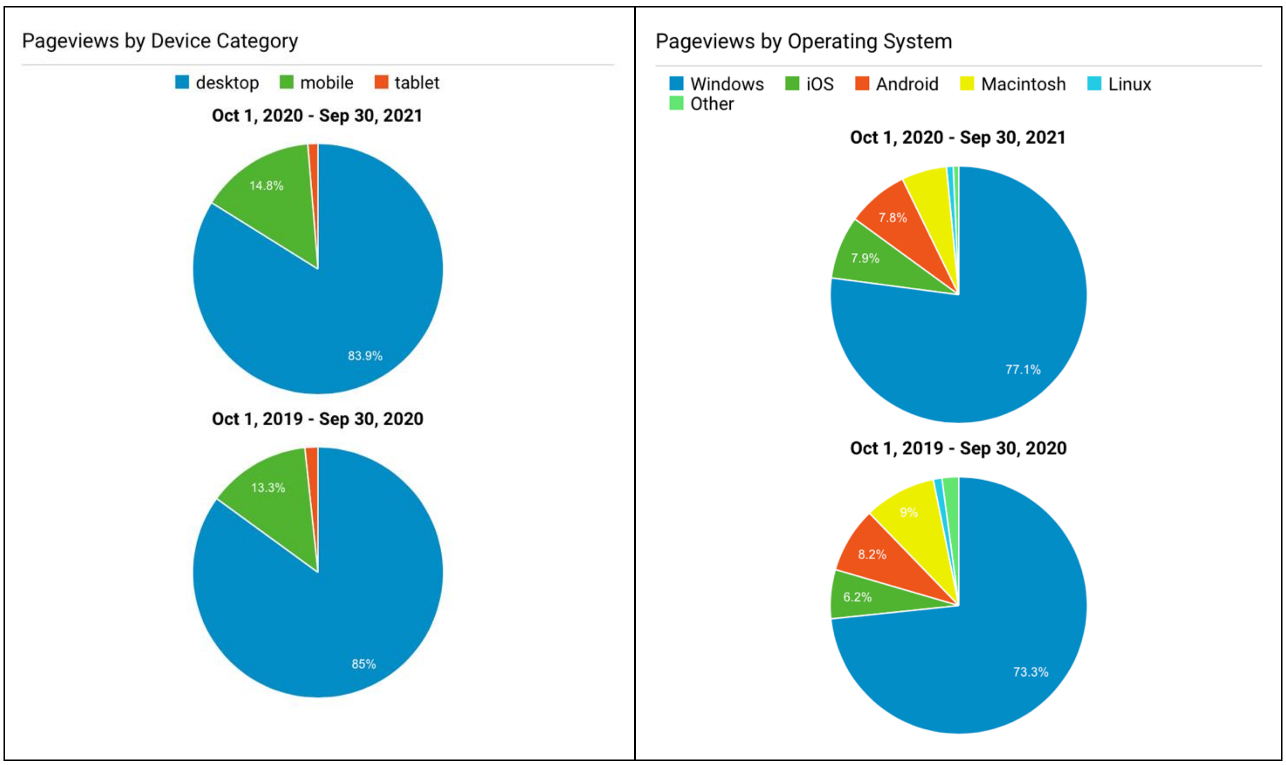

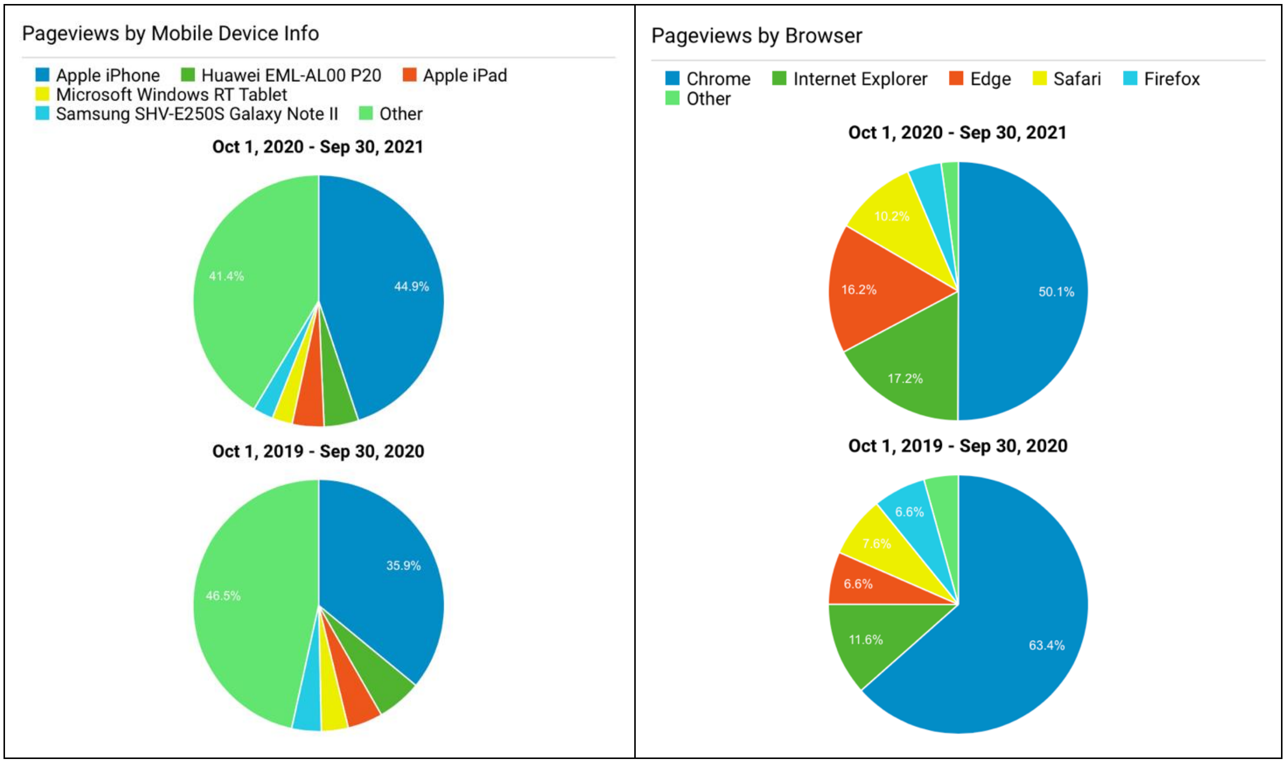

Figure 52. Google Analytics metrics for D&D KM-IT.

Subtask 3.4: Conclusions

FIU published additional technologies, vendors, and lessons learned on the KM-IT platform in addition to other relevant resources for the community, such as D&D related training, conferences and workshops. There were 72 technologies published on the D&D KM-IT website. In addition, website data analytics captured key metrics that helped the FIU developer focus on specific issues on the website. The content management efforts continue to keep the website current and informative for the D&D community.

Subtask 3.4: References

Waste Information Management System (WIMS), https://emwims.org/, Applied Research Center, Florida International University.

Google Analytics, https://analytics.google.com, Google Analytics, Google Inc.

Subtask 3.5: Marketing and Outreach

Subtask 3.5: Introduction

This task involves reaching out to sites/national labs to increase KM-IT user involvement as well as presentations at conferences and collaboration with the IAEA. In addition, the team focused on increasing engagement from DOE sites and national labs on D&D KM-IT by a series of methods such as TechTalks, public and internal newsletters.

Some specific activities for outreach and marketing of KM-IT included the following:

Newsletters and Mass Communications**:** Newsletters and online promotions are a great way to bring waves of traffic to the website. By using the registered users as recipients, users were kept up-to-date on new features and content on the D&D KM-IT.

Conferences and Workshops**:** Participation and presentations of KM-IT at industry conferences boosts awareness of the website and its capabilities to the target users. FIU presented KM-IT at conferences, such as the Waste Management Symposia, through a combination of oral and poster presentations as well as individual and small-group demonstrations and workshops hosted in the exhibition hall. At these events, the site features can be explained in detail and participants can share their feedback and ideas.

User Support and Ad Hoc Specialized Reports: This task includes supporting KM-IT users with a help desk role to resolve issues on a day-to-day basis, as well as developing specialized reports using the KM-IT system for unforeseen data requests from DOE or the EM community of practice.

Subtask 3.5: Objectives

The objective of this task is to reach the D&D community and educate them on the features available on the D&D KM-IT system. There are many industry leaders who work at various DOE sites and national labs that can benefit greatly from the capabilities that the system has to offer. In many cases, these individuals are not aware of the system, so by doing outreach and marketing, the system usage can be promoted while helping the D&D community meet their knowledge management needs.

Marketing and outreach are critical for the self-sustainability of the system as it introduces the system to subject matter experts who may not be aware of its features and capabilities. This task increased the footprint of the D&D KM-IT in the community by allowing users to discover the capabilities of the D&D KM-IT.

Subtask 3.5: Methodology

This task is an ongoing process that is executed over the course of the year. When new features or content is added to the system, DOE is notified and others in the industry are reached via email to get feedback and comments. This is done not only to communicate with DOE regarding accomplishments and milestones, but also to involve other leaders in the industry in the process of spreading the word about D&D KM-IT. When sending newsletters, FIU uses the D&D KM-IT as its recipients. Currently, there are 1,091 registered users in the system. FIU has also used the public distribution list provided by the Waste Management Symposia (WMS) to make announcements about the D&D KM-IT training workshop typically held at the FIU booth during WMS.

FIU uses a third-party application/service called Mailchimp to send newsletters to a large distribution list. This service supports email stats like opened emails and read emails, and it also tracks clicks. However, for official announcement of milestones and deliverables, FIU uses a typical email system to notify its stakeholders. During the course of this year, several emails were sent to DOE notifying them about new features, such as the development of a sub-module on the KM-IT platform to highlight current EM research efforts and activities in support of D&D.

Subtask 3.5: Results and Discussion

FIU presented a poster at the 2021 Waste Management Symposia virtual conference capturing the research and efforts on D&D KM-IT during 2020. The poster was titled "*D&D Research on KM-*

IT Platform". The following Figure 53 shows the poster prepared and presented at the virtual conference in March 2021.

Figure 53. D&D Research on KM-IT platform poster presented at WM2020.

This subtask also included developing newsletters for mass communication via email to keep users informed of new system features and other related activities. FIU sent a newsletter to the participants of the Waste Management Symposia announcing multiple topics. Below is sample collage of some of the newsletters sent to D&D KM-IT users followed by archive newsletters that can be accessed via the URL shown (Figure 54).

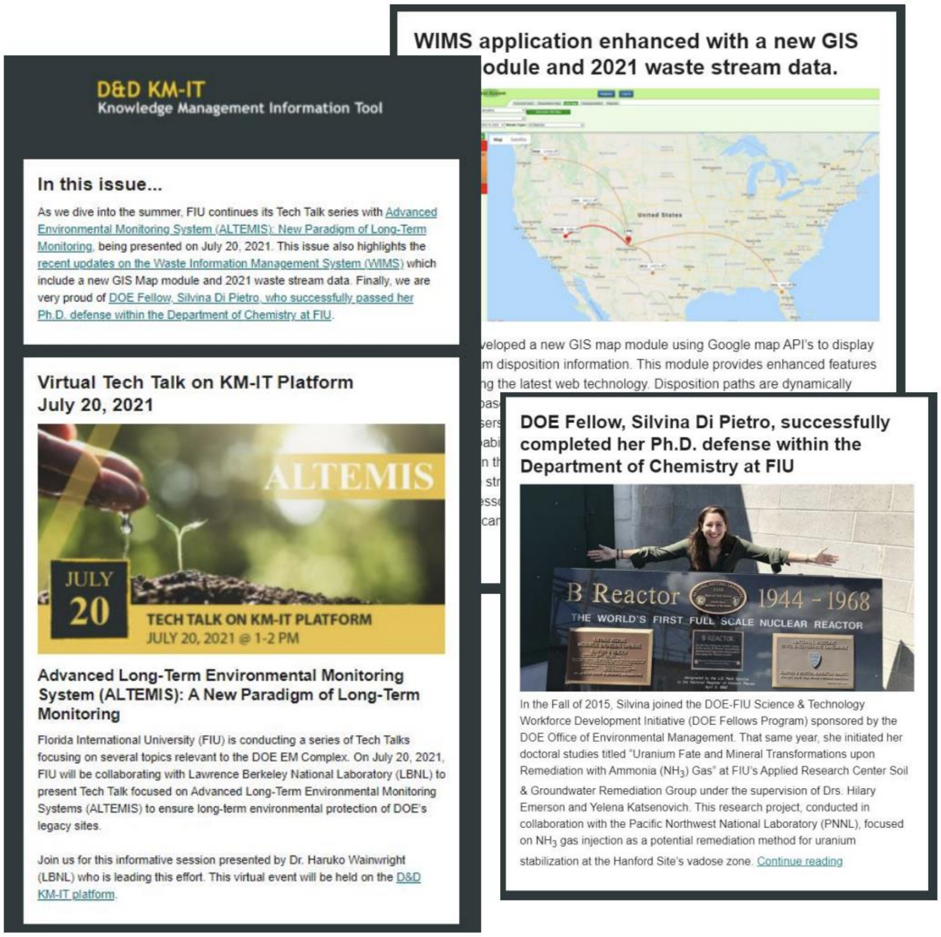

Figure 54. Sample newsletter sent to D&D KM-IT users.

Newsletter list:

- September Newsletter - https://mailchi.mp/26b9f80a3233/fiu-wms2019-4974082?e=[UNIQID]
- ALTEMIS Tech Talk Reminder - https://mailchi.mp/ffd3a465c46a/reminder-tech-talk-tuesday-1-pm-4940482
- July Newsletter - https://mailchi.mp/9624245af7f1/fiu-wms2019-4928650?e=[UNIQID]
- April Newsletter - https://mailchi.mp/fd2c92220169/fiu-wms2019-4842938?e=[UNIQID]
- Tech Talk Reminder - https://mailchi.mp/e2435953ff99/reminder-tech-talk-tuesday-1-pm
- December Newsletter - https://mailchi.mp/33b8c30022f4/fiu-wms2019-4803390?e=[UNIQID]

On September 29, 2020, the team engaged in a demonstration of the D&D KM-IT application for DOE EM officials as a follow-up to the year-end presentations. In this meeting, a detailed presentation of each module was performed and a discussion followed with the purpose of sharing ideas on how to increase participation by certain DOE sites and national labs. After capturing all the ideas, the team prepared and submitted a plan to DOE on how they intend to achieve this goal. The key points in this plan include:

1. Implementing Quarterly TechConnect Events – Online quarterly tech events will be organized that will allow subject matter experts (SME) to share their knowledge and experience with DOE EM sites and stakeholders. This will occur as one-hour events, which will include one or two guest speakers on relevant topics of interest to the community. The events will be recorded and published on D&D KM-IT along with other associated material such as the agenda, presentation slides and lessons learned for post-event viewing as well. A tentative schedule for TechConnect events is listed below. Topics will be decided after discussion with the speakers and team.
    a. SRS - o/a December 15, 2020
    b. WRPS - o/a March 30, 2021
    c. Oak Ridge - o/a June 30, 2021
    d. TD at EM HQ - o/a September 28, 2021
2. Enhancing connectivity/links with other databases – This involves exploring additional databases that the D&D KM-IT can integrate to make information available on the site, similar to what FIU is doing with OSTI. The D&D KM-IT currently can connect to OSTI and provide the information to its users without duplicating the data by using a sophisticated API published by OSTI. This capability will provide valuable information to users visiting the site that could lead to them returning and resulting in the increased traffic. As discussed during the September 28th, 2020 meeting, a potential link may be the database created/managed by Longenecker and Associates.
3. Enhancing user newsletter subscriptions – The current newsletter subscription will be modified so that users can get alerts when topics of interest are added to the D&D KM-IT. For instance, if a user is signed up to receive notification when new content is added (such as technologies, lesson learned, best practices, etc.), an email notification will be sent to the user.
4. Promoting KM-IT in internal DOE EM community newsletters – The tasks mentioned above can be promoted on internal DOE EM newsletters. Links to upcoming Tech Talks, new technologies or modules will increase the traffic to the site coming from DOE EM and site users.
5. Expanding the SME community across all disciplines at DOE-EM sites – FIU and DOE HQ will engage site contacts to create a working group that will increase subject matter experts in D&D areas. These areas will include robotics, sensors, machine learning and AI and many more based on the interest of the community. Meeting minutes, agendas, and schedules will be published on D&D KM-IT. SME will provide input and areas of interest, which will be highlighted on D&D KM-IT resulting in additional traffic across DOE sites.

The team started to address the Tech Talk initiative. These online tech events allowed subject matter experts (SME) to share their knowledge and experience with DOE EM sites and stakeholders. These were one-hour events, which included one or two guest speakers on relevant topics of interest to the community. The events were recorded and published on D&D KM-IT along with other associated material such as the agenda, presentation slides and lessons learned for post-event viewing as well.

The team finalized the topic that will focus on D&D technologies, specifically on fixative coatings supporting the SRNL facility. The team begun coordinating schedules with subject matter experts and has set the first Tech Talk to be scheduled for January 19, 2021. The team prepared a flyer (Figure 55) and a website for the event https://www.dndkm.org/TechTalk/ (see screenshot below) to promote the event. The website included meeting information, a link to the flyer and a link to Microsoft Apps that will be used for the event (Figure 56).

Figure 55. Tech Talk flyer scheduled for January 19, 2021.

Figure 56. Tech Talk website.

The team hosted 3 Tech Talks during this period. Below is the list of the topics and dates of the Tech Talks that were presented.

Successful Deployment of Fire-Retardant Fixative at SRS 235

On January 19, 2021, FIU collaborated with Savannah River National Laboratory (SRNL) focusing on the successful deployment of the fire-retardant fixative tested by FIU which was recently deployed on site at SRNL.

Use of Robotics in Nuclear Applications

On April 20, 2021, FIU collaborated with Washington River Protection Solutions (WRPS) focusing on the use of robotics in nuclear inspection and maintenance applications.

Advanced Environmental Monitoring System (ALTEMIS): New Paradigm of Long-Term Monitoring

On July 20, 2021, FIU collaborated with Lawrence Berkeley National Laboratory (LBNL) to present a Tech Talk focused on Advanced Environmental Monitoring System (ALTEMIS) to ensure long-term environmental protection of DOE's legacy sites.

Subtask 3.5: Conclusions

Outreach and marketing are critical elements towards the long-term sustainability of knowledge and are essential for the long-term strategic vision of D&D KM-IT. Moving forward, FIU will continue to participate in industry conferences (such as Waste Management Symposia) and other workshops to demonstrate and promote the KM-IT system. This allows for collaboration with other centers, facilities, and DOE sites to increase usage and subject matter specialist participation. In addition, FIU will continue to develop newsletters for mass communication via email to keep users informed of new system features and other related activities.

The Tech Talks were very successful and as a result, this effort will be designated as its own task in the following period.

Subtask 3.5: References

Deactivation and Decommissioning Knowledge Management Information Tool (D&D KM-IT), https://www.dndkm.org/, Applied Research Center, Florida International University.

Tech Talk on D&D KM-IT, https://www.dndkm.org/TechTalk/, Applied Research Center, Florida International University.

Subtask 3.6: D&D KM-IT System Administration

Subtask 3.6: Introduction

D&D KM-IT system administration is an ongoing task, which involves day-to-day administration of servers that house the KM-IT databases and web applications. This task includes updating patches and OS fixes, updating antivirus engines and definitions, updating drivers and assuring that the network (firewall, routers and switches) is working properly.

Subtask 3.6: Objectives

The KM-IT infrastructure is deployed, secured, and maintained in the FIU facility. The objective of this task is for researchers and DOE Fellows to continue to test, maintain, secure, and administer the KM-IT system to keep it reliable with no down time.

Subtask 3.6: Methodology

As mentioned above, the D&D KM-IT system administration is an ongoing task that involves hardware and software upgrades. Additional administration tasks during this period included the creation of the development environment for the D&D KM-IT to support Subtask 3.1 for example. This environment is a duplication of the production environment application and database. This environment must be constantly updated to replicate the production server. As the information on the production changes, these changes must be replicated on the development environment to keep both environments in sync. This requires additional administration of development files and database.

Subtask 3.6: Results and Discussion

Some of the efforts included backup of servers in preparation for the software upgrade outlined in Subtask 3.3. This involved creating incremental backups and snapshots of the application.

Some of the specific tasks included:

- Update of the DOE server room network switch from 24 port unmanaged switch to 50 port to managed switch – this switch provides network connectivity to the server running the KM-IT application.
- Starting the update of the DOE database server from 2017 to 2019.
    - New windows server with latest OS
    - Installation of SQL 2019 server
    - Starting the import of the DOE databases
- Update of security patches and applications for the servers and firewall of the DOE server room.
- Hardware updates (replacing hard drives and upgrading memory on server to increase performance and reliability).
- The team put together a layout for a new GPU server for the DOE AI work and placed the order to purchase.
- Maintenance and support of the DOE Fellows' remote access and local workstations.
- Software updates – security patches, development and framework updates.

- Assisting with access to development server for development team while working remotely.

Subtask 3.6: Conclusions

The team has successfully kept the D&D KM-IT application and production environment running with optimal performance. After all the hardware and software updates were done, the application did not experience any outages. As a result, the application continues to be more reliable because of the routine maintenance performed on the environment where the application is running.

Subtask 3.6: References

Deactivation and Decommissioning Knowledge Management Information Tool (D&D KM-IT), https://www.dndkm.org/, Applied Research Center, Florida International University.

Subtask 3.7: Cyber Security of D&D KM-IT Infrastructure

Subtask 3.7: Introduction

Cyber security of D&D KM-IT involves securing the network infrastructure that is deployed, secured and maintained in the FIU facility. This includes administration tasks described in Subtask 3.6, but also includes conducting routine cyber security tasks to test the network's vulnerability. This involves coordination between the FIU security team and DOE Fellows who learn cyber security skills while assisting staff do penetration testing and other tasks to test the overall security of the system at the application, database, and infrastructure levels.

Subtask 3.7: Objectives

The KM-IT infrastructure is deployed, secured, and maintained in the FIU facility. The objective of this task is for researchers and DOE Fellows to continue to test, maintain, secure, and administer the KM-IT system to keep it secured and up to date with industry standards. This is done to prevent any security breaches on the system and to train DOE Fellows on security tools used in the industry.

Subtask 3.7: Methodology

The KM-IT infrastructure is deployed, secured, and maintained in the FIU facility. This is a repetitive task, as researchers and DOE Fellows continue to test, maintain, secure and administer the KM-IT system. This involves the administration and upkeep of the application server, windows server and database servers of D&D KM-IT system. Penetration testing tools, malware analysis and reverse malware engineering techniques are used in the DOE Cyber lab to test and secure the KM-IT infrastructure. To keep this infrastructure secure, the team performs various tasks. For instance, each month FIU IT security scans the D&D KM-IT website and provides a report to the team on security vulnerabilities. On a weekly basis, Symantec/Norton scans the D&D KM-IT website for vulnerabilities and malware and sends a report to the team, which is then reviewed and analyzed. If anything in the reports looks critical, the team implements counter measures to minimize the risk of the vulnerability.

In addition, other tasks are executed related to disaster recovery, such as performing backups of the D&D KM-IT environment. These backups are incremental and full backup schemes are then moved to a separate NAS device outside the network. Finally, updates to the operating system are performed which include patches and other OS updates from the vendor. Typically, these updates are performed on the staging environment to make sure that they work properly before moving the changes to the production server. There are also other tasks that are performed to keep the application secured, but they are not necessarily done each month. These include:

- Update domain controllers and DOE environment domain.
- Update all SSL encryption for DnDKM-IT and WIMS websites.
- Follow the latest security policy recommendations from DOE.
- Monitor local users on the DnDKM-IT.
- Keep applications on the DnDKM-IT environment (SQL servers, IIS servers, ASP.Net).
- Monitor network switches and logs for permissions and traffic.
- Monitor users and bandwidth of the firewall.
- Keep NAT policies on the firewall up to date.
- Manage the firewall updates and policies.

DOE Fellows assist with many of these tasks. This allows them to get real life experience on cybersecurity and network administration that is way beyond the material they learn in the classroom. DOE Fellows have been actively working on this task. The team continued learning networking fundamentals by understanding layer 3 of the OSI networking model. This layer, called the Network layer, deals with Internet Protocol (IP) addresses. When a client tries to connect to a server, it tries to send a data packet using the server's public IP address. The router/gateway of the LAN sees the IP of the server, and it automatically knows that the server is outside of the LAN, so it forwards the packet to the largest WAN (the internet). The same process is reversed once the server receives the packet and wants to communicate back with the client machine. The team then experimented with IP addresses by pinging a server using the server's URL. If the ping is successful, meaning the server is running and it replies to the ping, the team can gather the public IP address related to that server. The first step of the Cyber Analysis workflow is to prepare and gather information about the target. Obtaining the public IP of a server is often one of the first steps in information gathering.

The cybersecurity team then focused on possible attacks that can be performed with the public IP of a machine. There are multiple approaches, but one of the easiest ones is performing an ARP poisoning attack that involves exploiting the Address Resolution Protocol by misleading the gateway to change the pairing in its CAM table. This allows attackers to execute a Man-In-The-Middle (MITM) attack where the attacker can see all the data packets entering or leaving a victim device in the LAN. More advanced concepts can be carried out using the MITM attack that involves changing HTTP requests and more, but the team only explored MITM attacks that involve reconnaissance. The team also continued the KM-IT infrastructure's content management efforts by editing obsolete vendor links that do not work anymore because the vendor has gone out of business.

Early on 2021, the DOE Fellows continued learning cybersecurity tools that are open-source and available in Linux machines. The first tool that was explored is THC Hydra. THC Hydra is a parallelized password cracker tool that supports various networking protocols to perform different attacks. The main feature of Hydra is that it allows penetration testers to remotely gain unauthorized access to a device. This tool can be used efficiently by specifying a file with a possible password; this permits rainbow table and dictionary attacks which are on average faster than just regular brute force attacks. The second tool that the team examined closely is called Nessus. Nessus is a popular open-source tool available for UNIX systems that is capable of performing vulnerability scanning of computer systems. The tool can be used for local and remote security checks of web servers. It features a graphical user interface that enables a seamless user experience for targeting domain name servers (DNS), databases, and specific operating systems.

Both THC Hydra and Nessus are tools that the cyber security team can potentially use to test the KM-IT infrastructure. A Hydra password cracker example for the KM-IT infrastructure would consist of a command that specifies a file with a list of potential passwords of the KM-IT web server, the IP address of the KM-IT web server, and the HTTP protocol. This would essentially perform a dictionary attack to more efficiently brute forcedly gain access of the KM-IT infrastructure as an admin. The Nessus tool can be used by specifying the IP address of the KM-IT web server as a target to perform a vulnerability scanning on. This will reveal any known vulnerabilities and open/closed ports in the KM-IT infrastructure that hackers could exploit.

Finally, other tasks are executed related to disaster recovery, such as performing backups of the D&D KM-IT environment. These backups are incremental and full back up schemes are then moved to a separate NAS device outside the network. Finally, updates to the operating system are performed which include patches and other OS updates from the vendor. Typically, these updates are performed on the staging environment to make sure that they work properly before moving the changes to the production server. The team has to also secure a testing domain that is being used on the staging environment for the DOE Fellows to test the KM-IT responsive design.

Subtask 3.7: Results and Discussion

The cyber security measures for the D&D KM-IT application were successfully implemented by the FIU team, and no breach of the system was detected with the procedures employed. In addition, the DOE Fellows were able to gain invaluable hands-on experience on cybersecurity and network administration, with exposure to penetration testing tools, malware analysis and reverse malware engineering techniques, to test, maintain, secure and administer the KM-IT system.

Subtask 3.7: Conclusions

Cybersecurity and administration of the D&D KM-IT application are ongoing processes to keep the application secure and reliable. The fact that there was no breach of the system detected can likely be attributed to the cyber security measures implemented, which is an indicator of the significance of this subtask and the need to maintain it as an ongoing support process for the D&D KM-IT application.

Subtask 3.7: References

Deactivation and Decommissioning Knowledge Management Information Tool (D&D KM-IT), https://www.dndkm.org/, Applied Research Center, Florida International University.

TASK 6: AI FOR EM PROBLEM SET (D&D): STRUCTURAL HEALTH MONITORING OF D&D FACILITY TO IDENTIFY CRACKS AND STRUCTURAL DEFECTS FOR SURVEILLANCE AND MAINTENANCE (SRNL)

Task 6: Introduction

The surveillance and maintenance (S&M) of nuclear-decommissioning infrastructure provide many challenges with respect to maintenance or decommissioning of the buildings. As these facilities await decommissioning, there is a need to understand the structural health of these facilities. Many of these facilities were built over 50 years ago and, in some cases, these facilities have gone beyond operational life expectancy. In other cases, the facilities have been placed in a state of "cold and dark" and they are sitting unused, awaiting decommissioning.

In any of these scenarios, the structural integrity of these facilities may be compromised, so it is imperative that adequate inspections and data collection/analysis be performed on a continuous and ongoing basis. There is a need for a framework to analyze the huge amount of data generated by the sensors on the nuclear reactor components as well as structures, to monitor the conditions of these buildings over a period of time.

Task 6: Objectives

This task is focused on investigating specific applications of artificial intelligence and big data technologies to solve DOE-EM problem sets and challenge areas, including potential applications of existing state-of-the-art technologies (e.g., imaging, robotics, big data, and machine learning/deep learning) to assess the structural integrity of aging facilities in support of ongoing surveillance and maintenance (S&M) across the DOE complex.

Task 6: Methodology

The focus of this research is divided into two distinct objectives. Each objective tackles and answers a different question which is essential for addressing the S&M challenges. The main questions are:

1. Is there an anomaly in the dataset (images)?
    - Determines if there are structural anomalies (cracks, etc.).
2. What and where are the anomalies?
    - Classify and locate visually the anomalies.

A single artificial intelligence methodology is not enough to solve the entire problem set. Therefore, each objective was solved with a different state of the art AI model and uses an ensemble approach to accomplish structural health monitoring for a better S&M activity.

1. **Anomaly Detection** - Answers the question: "Is there an anomaly in the data?"
    - Implementation of Auto Encoders (AE) with Convolutional Neural Network (CNN) layers and post image processing.
2. **Object Detection** - Answers the question: "What is the anomaly and where is it?"
    - CNN algorithms such as YOLOv3 (real time object detection).

- The above-mentioned neural network algorithms were modified to classify and locate cracks (not trivial; cracks are very challenging since they come in many shapes, forms, and sizes).
- Instance Image Segmentation methodology to identify the boundaries of the object.
- Identification of cracks to fabricate accurate metrics which will be used for forecasting.

Task 6: Results and Discussion

Subtask 6.1: Design & Development of Convolutional AutoEncoder Algorithm to Identify Cracks in D&D Mockup Facility

A state-of-the-art Convolutional Auto encoder (CAE) model, as shown in Figure 57, was developed for anomaly detection to identify cracks and structural defects on walls in the D&D mockup facility located at FIU. The mockup facility structure resembles the common structural health conditions in nuclear facilities in the DOE complex. This approach provides a robust solution to anomaly detection using unsupervised learning algorithms.

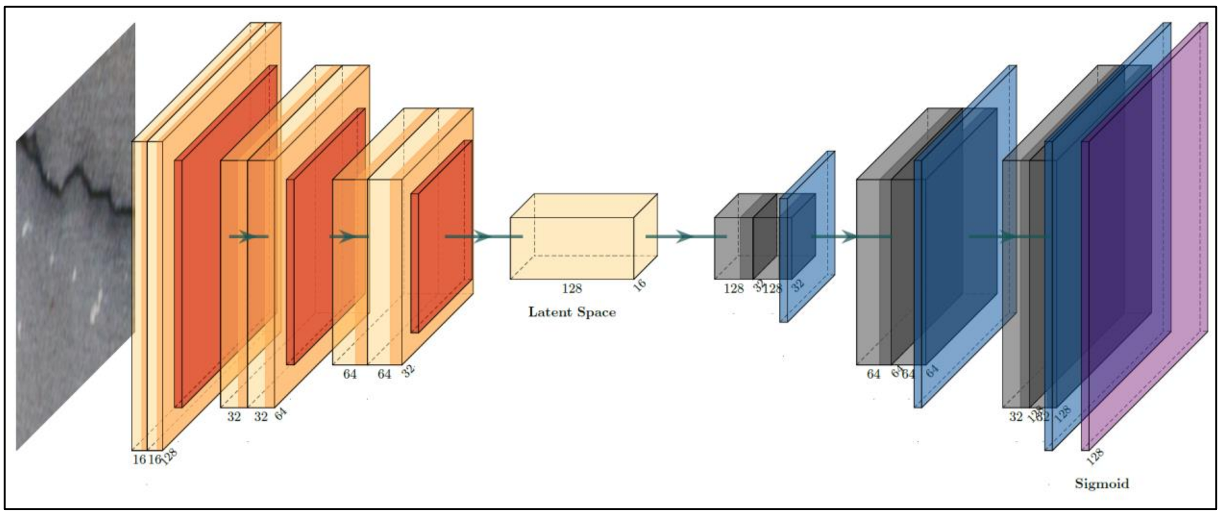

Figure 57. Convolutional Autoencoder (CAE) architecture developed by the FIU team. The model takes in an image in RGB format and tries to reconstruct it after compressing the spatial information into a 16x16x28 vector.

Post image processing methodology was used to generate a visual heat map of the anomalous areas in the imagery dataset as shown in Figure 58. Static and dynamic pixel thresholding was researched and implemented for improvements in overall detection accuracy.

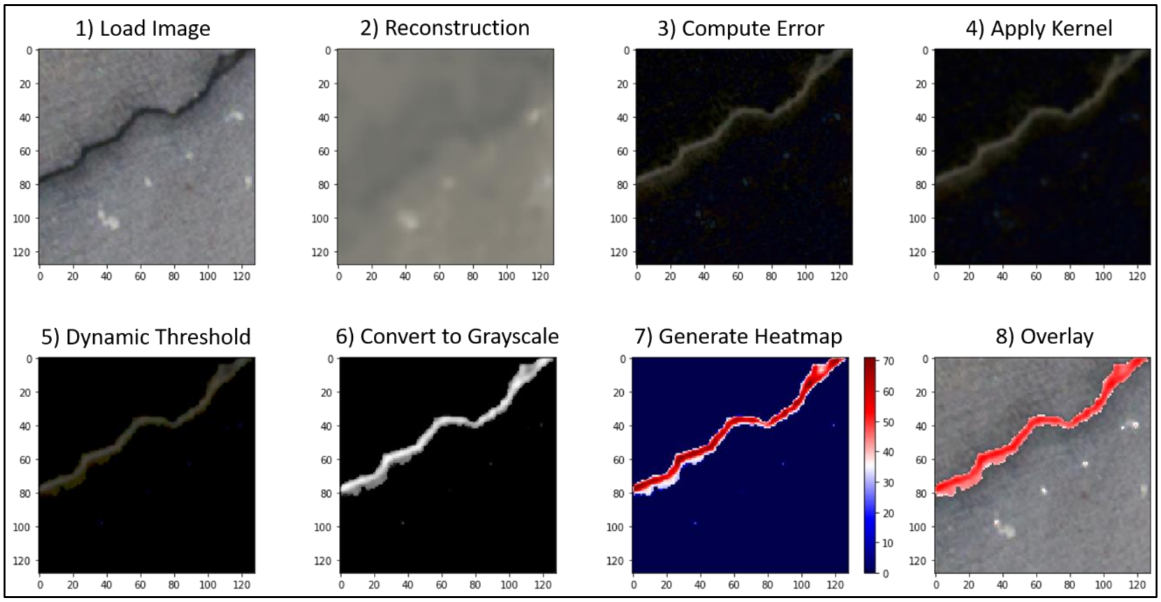

Figure 58. Image pipeline from start to finish for a single testing data sample that contains a crack.

The goal for this architecture was to detect anomalous conditions in an image and provide a visual heatmap of the identified areas having structural defects. An example of the visualization output is shown in Figure 59.

Figure 59. Fully analyzed image with anomaly detection heatmap overlaid for visual analysis.

Subtask 6.2: Use LiDAR Technology to Scan the Walls of the Hot Cell Testbed to Establish a Baseline Model using AI/Deep Learning Technologies

Purpose:

Collect LiDAR data for the purpose of training deep neural networks in classification and object detection tasks.

Data Collection:

LiDAR is a remote sensing technology which uses the pulse from a laser to collect data which can then be used to create 3D models and maps of objects and structures. This scanner was developed for the purpose of mapping structures and can generate detailed point clouds. The high level of detail captured in the point cloud, shown in Figure 60, makes it an ideal candidate for the task of detecting surface cracks and other deformities. The data obtained can be used to detect deterioration in the health of the structure.

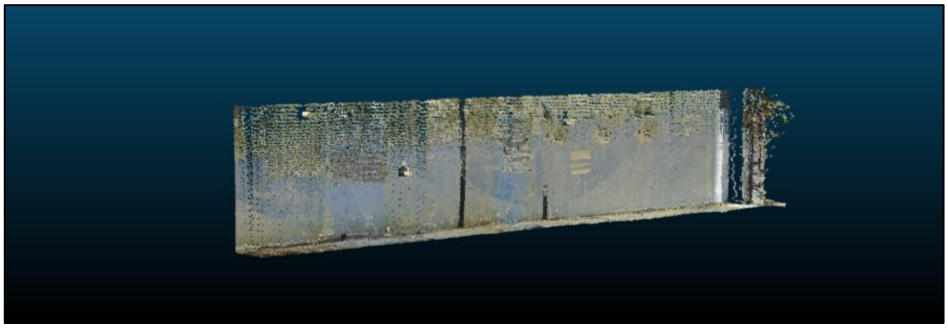

Figure 60. LiDAR point cloud data collected from the test facility at FIU.

Synthetic LiDAR data generation:

To build a baseline dataset for training neural network models in the either "classification" or "object detection" tasks the data must be as accurate as possible. At the moment, LiDAR data collected with current sensors are susceptible to noise and variability which can potentially degrade the performance of models. For this reason, the FIU team decided to simplify the problem and generate near perfect LiDAR data for wall scans. The approach is completely computer based and can be implemented with the current technology available.

The process starts by creating a generic wall, 10' x 8' x 4.5" (width x height x thickness), in a 3D modeling software as shown in Figure 61. Currently the free version of Google SketchUp Online [1] is being used for rapid prototyping of the walls. The wall is created by using the Rectangle tool to create the base 10' x 4.5" of the wall. Afterwards, the Push/Pull tool is used to pull the base to a height of 8'.

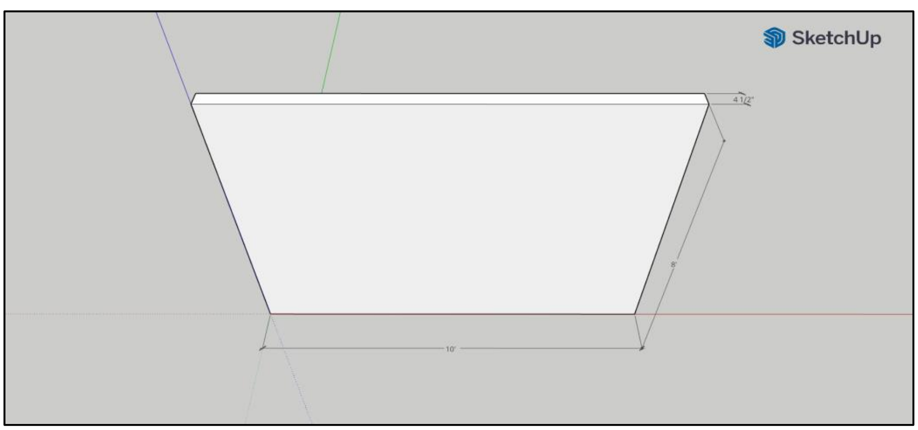

Figure 61. Generic 3D wall model created in the free version of Google SketchUp Online.

Since the file will be processed and converted to a point cloud data the back-side surface of the wall is removed so that no data is generated from it. To do this, the camera is rotated to the backside of the wall and the surface is selected. Afterwards, the delete key on the keyboard removes the selected surface from the wall. The 3D model with the back side of the wall removed is shown in Figure 62.

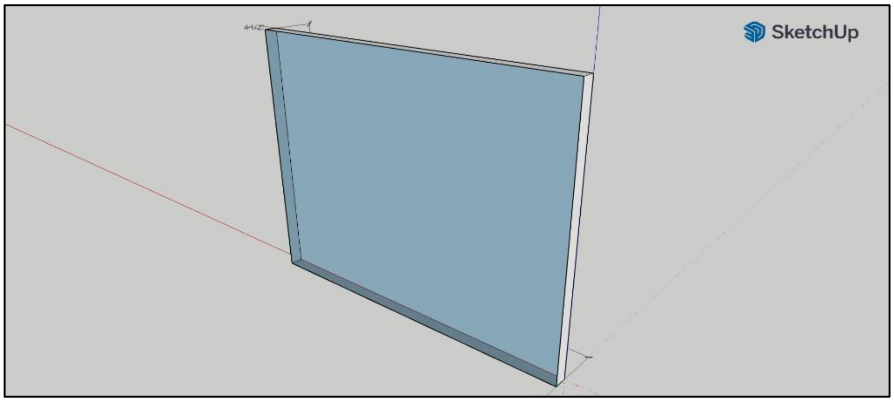

Figure 62. Backside surface of the wall removed.

Now that the wall has been created, it is exported as a stereolithographic file (.STL). This file type is processed in python to convert from the 3D object to the point cloud data. Using a python library called Numpy-STL [2] the exported file from SketchUp is import and visualized as shown in Figure 63**Error! Reference source not found.**. This step is performed to make sure that the file was saved correctly and that it is ready for processing.

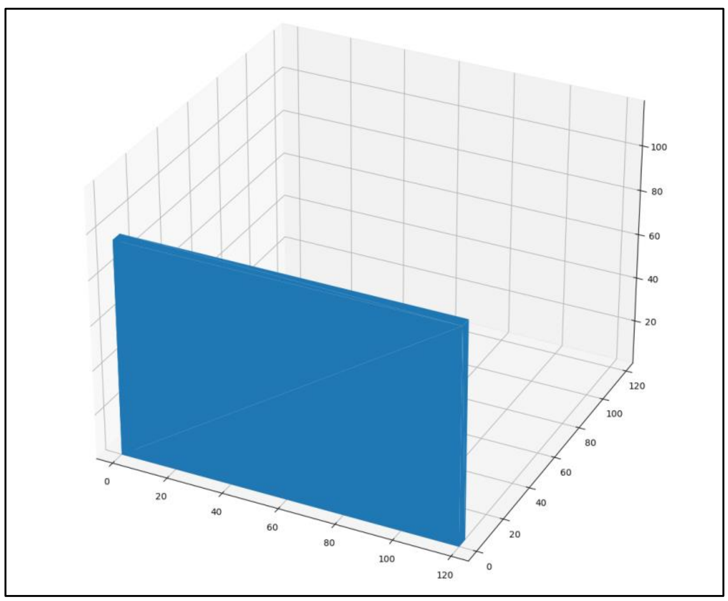

Figure 63. Numpy-STL library displaying the imported .STL file created in Google SketchUp Online.

If the 3D model would have a closed surface, we could then compute the volume using the get_mass_properties() function available in the imported object. Calculating volumetric information will be essential in future work for this project. A sample "cube" .STL file with dimensions 12" x 12" x 12" was used to verify that the function works correctly. The calculated volume for the "cube" was 1,728 in^3.

A python library Open3D [3] was used for STL to Point Cloud conversion. The first step after loading the file is to call the function PointCloud() which will build the point cloud data from the STL. Next, the point cloud points, colors, and normal vectors must be instantiated. We can now visualize the newly created point cloud. At this point, there will be only one point per vertex in the STL file and thus only 8 points will be present in the point cloud as shown in Figure 64.

Figure 64. Initial point cloud data generated by Open3D.

The point cloud at this stage does not represent what we expect from a LiDAR scan and further processing is required. We increased the number of points on the surfaces. To achieve this, we used the function sample_points_uniformly() from the imported mesh and specified the total amount of points desired. Increasing the number of points from 8 to 25,000 generates a point cloud as shown in Figure 65 that begins to resemble a typical LiDAR scan.

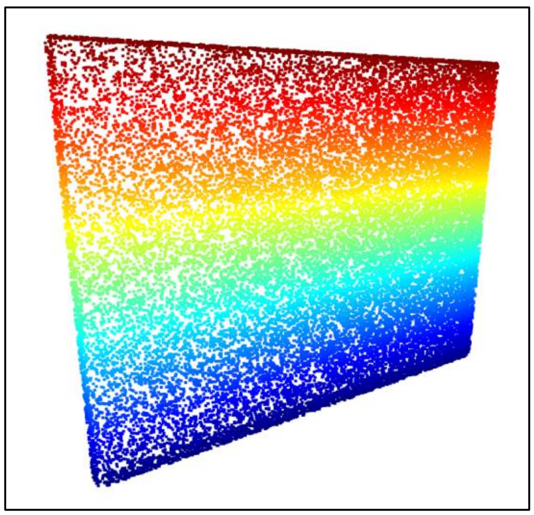

Figure 65. Point cloud generated by increasing the number of points from 8 to 25,000.

The color scheme is supposed to represent the distance from the main axis in the normal plane. In Figure 65 the axes are misaligned. The wall base was created along the XY plane and that is where the depth color mapping begins. To correct this issue, we can either rotate the wall such that the main surface of the wall (12’ x 8’) is on the XY plane or readapt the color depth mapping scheme. For simplicity, rotating the main surface of the wall to the XY plane and then generating the point cloud is shown in Figure 66.

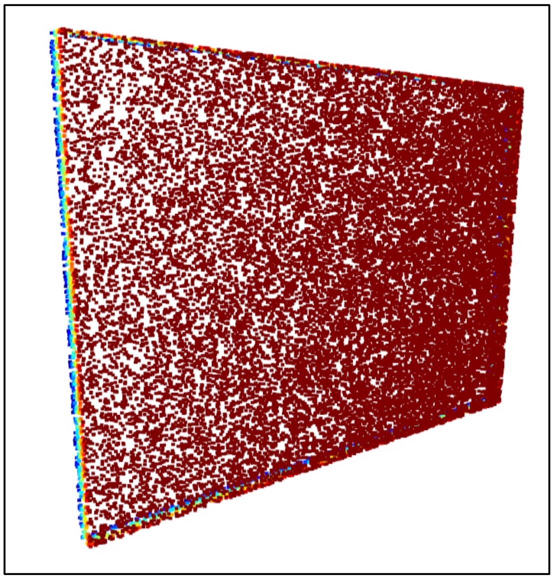

Figure 66. Point cloud generated of orienting the main wall surface to the XY plane.

Artificial Crack Generation:

Generating cracks artificially is not a trivial task. Preliminary literature review for realistic crack generation using physics informed modeling did not show any promising techniques. A more in-depth review was required to determine a good approach of generation synthetic cracks and its conversion to 3D object files.

A rudimentary crack was created using Google Sketchup. The crack is a simple deformation in the 3D test wall that was successfully imported into the Jupyter notebooks for processing. The deformation was generated by creating a closed loop polygon of a trivial shape and then using the push/pull tool pushed into the wall. This created a concave depression in the shape of the polygon into the wall. The main goal for testing this idea was to verify that the deformation would be converted to point cloud data once processed using the Open3D as shown in Figure 67.

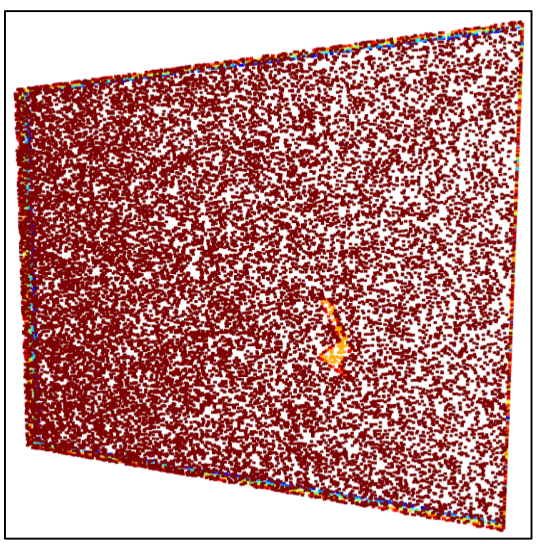

Figure 67. Point cloud generated showing synthetic crack in lower right quadrant (red and yellow points).

Additionally, the first iteration of converting 3D files into point clouds generated valid data but the points are scattered in a random Gaussian process. After reviewing some sample Lidar scans, specifically from the KITTI dataset [4], of walls and objects, it was noticed that the point cloud forms concentric scan lines because of how the scans are performed [5] and shown in Figure 68.

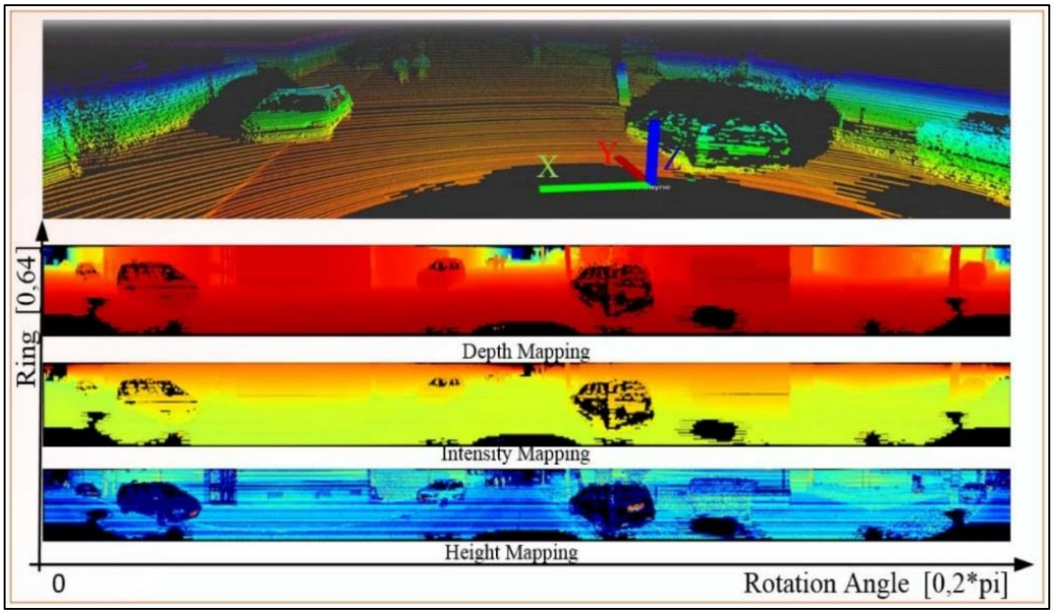

Figure 68. Image from [4] showing the point cloud data from a Lidar scan. Notice on the first row how the point cloud data forms concentric circles.

The Open3D offers two parameters that can be tuned to generate the point clouds. The first parameter is the number of points and that can be used to control the density of the information. The second parameter is the voxelation size which allows for the grouping of the points. A small grid search of these parameters was done to see if they can generate the point clouds, Figure 69, closer to actual Lidar scans.

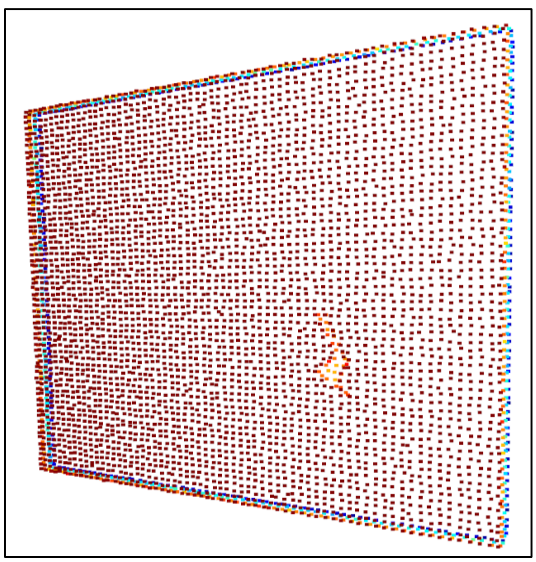

Figure 69. 3D point cloud generated with a voxelation size of 1.5 resembling closer to Lidar scans.

Results:

By testing different combinations of the two parameters the generated point clouds have gotten closer to actual Lidar scanning results. The new conversions show that the grouping and alignment of the points in the cloud are more symmetrical and uniform. The results are not perfect, in fact they are far from ideal, but the tuning of the parameters is heading in the right direction.

Subtask 6.3: Object Detection (2D Space) (NEW)

Deep learning algorithms for object detection in 2-dimensional space were applied for detecting and locating cracks in an image from a compromised nuclear facility structure.

VGG16 – Classification Model:
The FIU team is working on the crack detection mechanism based on a deep fully convolutional network (FCN), which includes the semantic segmentation on the cracks of the concrete images. In this study, we used VGG16 (pre-trained network), which will work as the backbone of the FCN's encoder. This model is trained and evaluated for image classification on the public concrete dataset [6] of 40,000 samples and a resolution of 227 × 227 pixel per images (Figure 70). The work consists of crack image classification using VGG16 networks and end-to-end training of the fully convolutional network.

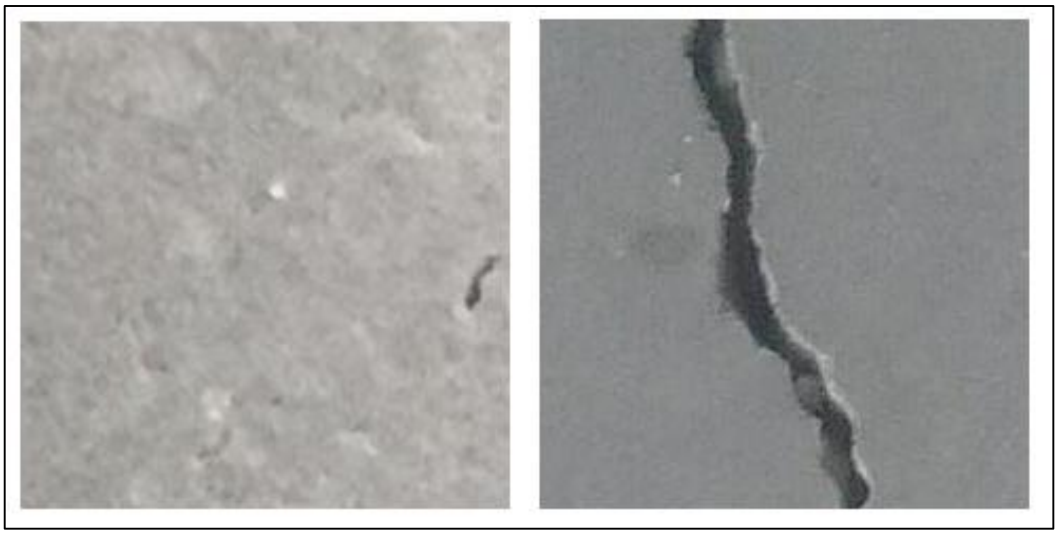

Figure 70. Image data samples. Left image is considered "non-crack" and right image is considered "crack".

The FIU team implemented the research by using the pre-trained model VGG16 and training on the concrete dataset (summary of model is given in **Error! Reference source not found.**). The classifiers are trained for 50 epochs with a batch size of 16. The dataset is first divided into two classes of crack and non-crack data with 20,000 images in each class. After that, in each class the dataset is divided into training, testing and validation. The model is trained with 16,000 images and 2,000 images are used for testing and validation in each class.

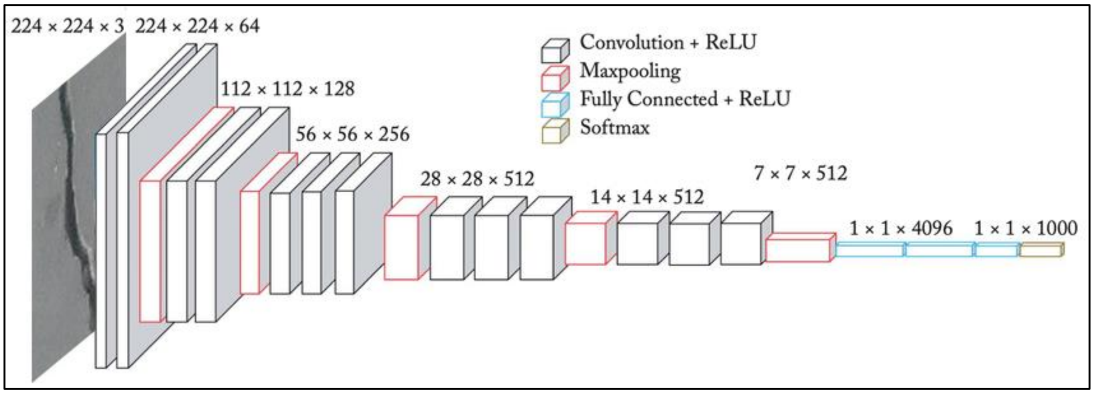

Figure 71. VGG16 model architecture summary.

YOLOv3 – Object Detection Model:

The YOLOv3 architecture [9], shown in Figure 72, was selected as the starting point for objection detection in this task. The speed and performance plus the team's experience with YOLOv3 made it a suitable choice as the primary architecture to research.

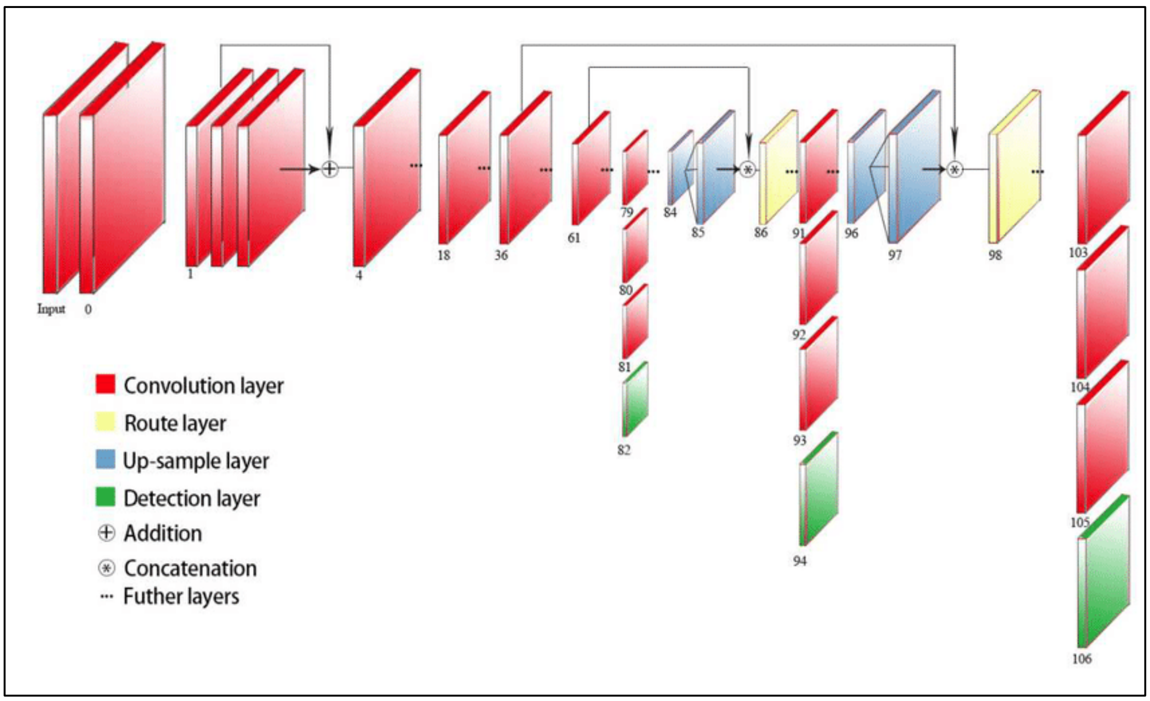

Figure 72. YOLOv3 model architecture summary.

To begin object detection in 2D space (images), a properly labeled dataset is required for the YOLOv3 [7] architecture. Currently, 20 images containing walls and cracks were collected from the open-source website Flickr [8]. The images were annotated in the YOLOv3 format using a tool called LabelIMG. The tool simplifies the labeling process by allowing the user to use a marquee selection tool to bind the object of interest for classification as shown in Figure 73. The file is saved in the Extensible Markup Language (XML) format which contains the image width, image height, object class, centroid, relative width, and relative height for all objects.

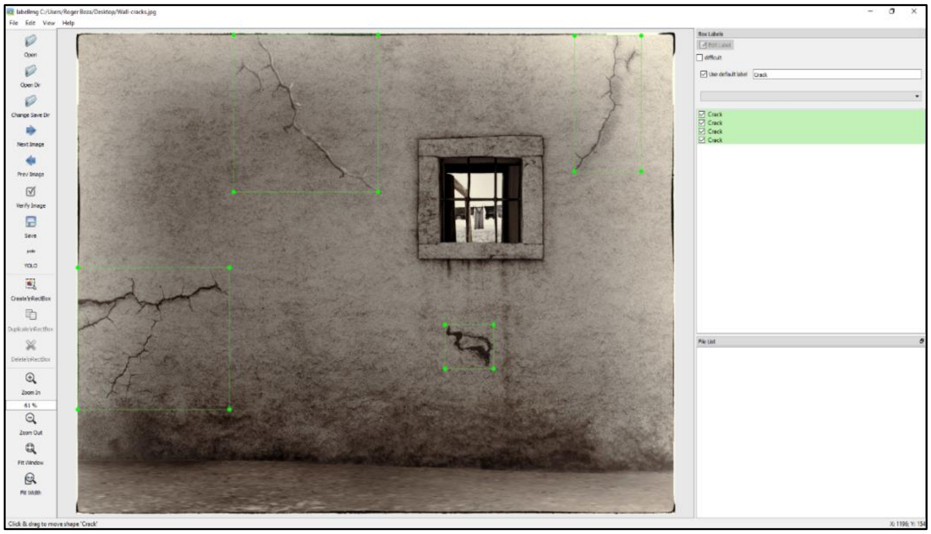

Figure 73. LabelImg graphical user interface showing the bounding regions for the "Crack" objects.

Data Collection and Augmentation:

A total of 51 images were collected from the open-source Flickr and annotated using LabelIMG. The image dataset contained cracks in wall sections and sides of buildings. There was some variance in the lighting and exposure of the images, as well as the type of landscape and environment. All 51 images, collage example shown in Figure 74, were used to train the YOLOv3 network.

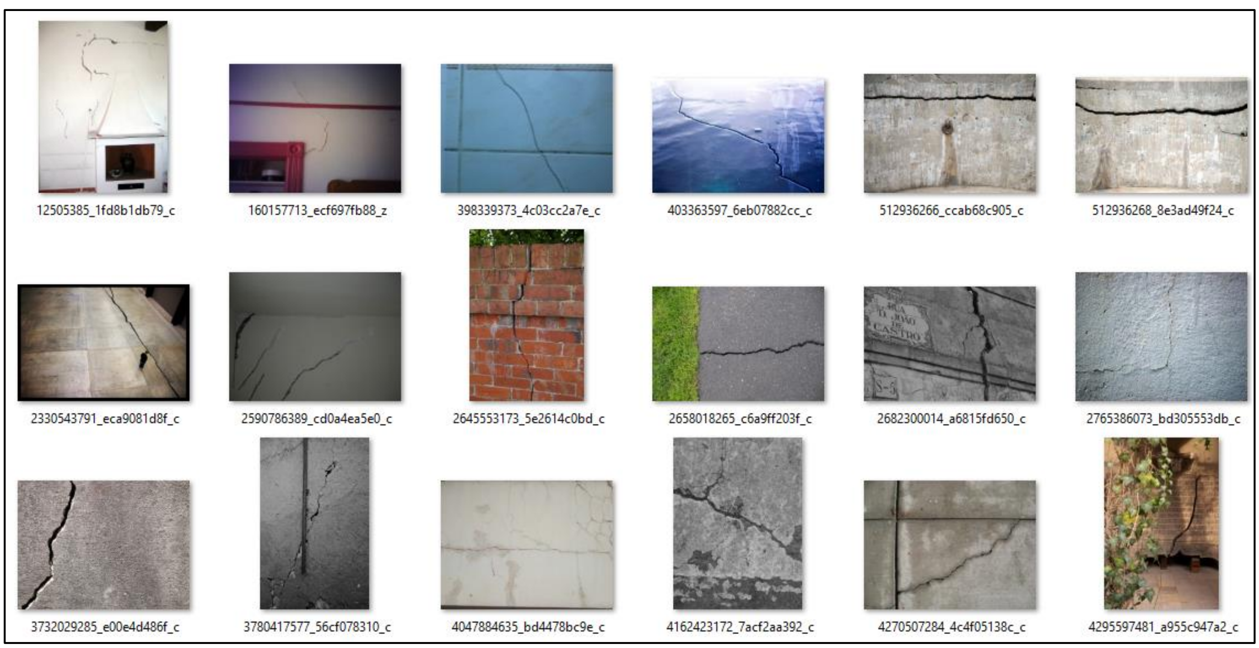

Figure 74. Image collage of samples in the training dataset collected from Flickr.

An additional 12 images, shown in Figure 75, were collected at random using Google search for the testing set. In the testing set, 2 images were chosen as adversarial cases. The first adversarial case was an image of a crack in a bridge and the second case was a crack on a staircase. These two images were adversarial cases for the model because they come from outside the training distribution since the network did not train with bridges or staircases.

Figure 75. Image collage of the testing dataset collected from Google search engine.

The current labeled dataset of 51 unique images was augmented using affine transformations with the help of an open-source python library named imgaug [10]. Imgaug makes the augmentation process simple and straightforward, especially when dealing with the annotation requirements for networks like the YoloV3 architecture. The annotations for YoloV3 require the centroid, relative width, relative height, and the object class to be specified per object. The common way to update the values is to re-annotate the augmented images and then proceed to model training. Using imgaug, we can apply random sequences of affine transformation and have the annotation values updated automatically.

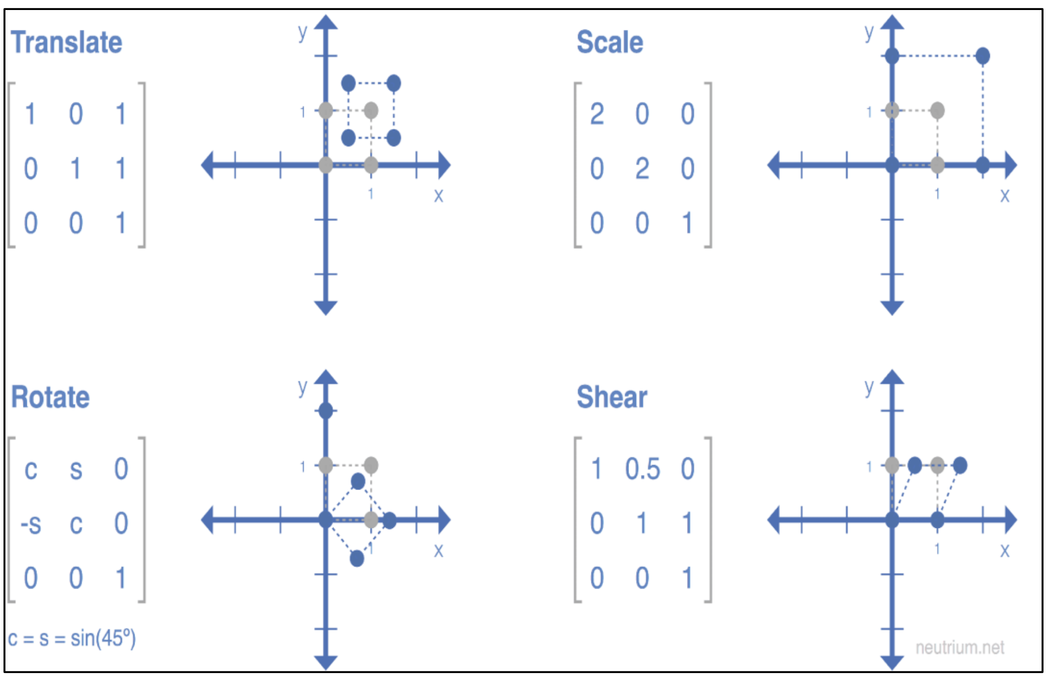

Figure 76. Matrix representation of affine transformations and their respective effect. Source: https://neutrium.net/mathematics/basics-of-affine-transformation/

The augmented dataset contained a total of 255 images. The composition of the set included the original 51 images and one image per affine transformation as shown in Figure 77. To create a larger data distribution, the dataset was augmented even further by having multiple types of affine transformations per image. The new dataset is composed of the 51 original images and 3 affine transformations per type as shown in Figure 78. Each transformation was done at random and within limits.

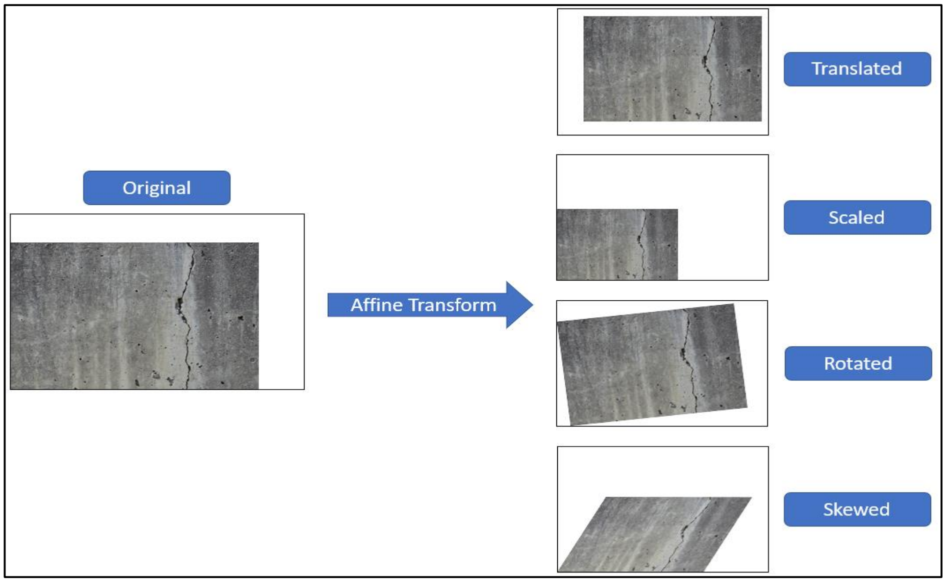

Figure 77. Affine image transformations applied to a sample training image.

For the translation, the range was set to 0-10% of the image width and height. For the scaling, the range was set to 0-50% of the original size. For the rotations, the range was set to 0-10 degrees. Lastly, the skewness had a range of 0-5. All values are also shown in Table 13.

.

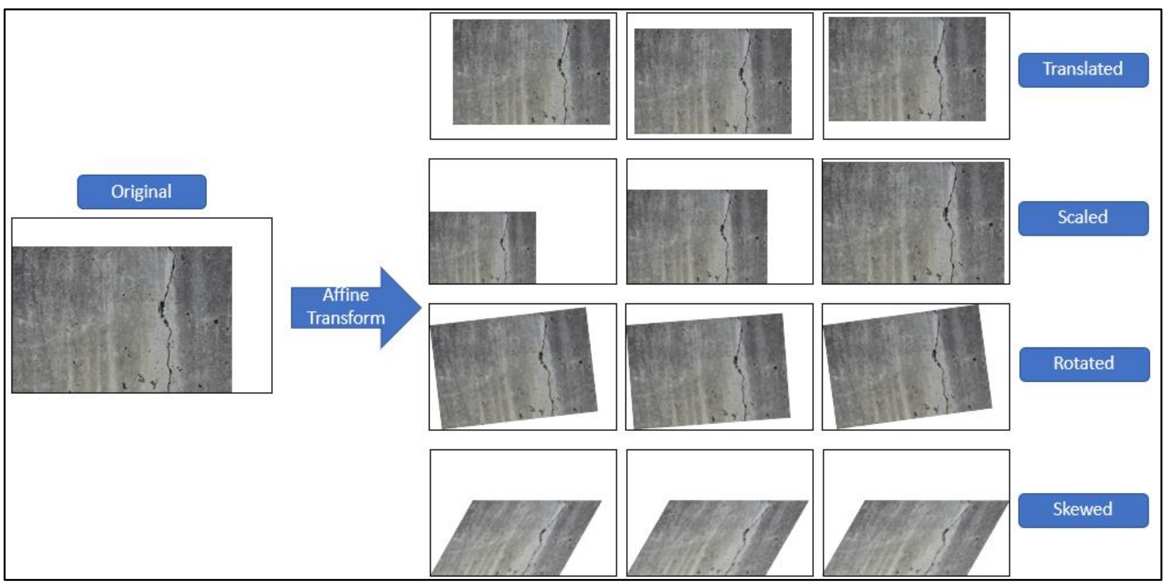

Figure 78: Multiple image transformations per affine type.

Table 13. Range Values for Affine Transformations

Affine transformation	Range
Translate	0 to 10 %
Scale	0 to 50 %
Rotation	0 to 10 degrees
Skew	0 to 5

The dataset was augmented, as mentioned, so that the training phase could expose the model to typical scenarios in the image capture process.

Model Training – YOLOv3:
All models were trained with knowledge transfer from the pre-trained Darknet weights. The models were trained in two phases. The first phase freezes the main body and only updates the weights added for the new object detection (coarse tuning). The second phases unfreezes the entire network and backpropagation can update all the weights in the model (fine tuning). This approach allowed the model to converge, shown in Figure 79, and showed promising results with a relatively small dataset.

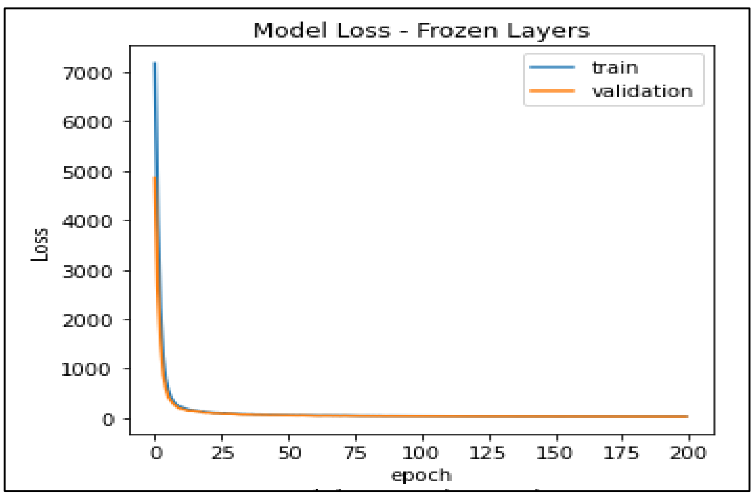

Figure 79. Line plot for the model loss in the frozen phase of training.

Multiple iterations of trainings are performed using YOLOv3 architecture to generate various models. Some models performed better than others in terms of false positives and false negatives. Hyperparameter tuning was done for the batch size, epoch count, confidence score, and intersection over union value. The combination of parameters is shown in Table 14.

Table 14. Hyperparameter Tuning Configuration Values

Parameter	Values
Batch size (frozen)	4, 8
Epoch count (frozen)	25, 50
Batch size (unfrozen)	4
Epoch count (unfrozen)	15
Confidence score	0.01, 0.1, 0.2
Intersection over union	0.01, 0.1, 0.2

Results:

The VGG16 classifier model performed well. It has been observed that during training the VGG16 classifiers achieved almost 0.999 accuracy. This is an indication that CNN's can extract meaningful features that allow the model to predict accurately.

The YOLOv3 models for object detection that were trained with the new augmented dataset outperformed all previous models. We noticed that the bounding boxes for the predictions were tighter around the identified concrete cracks, as shown in Figure 80. The main reason for the improvement was the variance introduced by the augmentation step in the training set.

Figure 80. Left: Crack detection performed with old model with loose bounding regions. Right: Crack prediction with the newest model and tighter bounding regions.

Subtask 6.4: Object Detection (3D Space) (NEW)

Deep learning algorithms for object detection in 3-dimensional space will be used for the task of locating cracks and determining if they have changed in size compared to a baseline. A deterioration score is calculated based on the difference between baseline information and current LiDAR scans using CNN models.

The dataset developed in Subtask 6.2 using the Lidar technology is used for this subtask. For this iteration, a single file was used to train the convolutional autoencoder as a proof of concept. The point cloud as shown in Figure 81 contains a wall structure with a door frame, interior door, and door handle. This point cloud was selected because it contains intricate geometries and does not exhibit any cracks. It fits the criteria for the baseline distribution.

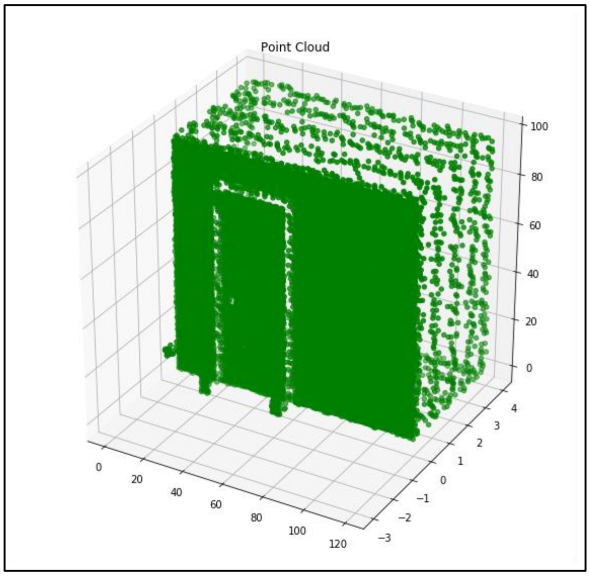

Figure 81. Synthetic point cloud visualization of a wall with a door.

To normalize the dataset, we need to accomplish two things. The first step is to translate the point cloud to the origin (0,0,0) about the point in the lowest left-hand corner. The second step is to scale the point cloud to a volumetric size that is suitable for input to the neural network. The team has decided that for the moment a cube that is 64 x 64 x 64 is sufficient for testing. The volumetric size is a tunable parameter and can be adjusted to increase the resolution of the data once transformed. The transformation yields a new point cloud as shown in Figure 82.

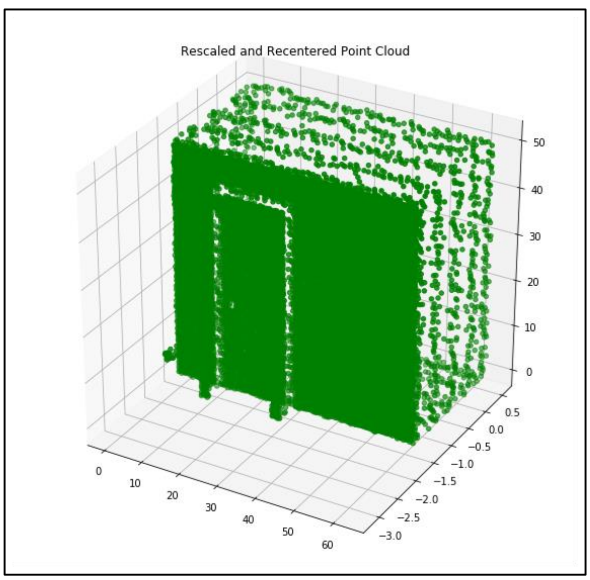

Figure 82. Point cloud that was translated and scaled to fit in the volumetric size of 64x64x64.

Once the point cloud has been transformed it has to be processed and discretized. The main issue with this is that the input to the neural network is a discrete value and we can have at most 64^3 inputs. The volumetric size puts a hard constrain on the number of points in the cloud. To overcome that effect, the transformed point cloud is converted into a new point cloud with a lattice grid implementation. Each point is moved to the closest lattice point during this process. The result can be seen in Figure 83.

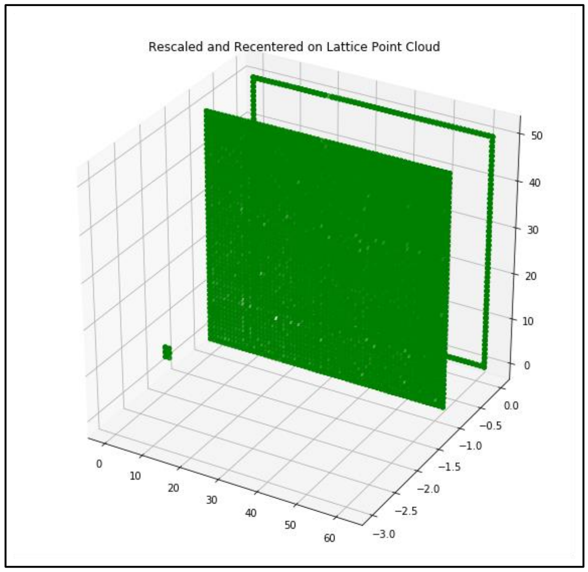

Figure 83. Point cloud that has been processed and converted to its lattice grid equivalent.

During the lattice grid process some points are going to be superimposed on top of each other. This creates redundancy and they can be removed safely. The lattice grid equivalent of the point cloud is guaranteed to be within the bounds of the volumetric size and will have only discrete, integer values, that will not exceed a count of 64^3.

Experimental Network:

The FIU team created an experimental convolutional neural network to work as an autoencoder that can accept the point cloud data generated from Lidar scans or the synthetic version being researched in Subtask 6.2. The idea is to normalize the point cloud using a boxelation technique to have a fixed input for the neural network. The network is trained as an autoencoder which must reconstruct the given input. Ideally, the convolutional autoencoder will reconstruct the point cloud as close as possible to the original sample.

In general, the network would be trained with point clouds of "normal" cases such as walls with objects but no cracks. Once that network converges and can recreate the data from the distribution in the training phase, we could feed it a point cloud that contains the crack defects. At this point, the network should try to do its best and reconstruct the crack, but it will not be able to do it very well. Comparing the unsuccessful reconstruction with the original sample data should yield significant error and thus the possibility of a heatmap implementation.

Model Training:

A neural network working as an autoencoder was created with 6 convolutional layers to learn the data distribution in the dataset. As shown in Figure 84, the network has over 67 million trainable parameters with a relative shallow configuration. Like any other neural network, the input layer to this one has a fixed size and thus the dimensionality of the data must match exactly. Since we are dealing with point clouds (LiDAR information), the data exhibits the 3 dimensions of space (x, y, z). The unbounded dimensionality of the data must first be normalized before being fed into the neural network.

```
Layer (type)                 Output Shape              Param #
=================================================================
input_5 (InputLayer)         (None, 262144)            0
_________________________________________________________________
dense_25 (Dense)             (None, 128)               33554560
_________________________________________________________________
dense_26 (Dense)             (None, 64)                8256
_________________________________________________________________
dense_27 (Dense)             (None, 32)                2080
_________________________________________________________________
dense_28 (Dense)             (None, 64)                2112
_________________________________________________________________
dense_29 (Dense)             (None, 128)               8320
_________________________________________________________________
dense_30 (Dense)             (None, 262144)            33816576
=================================================================
Total params: 67,391,904
Trainable params: 67,391,904
Non-trainable params: 0
_________________________________________________________________
```

Figure 84. Convolutional autoencoder architecture with 6 layers for point cloud data.

The neural network implemented as a convolutional autoencoder with the sample training case was able to learn the sample data and converged after 11 epochs (Figure 85).

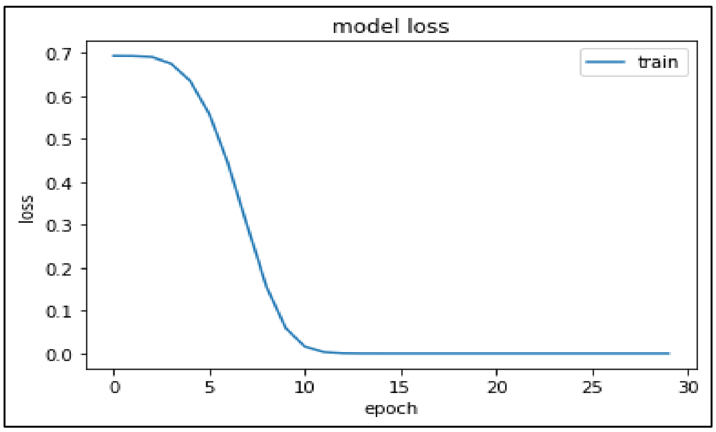

Figure 85. Model loss plot for the convolutional autoencoder. It shows that the model learns after about 11 epochs.

Results:

The experimental network can reconstruct the input data as shown in Figure 86. The reconstruction of the data is not perfect and further tuning needs to be done. Additional research into the model architecture can lead to better predictive capabilities.

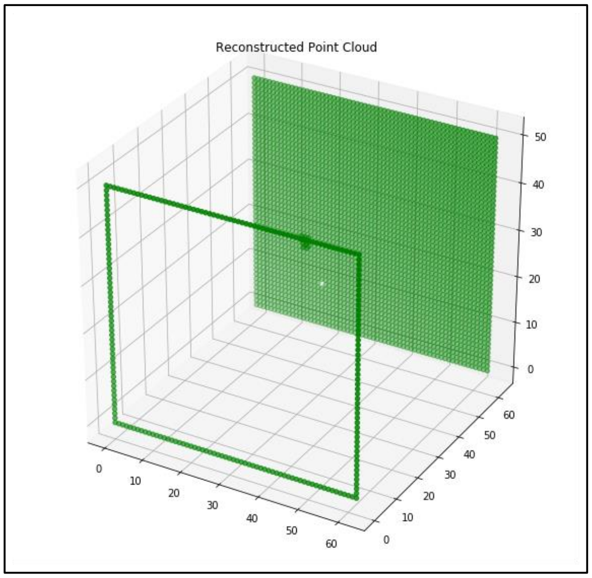

Figure 86. The reconstructed point cloud after the convolutional autoencoder's network predictions.

Task 6: Conclusions

The CNN model developed as part of Subtask 6.1 successfully detected cracks when implemented as an anomaly detector. This helped answer the question of "is there an anomaly in the data?" and provided a visual heatmap to show the sections considered anomalous. In Subtask 6.2, LiDAR data was collected for object classification and detection. We were also able to create a script that could generate point clouds similar to LiDAR scan from a 3D mesh file. This ability allows the team to create synthetic data that can be used and leveraged to train deep neural networks. To answer the question "what is the anomaly and where is it?" the team implemented the YOLOv3 neural network architecture in Subtask 6.3. In this subtask we were able to do a knowledge transfer from the publicly available pretrained weights and repurpose the model to learn where the cracks were in imagery data. The model successfully predicts where the cracks are located and bounds them with a rectangular box for visualization. As part of Subtask 6.4, the LiDAR data collected in Subtask 6.2 was analyzed. The pipeline created in this task had an adaptive data preprocessor to scale the point cloud information into a static input space. The neural network was able to accept the point cloud data and reconstruct it like Subtask 6.1. This work needs to be researched further to treat the application as an anomaly detector of the 3D spatial information.

Task 6: References

[1] Google Sketchup Online - https://www.sketchup.com/plans-and-pricing/sketchup-free

[2] Numpy-STL - https://github.com/WoLpH/numpy-stl

[3] Qian-Yi Zhou, et al. "Open3D: A Modern Library for 3D Data Processing". arXiv:1801.09847. (2018).

[4] A. Geiger, P. Lenz, C. Stiller, and R. Urtasun, "Vision meets robotics: The KITTI dataset," Int. J. Robot. Res., vol. 32, no. 11, pp. 1231–1237, Sep. 2013.

[5] X. Zhao, P. Sun, Z. Xu, H. Min and H. Yu, "Fusion of 3D LIDAR and Camera Data for Object Detection in Autonomous Vehicle Applications," in IEEE Sensors Journal, vol. 20, no. 9, pp. 4901-4913, 1 May1, 2020, doi: 10.1109/JSEN.2020.2966034.

[6] Çağlar Fırat Özgenel, “Concrete Crack Images for Classification”, Mendeley Data, v1, (2018), https://doi.org/10.17632/5y9wdsg2zt.1

[7] Joseph Redmon, et al. "YOLOv3: An Incremental Improvement." (2018).

[8] Tzutalin. LabelImg. Git code (2015). https://github.com/tzutalin/labelImg

TASK 7: AI FOR EM PROBLEM SET (SOIL AND GROUNDWATER) - EXPLORATORY DATA ANALYSIS AND MACHINE LEARNING MODEL FOR HEXAVALENT CHROMIUM [CR (VI)] CONCENTRATION IN 100-H AREA (PNNL) (NEW)

Task 7: Introduction

The Hanford Site 100 Areas contain monitoring data for groundwater wells (in situ sensing, water sampling), hexavalent chromium [Cr(VI)] pump and treat (P&T) activities (extraction and injection flow rates, weekly Cr(VI) sampling of influent water, etc.), as well as water table levels and river stage monitoring data. The analysis using artificial intelligence/machine learning (AI/ML) algorithms will help in understanding complex hydrogeological processes and interactions among the aquifers and the dynamic river stage in the Columbia River using these legacy datasets. Machine learning and deep learning models can be developed to identify patterns, address knowledge gaps and ultimately predict transport of Cr(VI) in the subsurface of the 100-H Area. The aim of this research is to develop a robust AI/ML-based platform for long-term monitoring, analysis and prediction of Cr(VI) contamination in the subsurface of the Hanford Site 100 Areas. AI/ML algorithms can leverage high-performance computing to predict the spatial and temporal distribution of Cr(VI) as well as help in identifying any spatiotemporal relationship in the dataset.

Task 7: Objectives

The overall goal of this research is to couple long-term monitoring data of hexavalent chromium (Cr(VI)) with AI/ML models to identify temporal and spatial relationships of subsurface chromium transport that reduces uncertainties in the conceptual site model (CSM).

Task 7: Methodology

FIU researched on the extended soil and groundwater dataset on the DOE Hanford Site 100 Areas to find spatiotemporal relationships between inland monitoring wells and shoreline hexavalent chromium [Cr(VI)] concentrations. The team investigated the last five years of data (2015 to 2019 inclusive) and followed the method outlined below to filter the wells based on the properties of the time series of the corresponding wells.

- Extract a subset of the 100 Areas dataset
- Filter wells with at least 1 data points in each year
- Equate the time axis of each wells time series
- Segregate wells into aquifer tube and groundwater wells
- Linear interpolate the time series (as Aquifer tubes have 1 data point / year approximately)
- smooth the time series with rolling mean window
- Exclude Aquifer tube with time-series mean Cr(VI) <10 μg/L
- Similarity analysis of remaining aquifer tubes mean time-series vs groundwater wells time series

To showcase the data filtering mechanism and similarity analysis demonstration, the subset of the dataset ranging from 2015/01/01 to 2019/12/31 was selected with Cr(VI) as the variable of consideration. The first filter criterion for wells' time series selection from the above subset of the dataset was conditioned as the presence of at least one data point per year in the range of the five years selected for processing. This filtering assumes that the selected wells would capture the year-wise dynamics of the variable under consideration.

(a) Five years pattern of datapoints avaiability

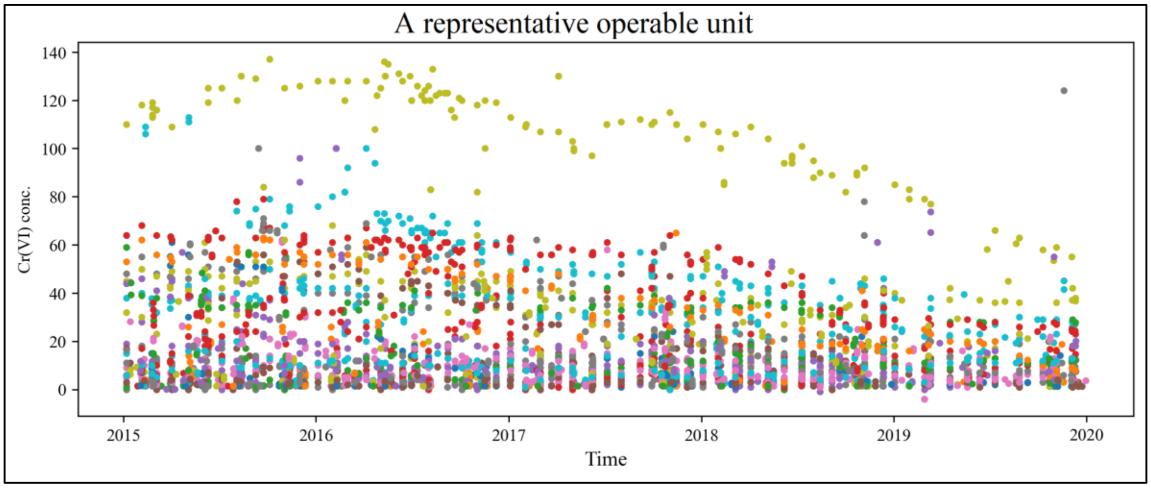

(b) Two months pattern of datapoints avaiability

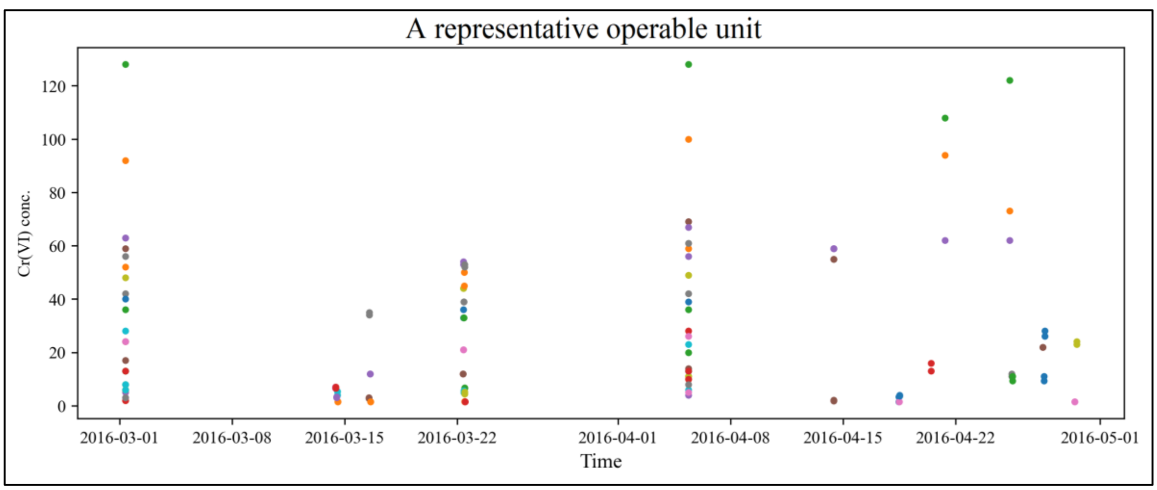

(c) Aquifer tube and Groundwater well data series segregation

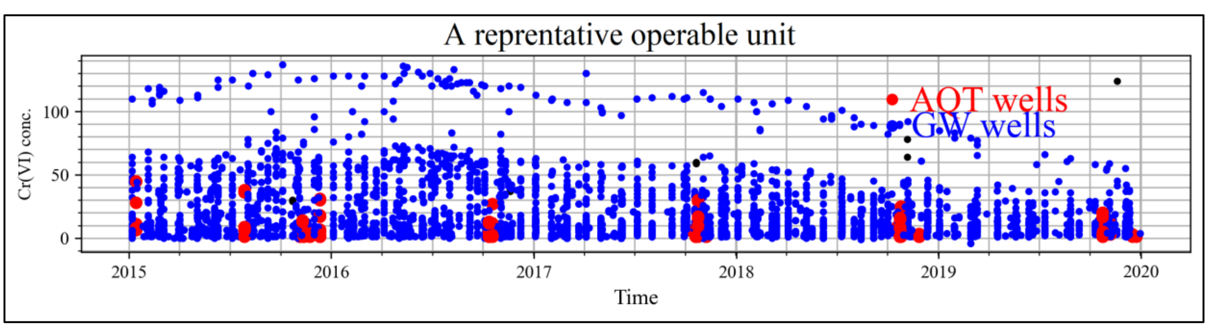

Figure 87. Raw data points' temporal pattern in the 100 Areas dataset: (a) Five years pattern, (b) Two months pattern, (c) Aquifer tube and groundwater well data series segregation.

The patterns of the data points depicted by Figure 87 (a) and (b), reveal that the data points are irregularly spaced over the time axis and the terminal data points of each time series may not fall on the same time point. Moreover, aquifer tubes' time series' have very sparse data points as they are sampled only in the fall each year which is apparent from Figure 87 (c) where it segregated the data points into these two groups. Thus, it entails equalization of the time series with the insertion of the terminal data points and interpolation to regularize over the temporal axis. For the terminal data point insertion, the closest head and tail data points were chosen to fill the terminal data point position. Linear interpolation was applied to interpolate the time series afterward. To smooth the time series, a rolling mean filter was applied, and the window was selected empirically as 90 days. This processed dataset is used to analyze the similarity measures between surface and groundwater Cr(VI) concentration.

As the surface water or aquifer tube data with Cr(VI) greater than the EPA recommended clean up level (CUL) of 10µg/L is one of the focuses of analysis, the team applied a second filter on the above-processed dataset to segregate the aquifer tubes for which the mean Cr(VI) of the time series exceeds this CUL. This filtered aquifer tube dataset was also used to measure the similarity pattern separately and compare it with the previous similarity measures.

ML modeling using aquifer tubes' mean Cr(VI) as Target variable:

To explore any probable spatiotemporal relationships between inland monitoring wells and shoreline hexavalent chromium [Cr(VI)] concentrations, FIU researched and applied machine learning (ML) algorithm on the extended soil and groundwater dataset on the Hanford site 100 Areas. In this regard, the Groundwater (GW) wells Cr(VI) concentration time series were the predictors, and the surface water or Aquifer tubes (AQT) Cr(VI) concentration time series were the target variable. As the focus of the exploration of the spatiotemporal relationship is to identify how the GW wells Cr(VI) concentration data are related to AQT Cr(VI) concentration, the ML algorithm was chosen to retrieve the predictors or features importance in the regression. These feature importance scores are then analyzed with the associated spatial data of these features (GW wells) to explore any relationship between the feature importance and GW wells' distance to the shoreline.

Feature (GW well) importance Score vs Distance to the shoreline:

In machine learning, feature importance refers to a score assigned to an input feature based on how useful that feature was in predicting the target variable. Although there are several types and sources of feature importance, such as statistical correlation scores, decision trees, and permutation importance scores, decision tree-based importance calculation was chosen for the current modeling. In this regard, Random Forest is an ensemble ML algorithm that constructs many individual decision trees in the training phase. Each decision tree is a set of internal nodes and leaves. The selected features in the internal node are used to make a decision on how to divide the dataset into two separate sets with similar responses within. This feature selection is done with some criteria, for instance, Gini impurity or information gain in classification task and mean squared error (MSE) reduction in regression task. For each feature, the average of the metric of selection criterion can be collected from the decision trees. Then the average over all the trees in the RF model would be the measure of the feature importance score for the features or GW well time series in our case.

ML modeling using Individual aquifer tube's Cr(VI) as Target variable:

In the previous ML modeling, the mean time series of all aquifer tubes in a respective operable unit was used as the target variable. As an alternate approach, each aquifer tube Cr(VI) was individually investigated in the ML modeling as target variables. Although most of the ML model resulted in a similar result of decreasing trend in feature vs distance to shore relation. There were some interesting observations surfaced from this data-driven approach. The major change in the case of an individual aquifer tube's Cr(VI) as the target variable from the previous modeling is that the distances were measured from individual respective aquifer tubes rather than the shoreline as depicted in Figure 88.

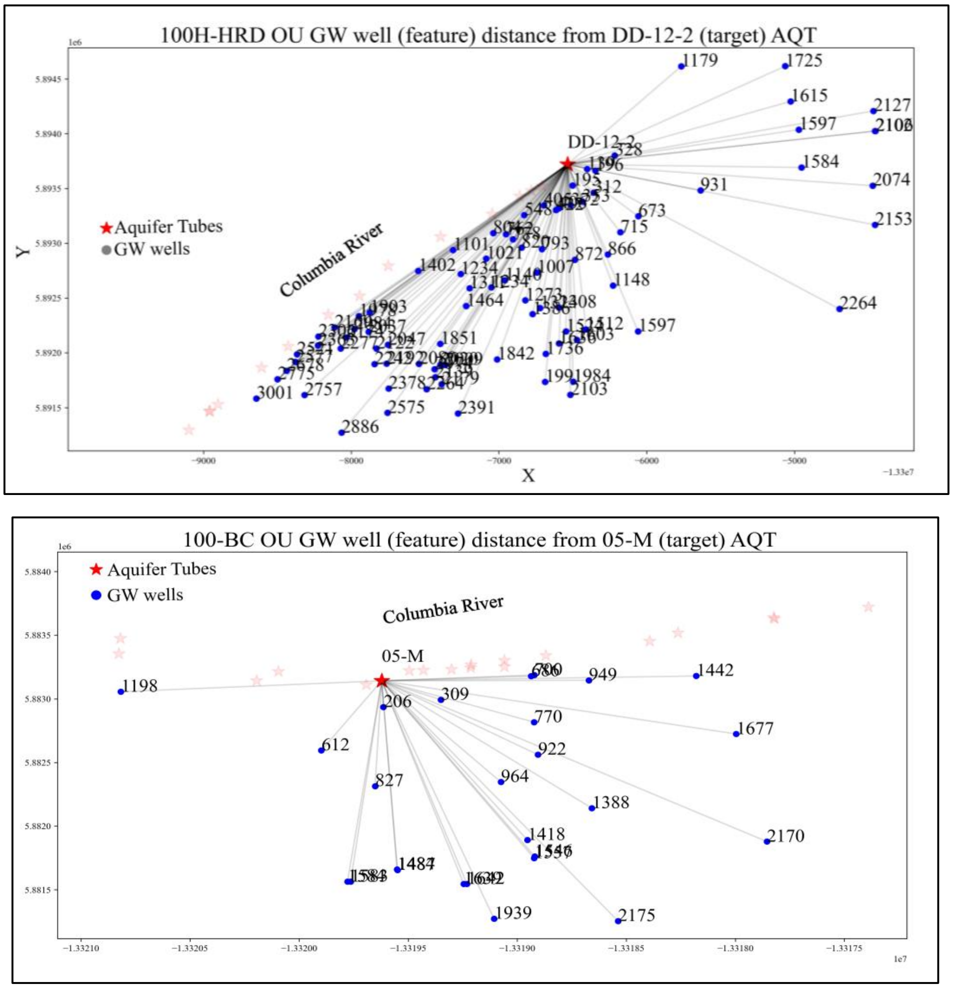

Figure 88. A representative depiction of distance calculation.

All the filtered aquifer tubes in 100-BC and 100-HRD have been individually used in the ML modeling; however, the major observations will be discussed with respect to a few aquifers' tubes.

Task 7: Results and Discussion

Subtask 7.1: Identification of Data Sources and Datasets from the Soil and Ground Water Repositories

The FIU team researched on the available repositories for soil and ground water datasets. Among the probable target data sources, the team has explored the data source PHOENIX from PNNL. The operable units (OU) consideration was extended from the initial 100-H Area to all OUs of 100 Areas of the DOE Hanford Site. Thus, 100-BC, 100-FR, 100-KR, and 100-NR OUs were included along with the initial OUs 100-HRD and 100-HRH in the dataset's consolidation. These extended datasets were gathered from the PHOENIX data-server, Figure 89.

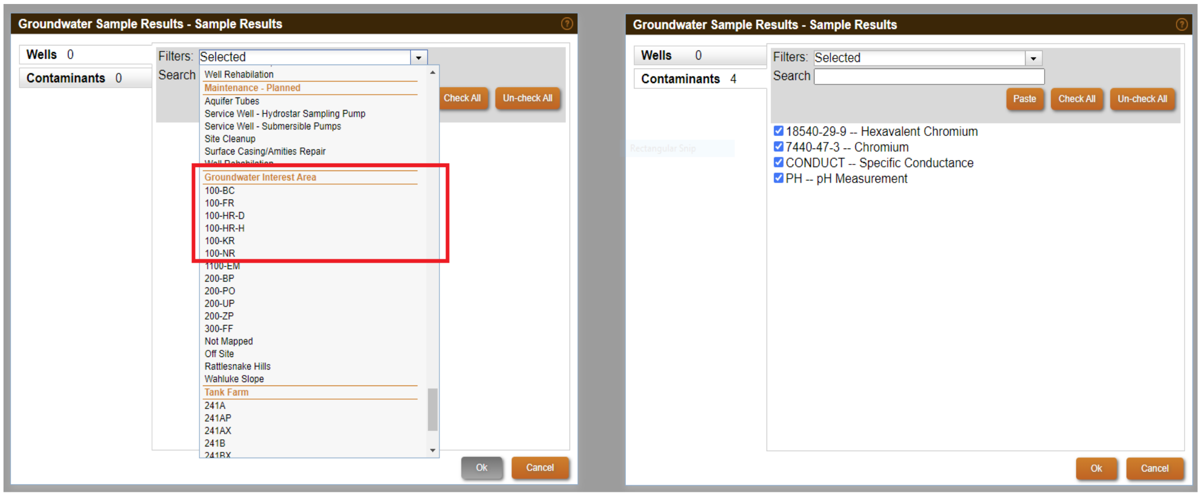

Figure 89. Extended dataset gathering from PHOENIX data-server.

The extended dataset of the entire 100 Area of the Hanford Site contains 2,323 wells as depicted by Figure 90. According to the attributes of the wells, there are 13 different types of the wells in the dataset, Table 15. However, for this AI task, ‘GROUNDWATER WELL’ (GW) and ‘AQUIFER TUBE’ (AQT) are of interest as the goal is to identify any spatiotemporal relationship between groundwater and surface water for Cr(VI) dynamics.

Table 15. Wells Attributes Of 100 Areas

Well Type	**Aquifer Tube**	Boring	Cancelled Site	Grounding Well	**Groundwater Well**	Hosted Piezometer	Independent Piezometer	Invalid	Piezometer Host	Proposed Site	Soil Tube	Unclassified	Vadose Well	**Total**
Number Of Wells	**508**	275	64	2	**961**	62	20	1	15	10	40	166	199	2323

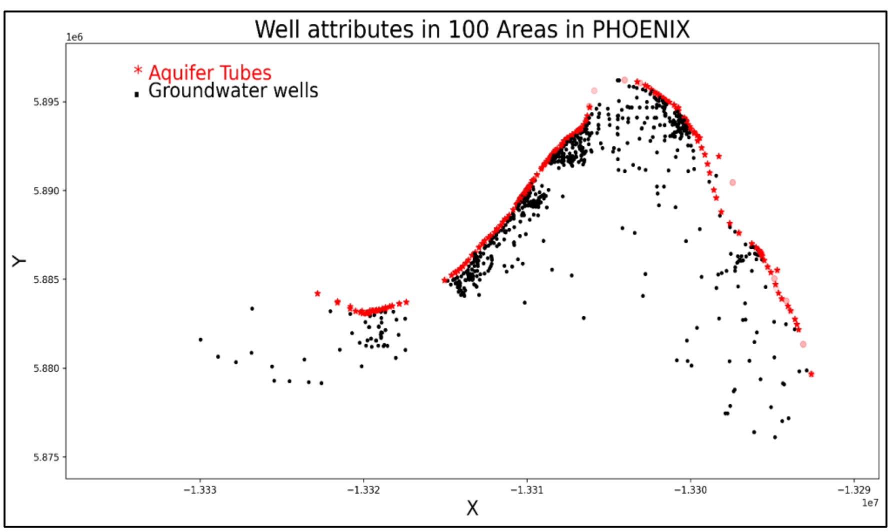

Figure 90. Well locations distribution in 100 Areas operable units in the Hanford site.

The GW wells and AQT distribution reveal that the number each type of wells vary OU to OU. The segregated 'GROUNDWATER WELL' and 'AQUIFER TUBE' for these 6 OUs are as depicted in Figure 91 and the varying numbers of wells per OUs are presented in Table 16.

Table 16. Operable Unit Wise Wells

Operable unit name	100-BC	100-FR	100-HR-D	100-HR-H	100-KR	100-NR
wells [(aqui. tube, gw wells)/total]	(75,59)/250	(84,83)/334	(97,252)/509	(101,164)/348	(58,142)/333	(93,261)/549

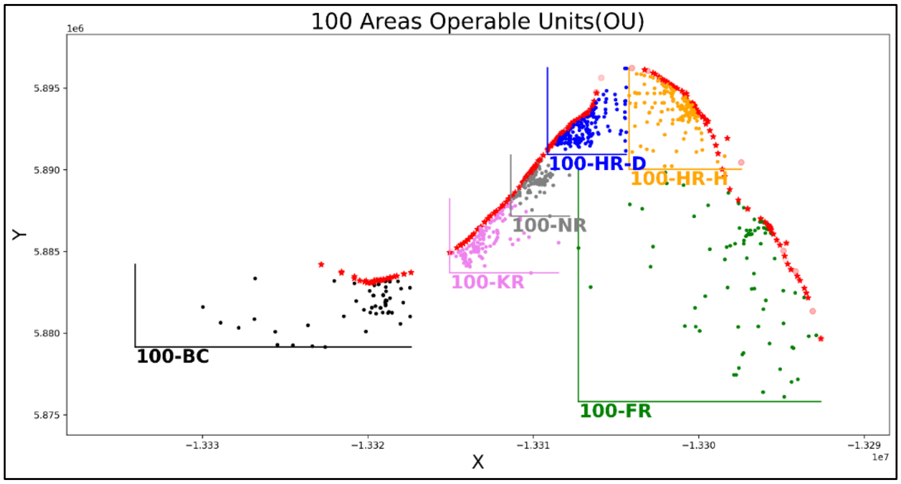

Figure 91. Different operable units and wells in 100 Areas.

In total there are 2,323 wells in the Hanford 100 Areas, and most of the wells do not contain various analytes/variable data required for modeling. Table 17 presents the data availability of various OUs. Cr (VI) concentration data availability for the OUs in 100 Areas are also depicted in Figure 92.

Table 17. C(VI) Data Availability of Various Operable Units in 100 Areas.

Analyte/Variable	100-BC	100-FR	100-HR-D	100-HR-H	100-KR	100-NR	Total wells/2323
Cr(VI)	122/250	106/334	329/509	229/348	192/333	86/549	1064

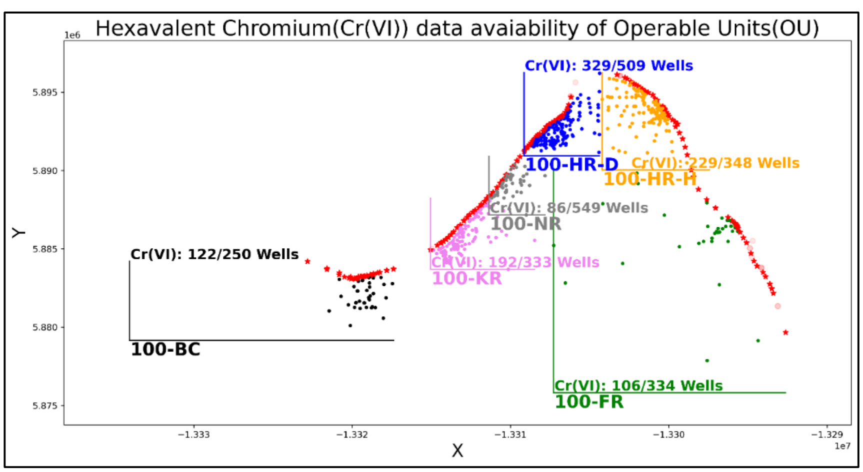

Figure 92. Hexavalent chromium [Cr (VI)] data availability of wells in 100 Areas.

The dataset exploration reveals that the mean and variance intensities of Cr(VI) in 100 Areas OUs have gradually decreased over time. Figure 93 depicts the gradual progression of hexavalent chromium [Cr(VI)] concentration in Hanford Site 100 Areas.

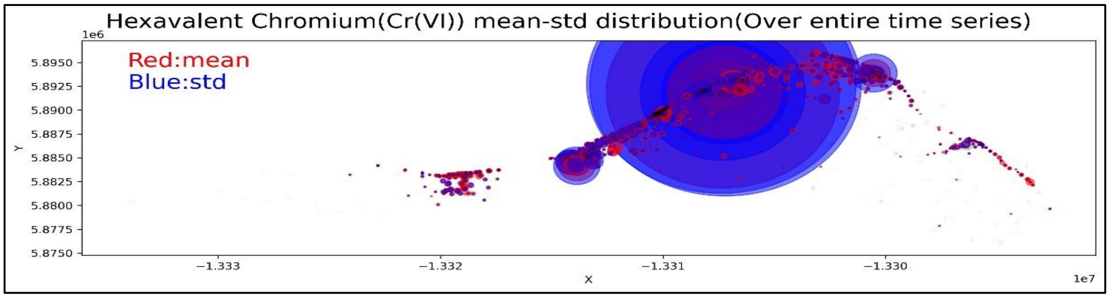

2010-2011 2014-2015 2019-2020

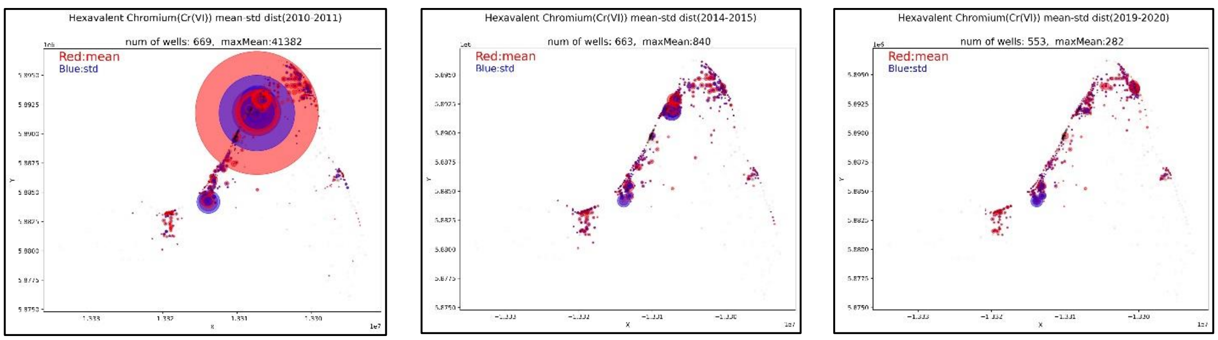

Figure 93. Hexavalent chromium [Cr(VI)] concentration variation over time.

Subtask 7.2: Data Pre-Processing and Exploratory Data Analysis to Evaluate the Chromium Concentration in the Samples

In line with AI/ML-based exploration of spatiotemporal relationships of groundwater and surface water Cr(VI) concentration, the FIU team looked into the overall statistical features of the time series of the groundwater and surface water Cr(VI) data. For this, all the time series in the groundwater wells or aquifer tubes group were averaged over the time axis to create a single time series for each group in respect of operable units. The operable unit-wise resultant time series for groundwater wells and aquifer tubes are presented in Figure 94. The average time series for the groundwater wells and aquifer tubes resulted after the use of filter 1, is depicted by the dotted red and bold green plots in Figure 94, respectively. On the other hand, the filter 2 resulted aquifer tubes' average time series are depicted by the bold red plots in Figure 94.

No data filter case	With data filter

Figure 94. Averaged time series of ground water wells and aquifer tubes time series after the application of dataset filter 1 & 2 vs. no filter case.

As a subjective assessment, the weak similarity of groundwater and surface water Cr(VI) concentration is apparent for operable units 100BC, 100HRD, and 100HRD in Figure 94. For quantitative assessment, cosine similarity and Pearson correlation coefficient were applied. As presented in Table 18, the cosine similarity of ground and surface water Cr(VI) for each operable unit as well as the 100 Areas as a whole is close to 1 which signifies the orientation wise the time series are very similar. Moreover, the concise set of aquifer tubes dataset due to the application of the dataset filter 2 slightly improves the cosine similarities. On the other hand, the Pearson correlation coefficient showed a mixed result for different operable units. The time series sustained through the dataset filter 1, resulted positive or close to 0 Pearson coefficient for most of the operable units except 100HRH, which is slightly negative. Interestingly, when dataset filter 2 was applied, the correlation coefficient greatly improved for 100BC, 100HRD, and 100HRH.

Table 18. Quantitative Measures of Similarities

OU name	AQT (No filter)	GW and AQT similarity measures		AQT (filter 1)	GW and AQT similarity measures		AQT>=10µg/L (filter 1 & 2)	GW and AQT similarity measures	
		Pearson	cosine		Pearson	cosine		Pearson	cosine
100BC	59	-0.0466	0.9923	19	**0.0276**	0.9918	14	**0.2886**	**0.9929**
100KR	55	-0.7135	0.9731	44	**0.1514**	0.9889	4	-0.2636	0.9723
100NR	16	0.5409	0.9990	9	0.3903	0.9947	0	-	-
100HRD	67	0.7879	0.9705	15	0.0127	0.9215	3	**0.2419**	**0.9308**
100HRH	58	0.3221	0.9902	18	-0.0230	0.9808	2	**0.4417**	**0.9847**
100FR	12	0.1916	0.9951	5	**0.2639**	0.9824	0	-	-
ALL 100 Areas	267	0.1323	0.9953	110	**0.6909**	0.9833	23	0.6044	**0.9846**

Finally, the two metrics of similarity measures for the whole 100 Areas dataset filtered using the two filters described in the method, reveal that the groundwater and surface water Cr(VI) concentration time series are highly correlated temporally as their cosine similarity score is 0.9846 (filter 1 & 2) and Pearson correlation coefficient is 0.6909 (filter 1) as presented in Table 17 and Table 18. The Figure 95 present these time series related to the whole 100 Areas.

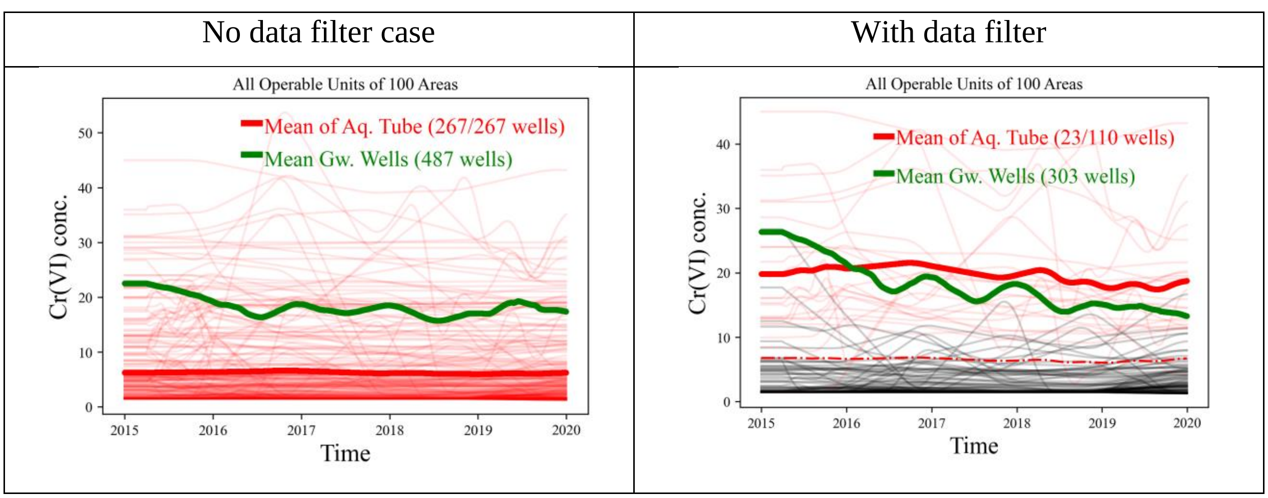

Figure 95. Complete 100 Areas ground water and surface water Cr(VI) time series similarity.

Using the aforementioned filtering method for GW wells and AQT, a usable dataset was extracted considering the 100-BC operable unit of the Hanford Site. An RF regressor model was trained using the GW wells time series as the features and mean aquifer tubes time series as the target variable. From the trained model, the GW wells or feature importance scores were extracted as presented in Table 19 and depicted by Figure 96.

Table 19. 100-BC GW Well (Feature) Importance Score

GW well name	RF feature Importance score
199-B3-1	0.167612
199-B3-47	0.157865
199-B3-50	0.105797
199-B3-51	0.104468
199-B3-46	0.096134
199-B5-10	0.0662539
199-B5-5	0.0658255
199-B4-18	0.0561685
199-B4-7	0.0347565
199-B5-12	0.0310425
199-B8-9	0.0201682
199-B4-4	0.0162003
199-B3-52	0.0101805
199-B2-13	0.00802842
199-B5-2	0.00797314
199-B4-14	0.00760333
199-B5-9	0.00750724
199-B4-16	0.00703179
199-B5-11	0.00522866
199-B9-3	0.00510556
199-B5-6	0.00497722
199-B4-8	0.0047335
199-B2-16	0.00378119
199-B2-14	0.00302549
199-B5-13	0.00160271
199-B4-1	0.000930526

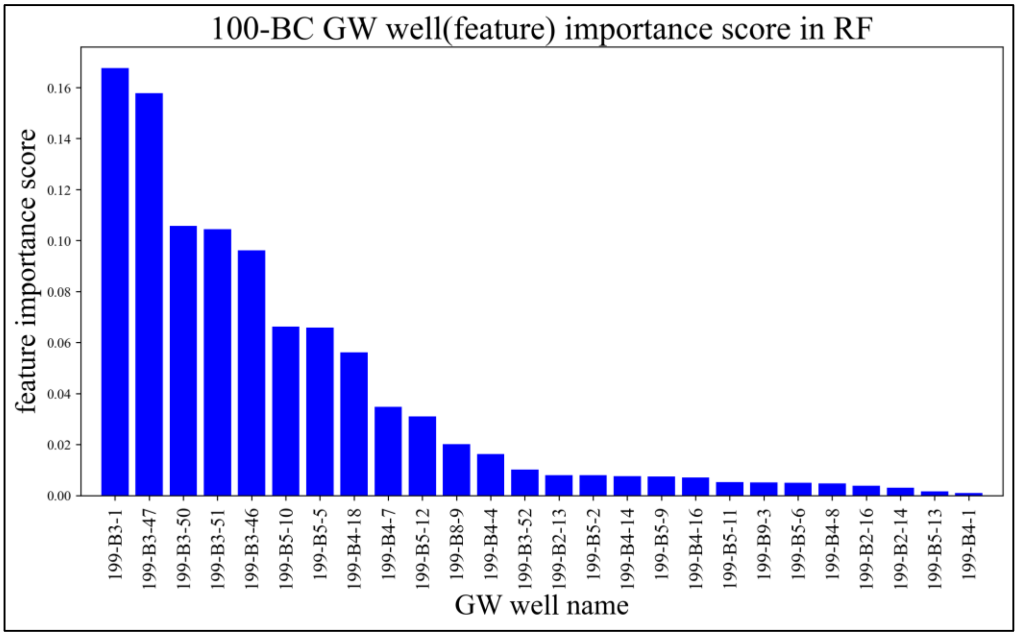

Figure 96. 100-BC GW well (feature) importance score.

For a subjective assessment, these importance scores are projected according to their actual location as shown in Figure 97. The red stars are the AQT locations which indicates the approximate shoreline, and the various colored circles are the GW well location. The GW wells associated circles' size and color depict the corresponding importance scores, where bigger and towards red signifies more feature importance. From the subjective assessment, it is apparent that the more important GW wells or features are closer to the shoreline.

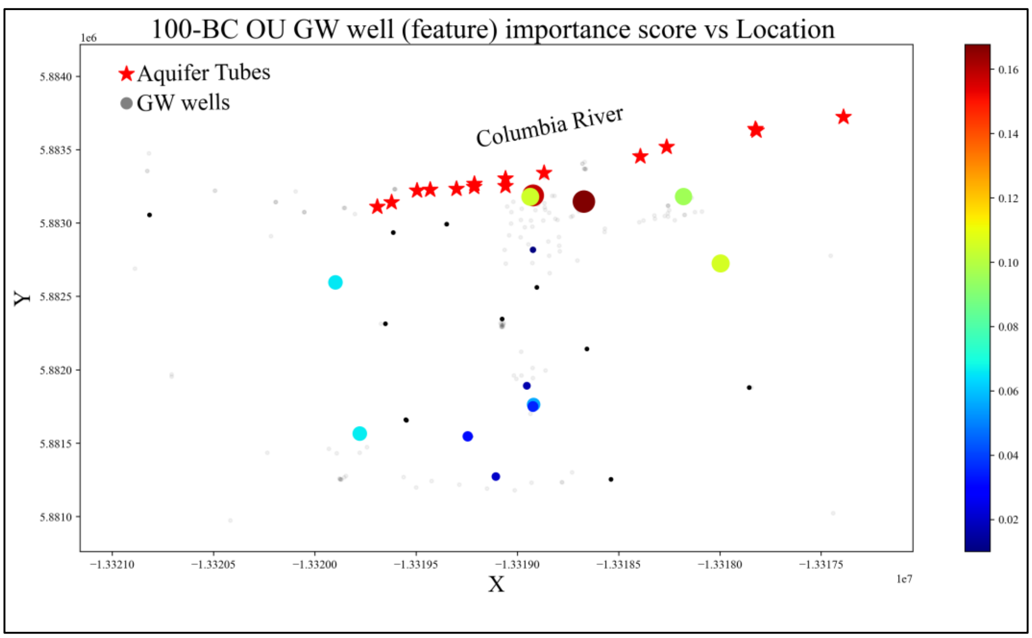

Figure 97. 100-BC GW well (feature) importance score vs actual location of the GW wells.

The distance of the GW wells from the shoreline was approximated using the nearest AQT locations. These distances to shoreline vs feature (GW well) importance are plotted and are as shown in Figure 98. For analyzing distance to the feature importance relationship, a regression analysis was performed, where the less important features are excluded using a threshold of 0.02

in the case of 100-BC OU. The regression analysis depicted by the green line in Figure 98 reveals that the important feature or GW wells are linearly distant from the shoreline.

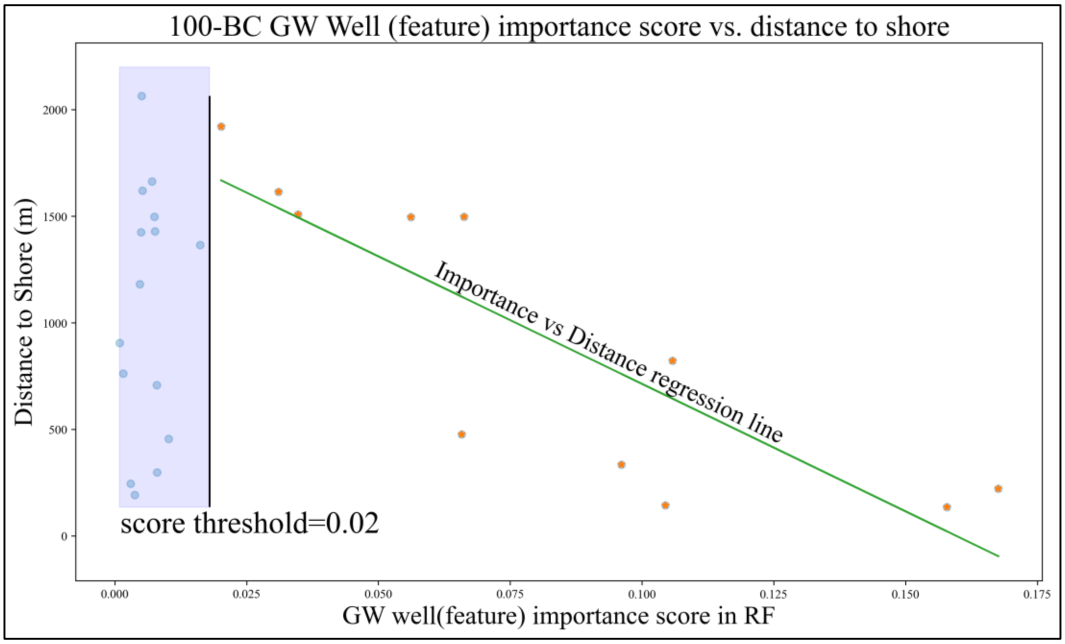

Figure 98. Feature importance score vs distance to river shoreline.

The GW wells' feature importance scores spatial distribution for 05-M aquifer tubes along with feature score vs distance to target aquifer tube relation are presented in Figure 99. Using the distances of the GW wells from the target aquifer tube and the respective features' importance, a regression line was fitted for this representative aquifer tube. In the regression line fitting the dynamic threshold of 5% of the maximum feature importance value resulted in 0.018, as the minimum feature importance value to be considered in the regression line fitting. In the case of 05-M aquifer tube, the nearer GW wells' feature has higher feature importance values and there is a decreasing trend in feature score vs distance to this aquifer tube relation was observed. This phenomenon of decreasing trend in the feature score vs distance to the target aquifer tube relation was also observed in most of the aquifer tubes considered under the 100-BC operable unit.

(a)

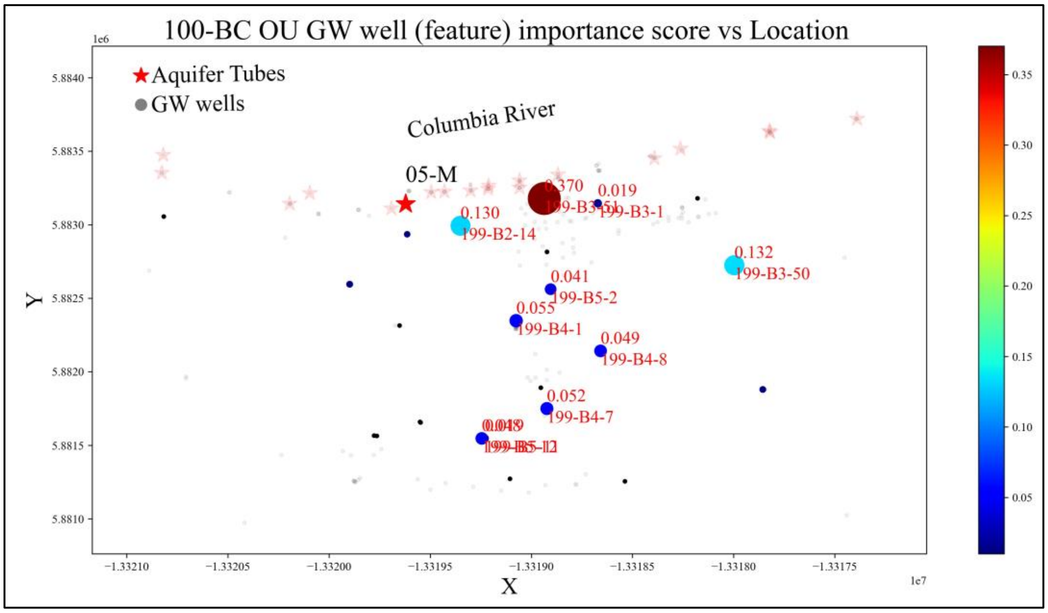

(b)

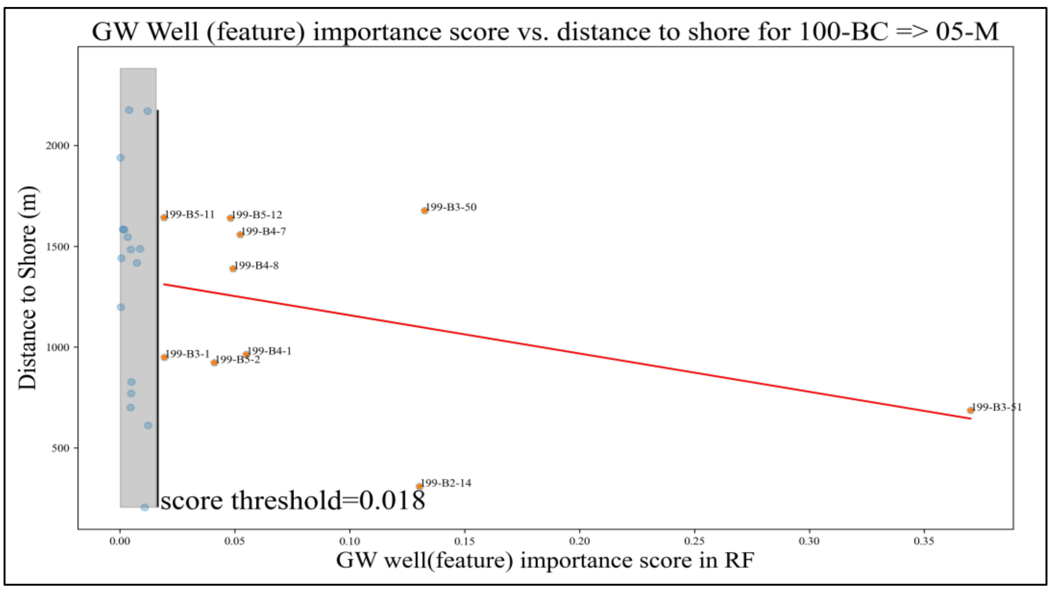

Figure 99. Aquifer tube 05-M (a) feature importance score spatial distribution, (b) feature score vs distance to target aquifer tube 05-M relation.

Although we observed a decreasing trend in feature score vs distance to C8841 aquifer tube relation, some intermediate distanced GW wells showed lower feature importance in ML modeling in the case of this aquifer tube as highlighted by the blue boundary in Figure 100 (a). However, for this aquifer tube, the nearest GW well 199-B2-13 got the highest feature score.

(a)

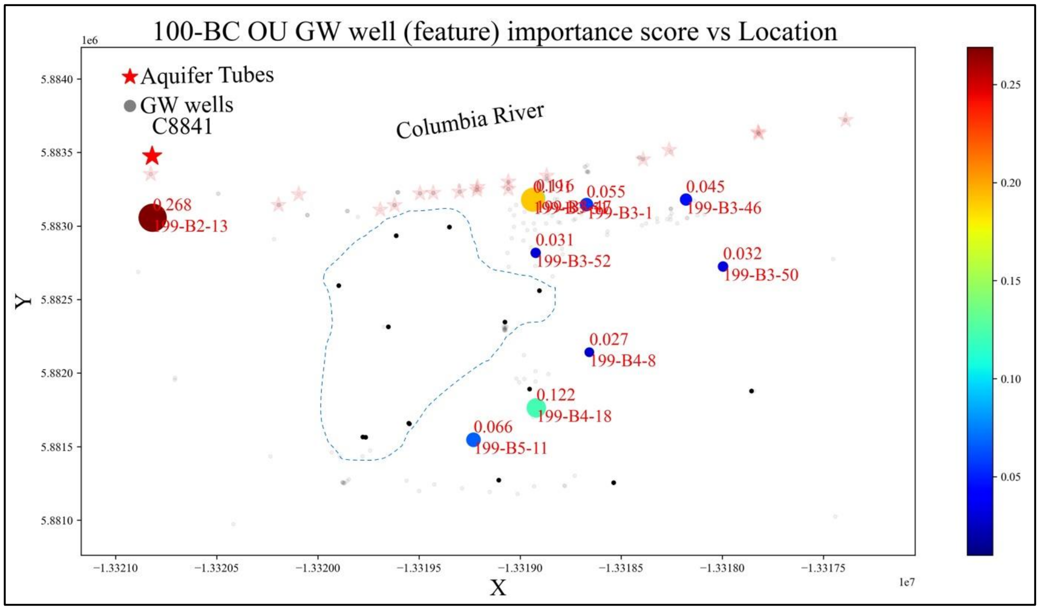

(b)

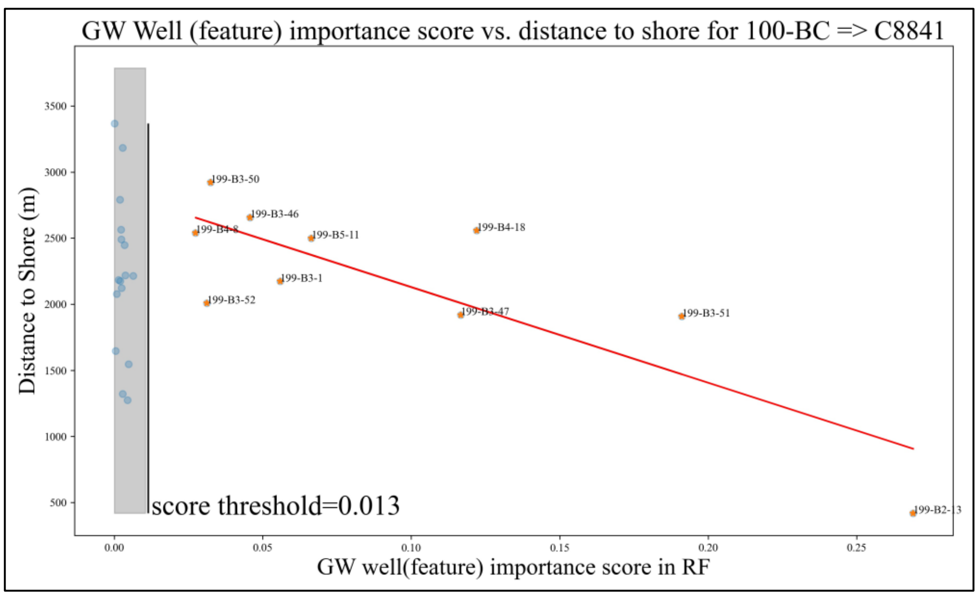

Figure 100. Aquifer tube C8841 (a) feature importance scores spatial distribution, (b) feature score vs distance to target aquifer tube C8841 relation.

Apart from the above decreasing trend in feature score vs distance relationship, some aquifer tubes showed an opposite trend as depicted in Figure 101 for the aquifer tube C8861. More interestingly, the highest scored GW wells feature location is the most distant wells for this aquifer tube C8861 as highlighted by the blue arrow in Figure 101 (b).

(a)

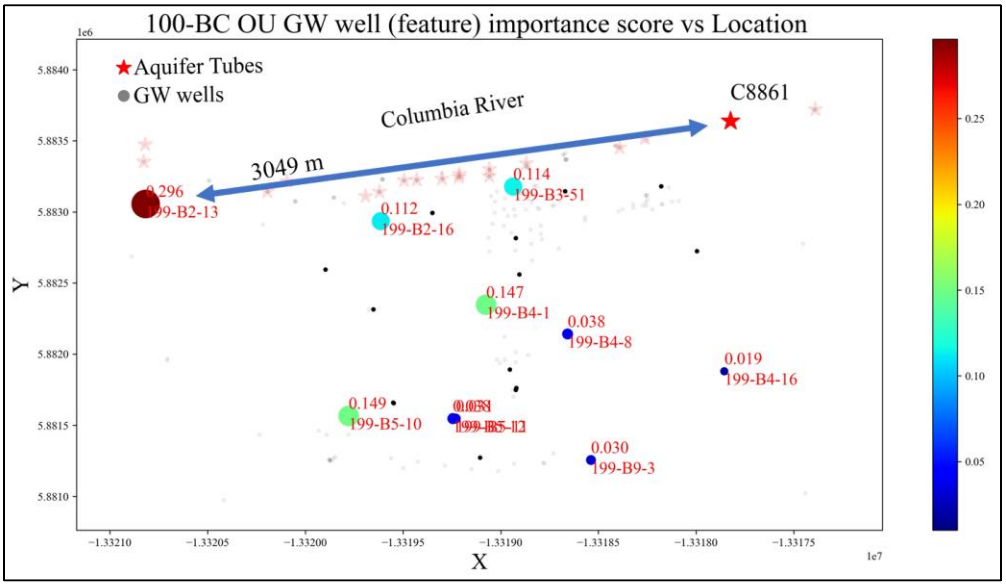

(b)

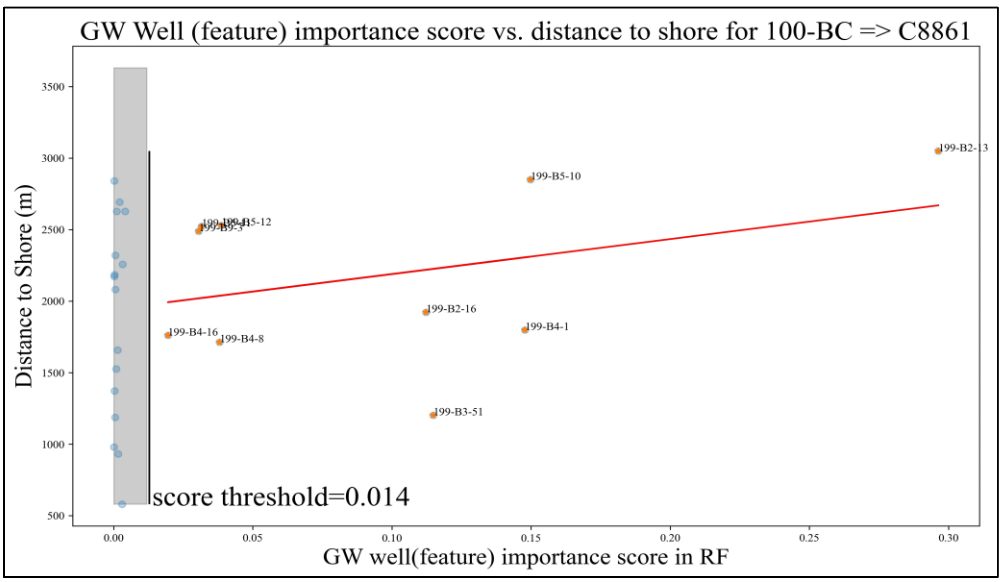

Figure 101. Aquifer tube C8861 (a) feature importance scores spatial distribution, (b) feature score vs distance to target aquifer tube C8861 relation.

In case of 100-HRD OU, out of 252 GW wells and 97 aquifer tubes, 87 GW wells, and 15 aquifer tubes sustained the data filter. Alike 100-BC, most of the individual aquifer tube machine learning models showed a decreasing pattern of feature importance for GW wells as predictors. Figure 102 depicts the spatial distribution of the GW wells or feature importance for aquifer tube DD-12-2 as a representative well. Subjectively it is apparent that closer GW wells to the target aquifer tube DD-12-2 have higher feature importance values.

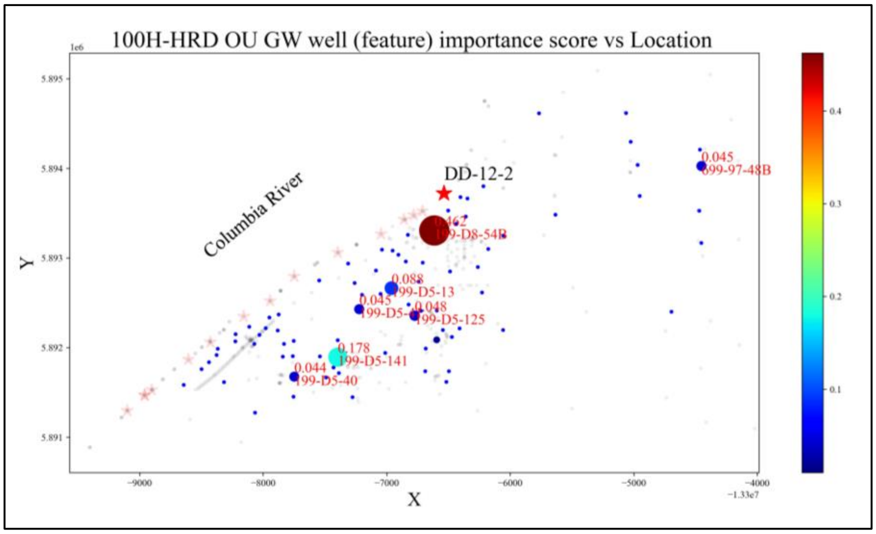

Figure 102. Spatial distribution of the GW wells or features importance of a representative aquifer tube with decreasing feature importance relation in respect of increasing distance to target aquifer tube.

In the regression line fitting between the distances of the GW wells from the target aquifer tube and the respective features' importance, the dynamic threshold of 5% of the maximum feature importance value resulted in 0.023 as the minimum feature importance value to be considered in this representative aquifer tube. The red regression line in Figure 103 depicts the decreasing feature importance relation with respect to increasing distance to the target aquifer tube.

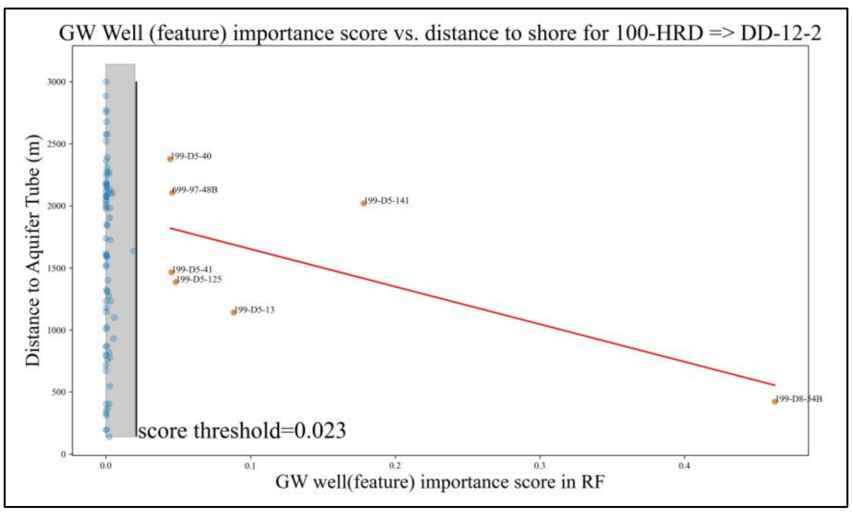

Figure 103. Spatiotemporal relationship identification by feature importance vs distance to aquifer tube regression line fitting of a representative aquifer tube with decreasing feature importance relation in respect to increasing distance to target aquifer tube.

Among the 15 filtered aquifer tubes from 100-HRD, 12 showed the decreasing feature importance relation with respect to increasing distance to target aquifer tube alike the representative aquifer tube DD-12-2 presented above. However, 3 of the aquifer tubes showed the opposite trend in the distance vs features importance relation, and the relation for a representative aquifer tube is present in Figure 104 and Figure 105.

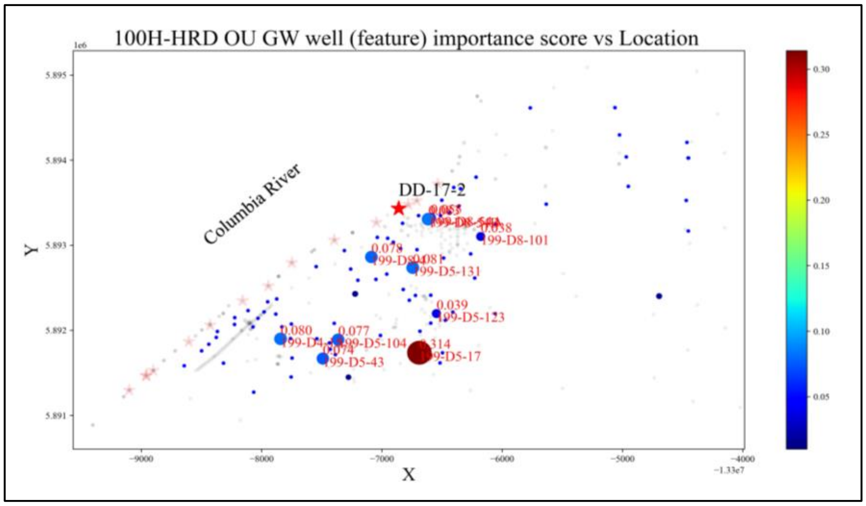

Figure 104. Spatial distribution of the GW wells or features importance of a representative aquifer tube with increasing feature importance relation in respect of increasing distance to target aquifer tube.

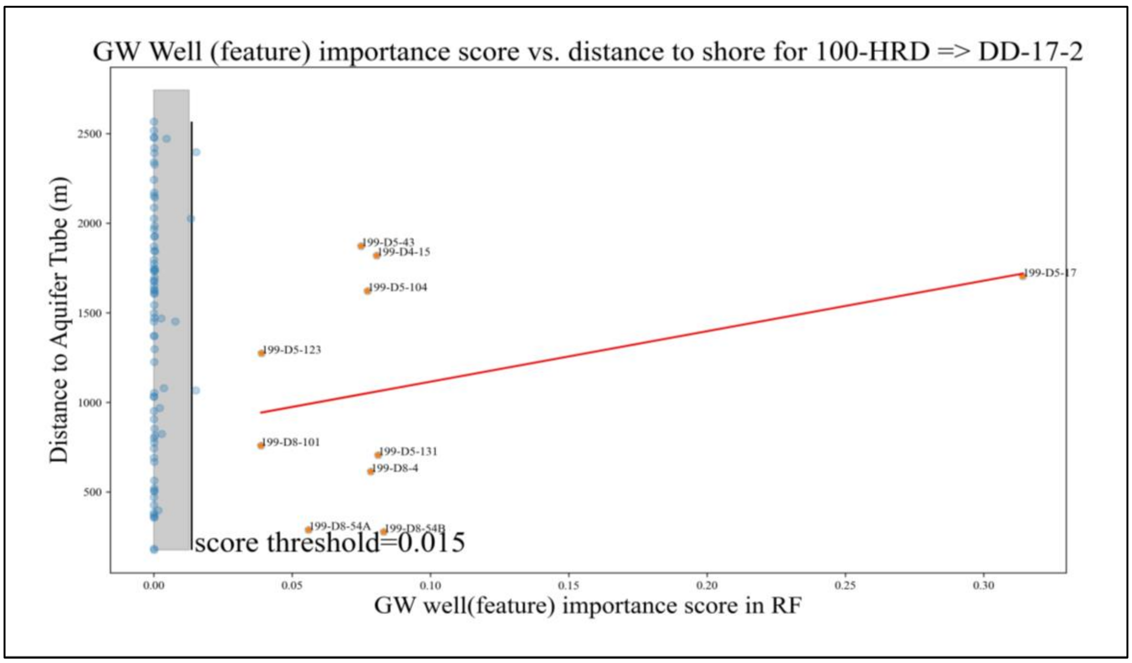

Figure 105. Spatiotemporal relationship identification by feature importance vs distance to aquifer tube regression line fitting of a representative aquifer tube with increasing feature importance relation in respect of increasing distance to target aquifer tube.

Using all the individual regression lines for aquifer tubes, a grand regression line was fitted to get an overall picture of the spatiotemporal relationship in respective operable units. The resultant regression presented by the bold line plot in Figure 106 depicts an overall decreasing feature importance relation with respect to increasing distance to target aquifer tubes for the 100-BC operable unit.

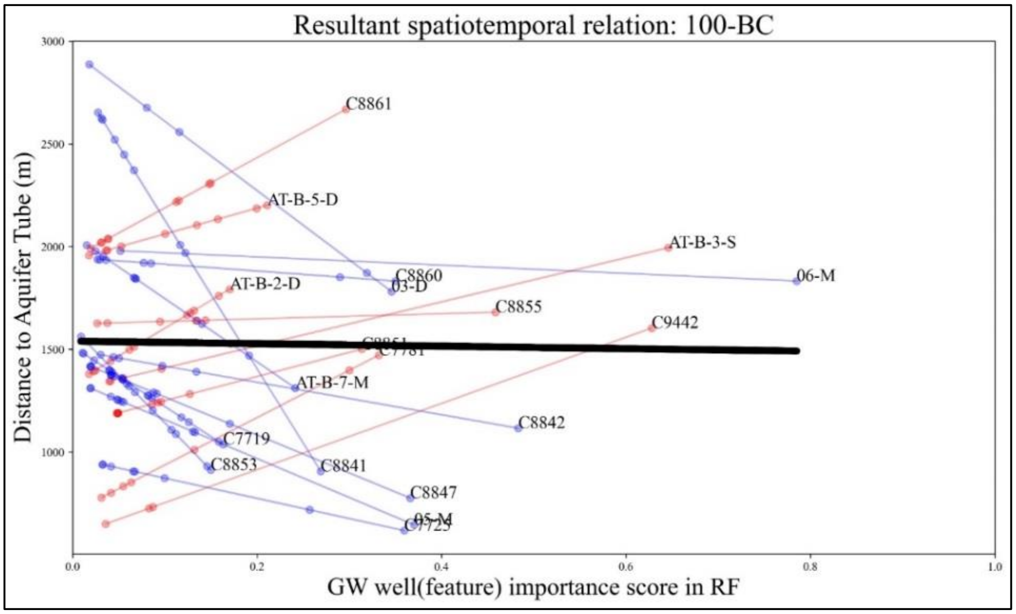

Figure 106. Spatiotemporal relationship identification by feature importance vs distance to aquifer tube regression line fitting of a representative aquifer tube with decreasing feature importance relation in respect of increasing distance to target aquifer tube for 100-BC.

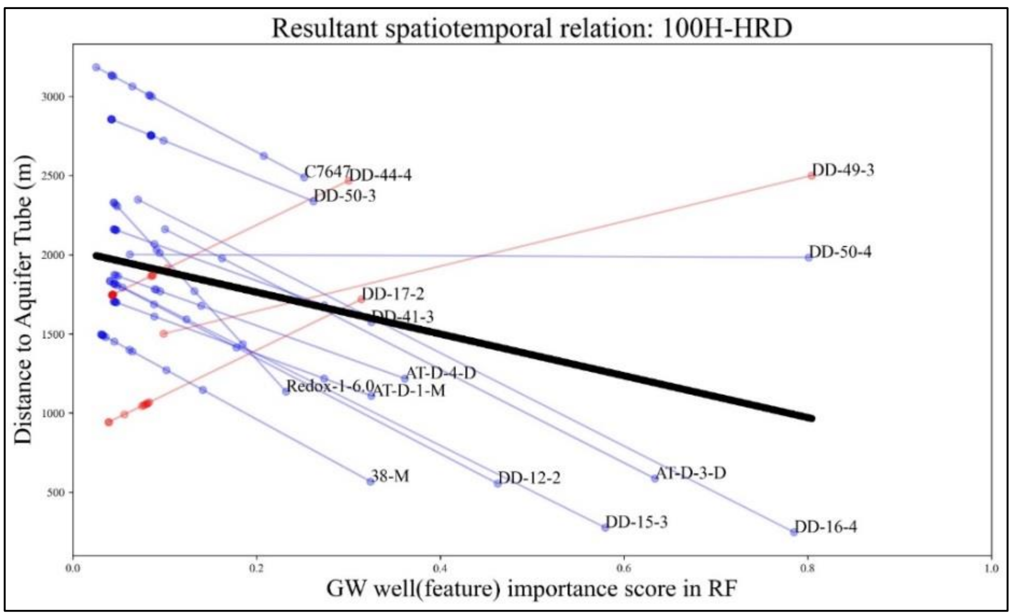

Figure 107. Spatiotemporal relationship identification by feature importance vs distance to aquifer tube regression line fitting of a representative aquifer tube with decreasing feature importance relation in respect of increasing distance to target aquifer tube for 100-HRD.

Based on the analysis for 100-HRD operable unit, the resultant regression line showed an overall decreasing feature importance relation with respect to increasing distance to target aquifer tubes, which is stronger than for 100-BC as depicted by Figure 107.

Subtask 7.3: Machine-Learning and Deep-Learning Model Development for Anomaly Detection

Towards the goal of developing an anomaly detection system for chromium concentration, FIU investigated a deep learning approach for this subtask. In particular, we use the Long Short-Term

Memory (LSTM) cell-based neural network architecture for the anomaly detection system development. As the 100-H Area Cr (IV) dataset does not have any label for anomalous data points, a semi-supervised approach was taken for the overall anomaly detection problem-solving. In this approach, a stacked-LSTM neural network is implemented for the time series signal encoding and decoding application. In this architecture, the encoder part of the network tries to learn from the training signal and the decoder part tries to reconstruct the signal using the learned parameters. The maximum value of the Mean Absolute Error (MAE) between the training and reconstructed training signal is used as the threshold for the anomaly detection on the test signal in this approach. As this threshold or the anomaly detection criterion is based on the training signal, this approach resembles the semi-supervised approach of anomaly detection.

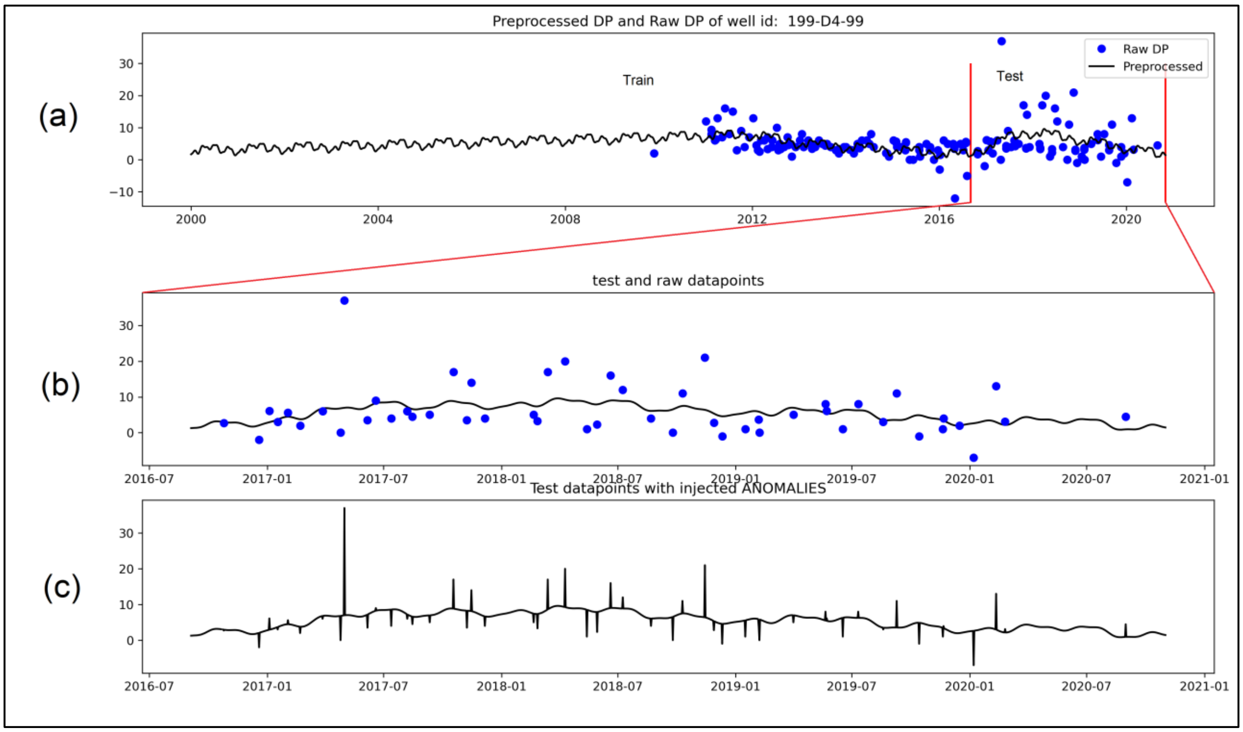

Figure 108. Training and test signal. (a) 75/25 split of the datapoint. (b) Replacing some test datapoints anticipating anomaly injection. (c) Final test datapoints.

A representative well's (199-D4-99) chromium concentration time series is presented in Figure 108. Figure 108 (a) presents the raw data points and the preprocessed time series. This time series was split into a 75/25 ratio for training and testing of the anomaly detection assessment. To introduce anomalous data points in the test signal, the corresponding data points of the raw data points time stamp were replaced by the value of the raw data point in the test signal which is depicted by Figure 108 (c). To train the network, adam optimizer was used and the MAE was selected for the objective function. The training and validation MAE losses for various epochs are presented in Figure 109.

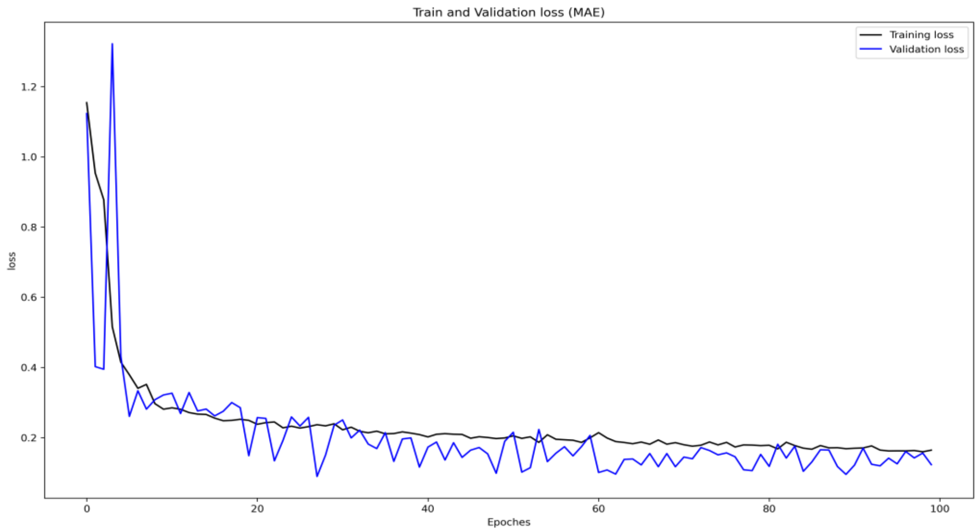

Figure 109. Training and validation loss.

The training time series were reconstructed using the trained model's predictive function which is depicted by Figure 110(a). Afterward, the MAE losses between the original training time series and the reconstructed time series were calculated. As presented in Figure 110(b), the maximum value of the MAE loss in the training time-series reconstruction was selected as the criterion for anomalous point detection for further steps.

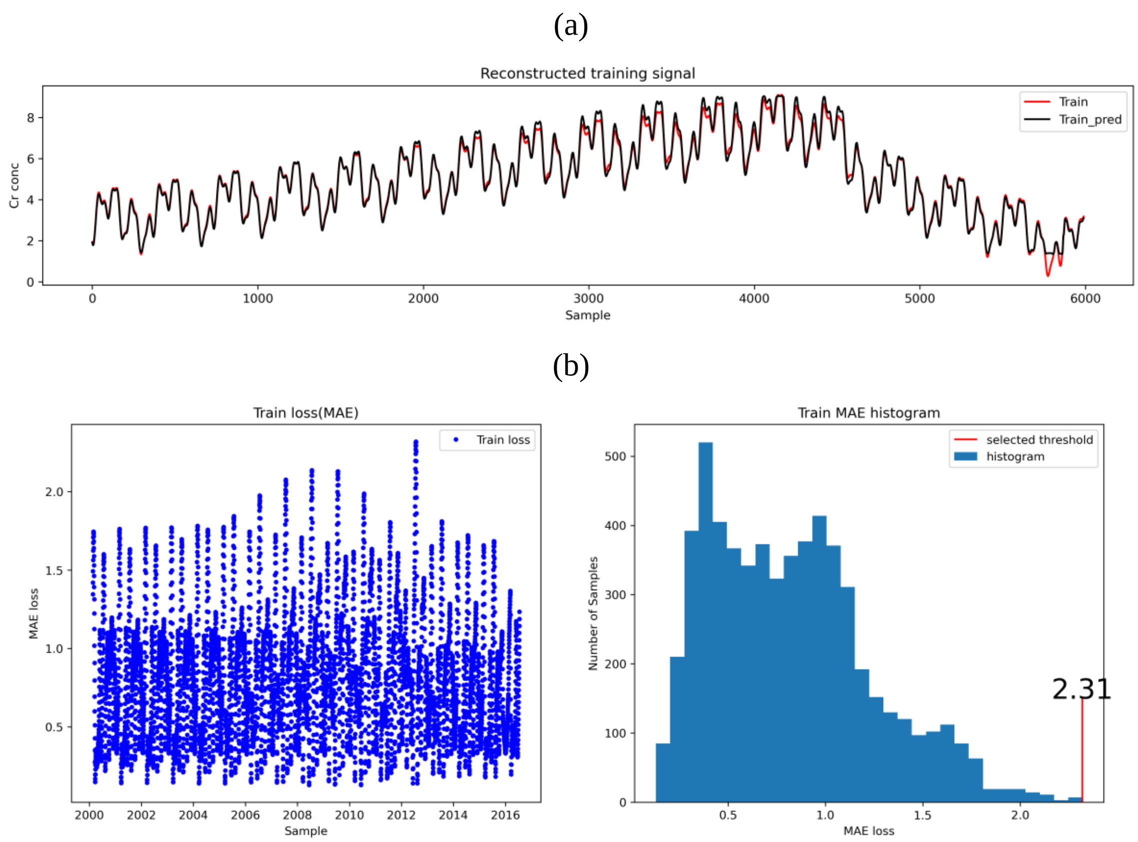

Figure 110. (a) reconstructed time series using the trained model. (b) MAE loss between training and reconstructed time series and automatic selection of the anomaly detection threshold.

The anomalous data point injected test signal presented by Figure 108 (c) was used for predictive reconstruction of the test data points which is presented in Figure 111(a).

(a)

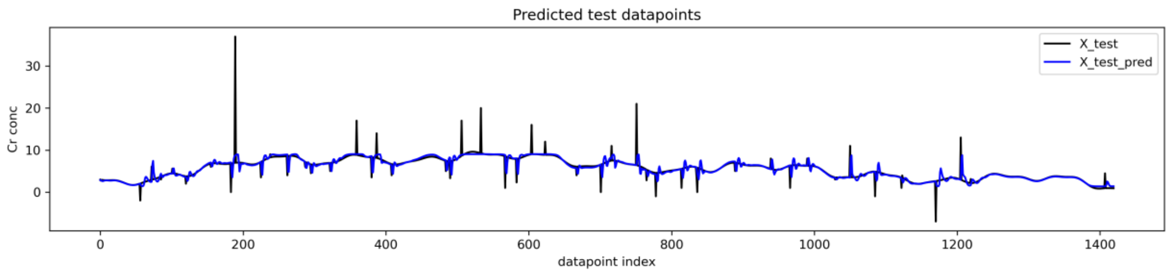

(b)

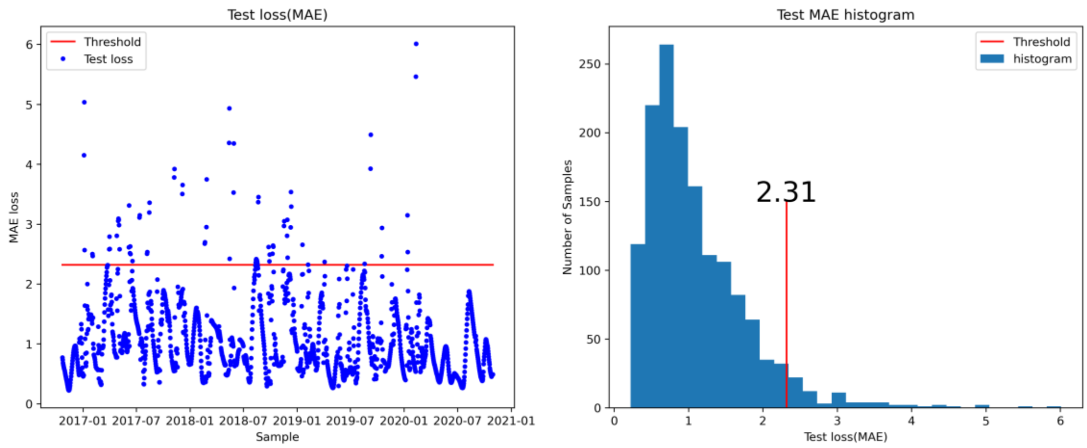

Figure 111. (a) Predictive reconstruction of test time series. (b) MAE loss between test and reconstructed time series and MAE loss distribution.

Based on the test MAE distribution and the MAE threshold selected in the training phase, certain data points were marked as anomalous data points by the system. The test timeseries, injected anomalous data points and detected anomalous data points are presented in Figure 112.

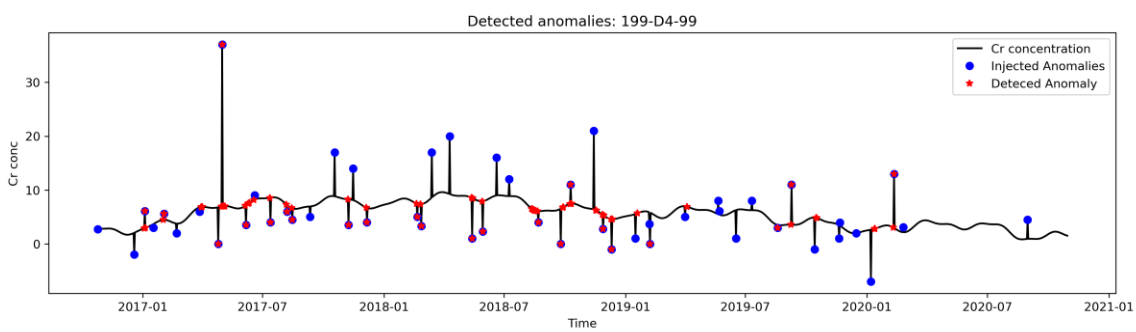

Figure 112. Detected anomalous data points.

Among the 1470 data points in the test time series, 74 data points were marked as anomalous data points by the system. However, 23 of the 51 injected anomalous points were among these detected anomalous data points. Thus, the designed network needs to be further tuned to improve the anomaly detection performance as a next step.

Task 7: Conclusions

The overall relationship for 100-BC and 100-HRD showed a decreasing feature importance relation with respect to increasing distance to target aquifer tubes. However, for 100-HRD operable unit, the resultant regression line showed an overall decreasing feature importance relation with respect to increasing distance to target aquifer tubes which is stronger than for 100-BC.

Task 7: References

Trinh, Hoang Duy, et al. "Detecting mobile traffic anomalies through physical control channel fingerprinting: A deep semi-supervised approach." IEEE Access 7 (2019): 152187-152201.

TASK 8 AI FOR EM PROBLEM SET (SOIL AND GROUNDWATER) - DATA ANALYSIS AND VISUALIZATION OF SENSOR DATA FROM WELLS AT THE SRS F-AREA USING MACHINE LEARNING (LBNL, SRNL) (NEW)

TASK 8: Introduction

The ALTEMIS team has procured about twenty new sensors, the In-Situ Aqua TROLL 500, to install at different existing well locations at the SRS F-Area. Nine of these sensors collect over 10 parameters and the remaining sensors collect only 3 parameters: pressure, specific conductance, and temperature. The locations for the nine sensors with many parameters have been predetermined by experts and will be installed along the central line of the plume. The challenge of sensing location selection arises from the fact that a limited number of new sensors can be deployed in existing location towards effective sensing for the overall dynamics. In addition, there are hundreds of analytes to be monitored in the groundwater, and it is not feasible to sense all of them with the new sensors. Thus, it is necessary to identify a small subset of analytes or variables whose dynamics can represent the overall dynamics of all the pollutants in the monitoring area.

Task 8: Objectives

The main objective of this task is to determine the most optimal locations to place an additional 10 to 15 Aqua TROLL 500 sensors. The well locations should be chosen with the aim of capturing the overall contamination and groundwater movement.

Task 8: Methodology

The FIU team has developed a robust pipeline to select optimal sensor placement using a bagging approach. The four major steps in the implementation are exploration and preprocessing of the data, spatial estimation, the optimization algorithm, and finally the majority voting process.

Task 8: Results and Discussion

Subtask 8.1: Exploratory Data Analysis

Purpose:

Understanding the data is key to effectively solving the sensor optimization problem. The purpose of this subtask is to understand both the spatial and temporal distribution of the F-Area dataset and develop tools to guarantee the data is of high quality and can be used for complex algorithms.

Time series exploration:

As part of the exploration phase a function called *plot_all_time_series* was created to understand the distribution of the data. This function plots all the start/end dates and helpful to identify the common date ranges where there is available data. Figure 113 below shows an example of the function containing time series of length at least 500 days. This analysis is used for the time series selection process in later sections.

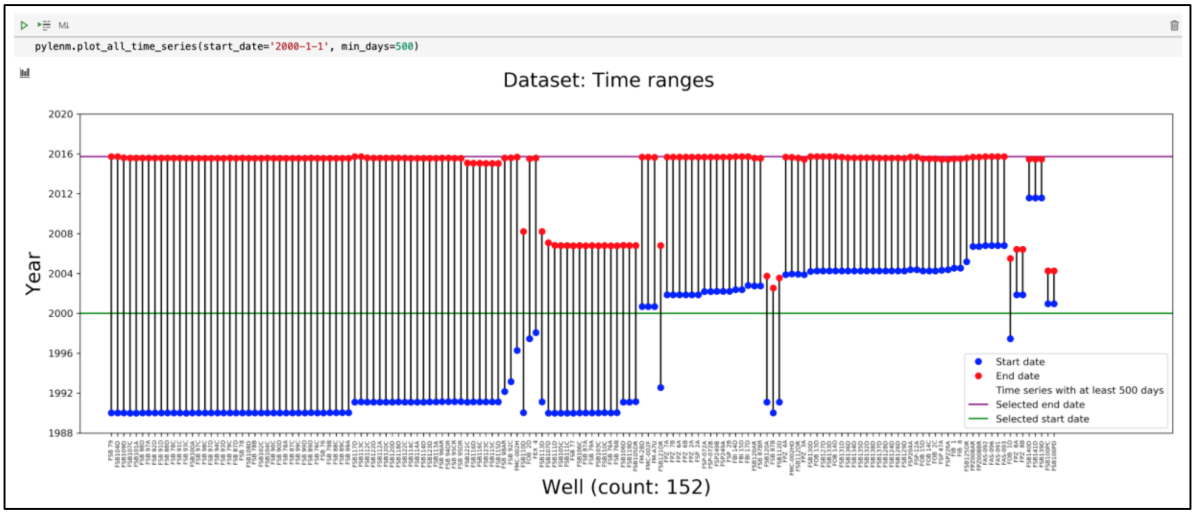

Figure 113. plot_all_time_series function plotted for time series with at least 500 days of data.

Resampling and Interpolation:

The F-Area groundwater dataset is sporadic in terms of collection dates, which is an undesirable feature for the analysis. To fix this issue, data resampling is required to align all the separate time series on the same dates. This restructuring also introduces a whole lot of missing cells in the table since we are altering the dates from the original dataset. As a result of this, interpolation is essential. This process involves strategically replacing missing data with estimated values to properly apply subsequent algorithms.

Selection of appropriate data:

The dataset contains more than 100 different analytes. To generate a thorough optimization that reflects overall plume movement, a subset of key analytes needs to be selected. With the help of the subject matter experts from the ALTEMIS team, 8 analytes were selected as the main driver for the optimization problem. The selected analytes are listed as follows: water table, water temperature, pH, specific conductance, uranium-238, iodine-129, strontium-90 and tritium. In addition, only the 'D' wells, which are part of the upper aquifer, are included as part of the dataset since the sensors will be placed in the upper aquifer for monitoring. Lastly, thanks to the plot_all_time_series function, time series that were lacking too much information were filtered out from the scope of analysis.

Subtask 8.2: Identify the Master/Proxy Variables

Purpose:

The purpose of this subtask is to identify a subset of analytes as master variables whose transport dynamics reflect the overall dynamics of the other variables, in particular water table and contaminant concentrations.

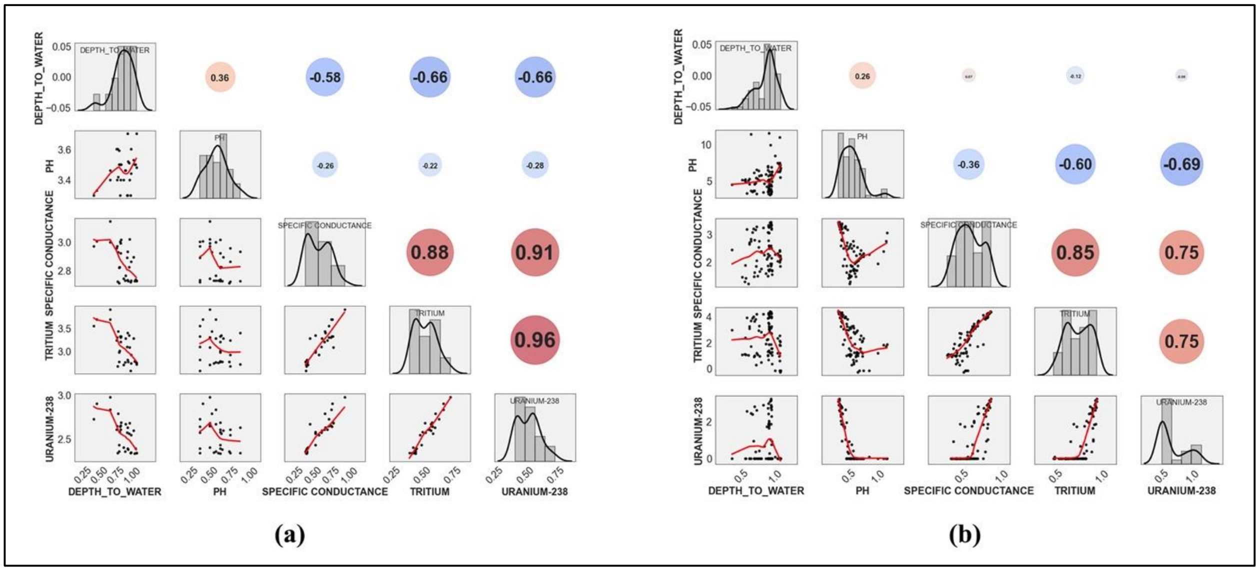

Figure 114. (a) Temporal correlation plot among analytes at FSB95DR between 02/09/1993 and 07/30/2013 log concentrations. (b) Spatial correlation plot for all wells among analytes on 02/21/1993 with a lag of 12 days (02/09/1993 - 03/05/1993) log concentrations.

Results:

Through correlation analysis using of proxy variables against contaminant concentrations functions created in subtask 8.1, it is clear that specific conductance (SC) and tritium have very high correlations in both the spatial and temporal directions. This indicates that SC is a good proxy for tritium. In addition, SC has high correlations with uranium-238 as well. The correlation is weaker however in the spatial direction but remains strongly correlated.

Subtask 8.3: Machine Learning Model Development & Optimization for Sensor Placement in Groundwater Wells

Purpose:

This task intends to infer the transport dynamics of many analytes based on the data collected from a reduced number of sensor placement. As this inference will be made using feature correlation analysis and weighting, its accuracy will depend on the sensor locations' capability of capturing the collective gradient of these feature values temporal data.

Spatial Estimation:

A critical aspect of the optimization is to consider the spatial aspect of the dataset. The dataset contains concentration values for each of the eight studied analytes at each well location. To understand the dynamic of the plume in respect to each individual analyte, estimated values in between wells need to be generated for the entire F-Area. In other words, spatial estimation must be performed to properly perform analysis. A popular method known as Kriging or Gaussian Process Regression (GP) was used to spatially interpolate the data. The advantage of using a GP is its ability to spatially estimate in a normal distribution, which is useful for generating a realistic map. An example of one of the many spatial interpolated maps can be seen in Figure 115 below. The map generated using all the wells is known as the reference field or the ground truth map. The values contained by the reference field maps are utilized in the optimization step.

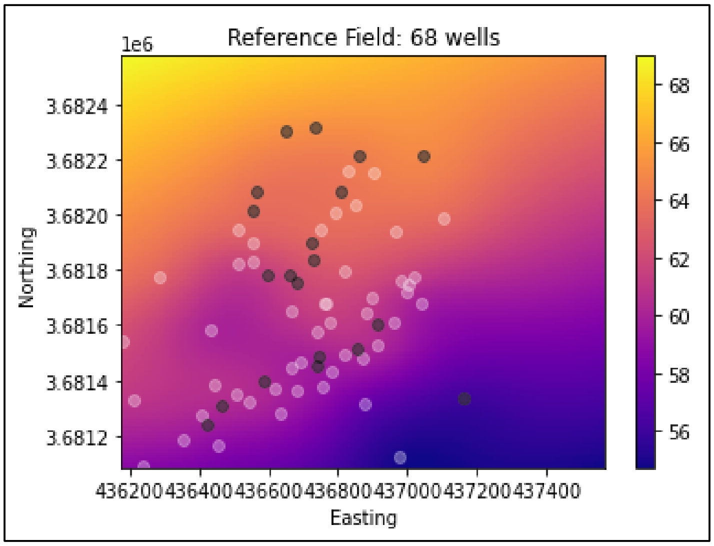

Figure 115. Water table interpolated map (Ground truth map) of the F-Area of 'D' wells using the average value over the entire time series.

Optimization Algorithm:

The overall optimization solution works by combining the results of individual optimized solutions with the bootstrap aggregation (bagging) approach. The aggregation details using majority voting will be discussed in a later section. The individual optimization serves to optimally select 15 to 20 sensor placement locations for an individual time step. The main idea of the optimization is to minimize the overall error between the high-quality reference field and the spatial interpolated map with the 15-20 subset wells. The mean squared error (MSE) was used as the error metric for this problem. The selection of the subset well locations is performed using below mentioned algorithm.

Individual time-step sensor placement selection algorithm (pseudocode) description:

- **Input:**
  - List of all available well locations to choose from
  - [max_wells]: Maximum number of wells to select
  - List of starting wells (if any)
- **Algorithm:**
  1. If there is a list of starting wells, they will be chosen first as the optimal locations.
  2. Run this process for ([max_wells] - # of starting wells) number of times:
     a. For each of the available wells remaining:
        i. Create a GP using the current well + the starting wells + previously selected wells.
        ii. Calculate the MSE (mean squared error) between the GP from **Step 2.a.i.** and the Ground truth GP.
     b. The well combination that contributes the least MSE from **Step 2.a.** is chosen and added to the list of selected wells.
- **Output:**
  - List of selected well names in the order from most optimal to least optimal.

Figure 116 below demonstrates the results of the selection algorithm applied to water table data using averaged values between 02/29/2004 and 06/06/2004. The 20 wells (shown with black dots on the right side of the figure) are the identified wells that generated a spatially interpolated map with the least amount of error. In other words, these 20 selected wells best match the results generated using all the available wells. The algorithm is successful in mimicking the behavior of 68 wells using only 20 wells.

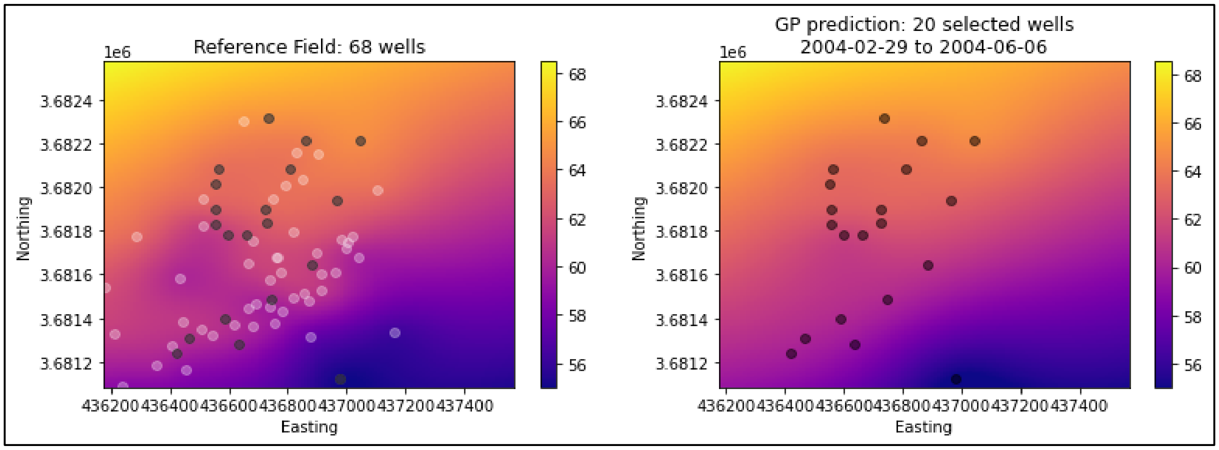

Figure 116: Selection algorithm applied to water table data with averaged values between 02/29/2004 and 06/06/2004.

Majority voting:

I. Dividing the time series into buckets of equally spaced ranges.

The spatial information and temporal data need to be combined for the optimization to work properly for the best set of wells selection. The optimization algorithm described previously considers the spatial aspect of the problem but is missing the temporal aspect, which is responsible for capturing the change in concentrations over time. Unless the time-series stays steady and constant through time, which is typically not the case. The resulting wells will not capture the overall analytes movement. To combat this issue, a bagging approach was implemented to divide each time series into a bucket of equally sized ranges and calculated the average of each range. These values are passed as input to the algorithm the same number of times as the size of the bucket. The bucket sizes are shown in Table 20 below. The decision to select multiple segmentation sizes is to maximize the likelihood of capturing the temporal dynamics of the variables.

Table 20. Time Series Segmentation

Number of buckets in segmentation	Approximate days in each bucket
45	98
90	56
135	28
225	14

II. Majority voting process description

As was mentioned before, for each time range, we perform the well selection algorithm, which outputs a list of well names. At each iteration (one of the 45, 90, 135, 225 ranges), the list of wells are saved to a Data frame. Once the algorithm completes its last iteration and we have a list of 20 wells outputted for each of buckets based on the majority voting. In other words, we count the number of occurrences of each unique well location and calculate the percentage. For example, if well "FSB105DR" appeared 43 times, we say that it has a 95.5% (43 ÷ 45) occurrence rate. This process is repeated for each of the eight analytes and for each bucketing window. A visual representation of the process is shown in Figure 117 below.

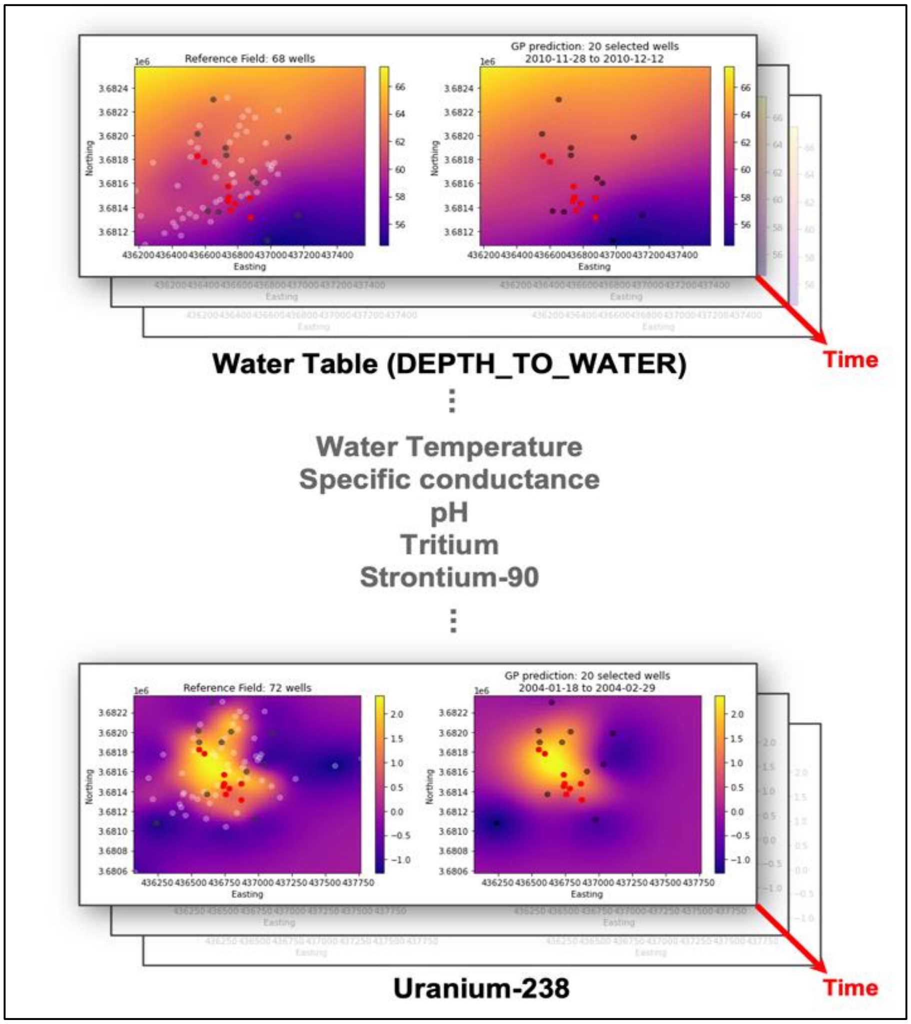

Figure 117. Optimization process through aggregation of time series buckets for each analyte.

After running the algorithm for each of the eight analytes at each bucket length (45, 90, 135, 225), we are left with many files with a sorted list of the occurrence count for each well. A total of 32 files will be generated based on 8 analytes and 4 buckets. We ran the above-described process 2 sets of times, (1) providing the algorithm with a list of preselected well locations that we call "with preset" and (2) not providing any well locations and letting the algorithm to make all of the decisions strictly based on the raw data that we call "without preset". We ran these two versions to determine if some wells were in agreeance between the two simulations.

Results:

After aggregating all the occurrences of the well selection among all the 32 files generated using the python script, we compiled an excel sheet with the results. To simplify the meaning of the results, we converted the occurrence count into a percentage by dividing the occurrence by 32. As there were 4 bucketing windows and 8 analytes in total, the highest possible occurrence for any well is 32. An occurrence count of 32 signifies that the well was selected by each analyte in each bucketing window. The last column of Table 21 and Table 22 show the occurrence percentage by well for the "without preset" version and the "with preset" version respectively.

Table 21. "Without preset" Well Selection Results

Rank	well name	W/O preset Run 1 (Count)	W/O preset Run 2 (Count)	W/O preset Run 1 (%)	W/O preset Run 2 (%)	W/O preset AVGERAGE
1	FEX 4	30	26	93.75%	81.25%	87.50%
2	FSB135D	24	24	75.00%	75.00%	75.00%
3	FSB 91D	24	20	75.00%	62.50%	68.75%
4	FSB 92D	24	20	75.00%	62.50%	68.75%
5	FSB126D	22	21	68.75%	65.63%	67.19%
6	FSB 87D	18	23	56.25%	71.88%	64.06%
7	FSB124D	20	20	62.50%	62.50%	62.50%
8	FSB 93D	22	16	68.75%	50.00%	59.38%
9	FBI 17D	19	16	59.38%	50.00%	54.69%
10	FSB132D	16	19	50.00%	59.38%	54.69%
11	FSB130D	18	16	56.25%	50.00%	53.13%
12	FSB 99D	20	13	62.50%	40.63%	51.56%
13	FSB 97D	17	16	53.13%	50.00%	51.56%
14	FSB128D	14	19	43.75%	59.38%	51.56%
15	FSB 79	16	16	50.00%	50.00%	50.00%
16	FSB112DR	12	20	37.50%	62.50%	50.00%
17	FSB 95DR	15	16	46.88%	50.00%	48.44%
18	FSB 98D	12	19	37.50%	59.38%	48.44%
19	FSB136D	11	20	34.38%	62.50%	48.44%
20	FSB118D	17	13	53.13%	40.63%	46.88%
21	FSB138D	13	17	40.63%	53.13%	46.88%
22	FSB 78	17	12	53.13%	37.50%	45.31%
23	FSB137D	15	14	46.88%	43.75%	45.31%
24	FSB104D	12	16	37.50%	50.00%	43.75%
25	FSB 94DR	15	11	46.88%	34.38%	40.63%
26	FOB 13D	11	15	34.38%	46.88%	40.63%
27	FSB120D	12	13	37.50%	40.63%	39.06%
28	FSB134D	11	14	34.38%	43.75%	39.06%
29	FSB133D	10	15	31.25%	46.88%	39.06%
30	FSB125DR	13	11	40.63%	34.38%	37.50%
31	FSB122D	12	12	37.50%	37.50%	37.50%
32	FSB117D	12	11	37.50%	34.38%	35.94%
33	FSB108D	13	8	40.63%	25.00%	32.81%
34	FBI 15D	9	12	28.13%	37.50%	32.81%
35	FOB 14D	9	12	28.13%	37.50%	32.81%
36	FSB127D	12	7	37.50%	21.88%	29.69%
37	FSB114D	8	8	25.00%	25.00%	25.00%
38	FSB123D	8	8	25.00%	25.00%	25.00%
39	FSB 76	9	5	28.13%	15.63%	21.88%
40	FSB 88D	5	8	15.63%	25.00%	20.31%
41	FSB115D	8	4	25.00%	12.50%	18.75%
42	FSB129D	8	4	25.00%	12.50%	18.75%
43	FBI 14D	4	8	12.50%	25.00%	18.75%
44	FSB131D	4	6	12.50%	18.75%	15.63%
45	FSB 90D	4	5	12.50%	15.63%	14.06%
46	FOB 15D	4	4	12.50%	12.50%	12.50%
47	FSB109D	3	3	9.38%	9.38%	9.38%
48	FIB 1	#N/A	#N/A	#N/A	#N/A	#N/A
49	FIB 8	#N/A	#N/A	#N/A	#N/A	#N/A
50	FPZ 4A	#N/A	#N/A	#N/A	#N/A	#N/A
51	FPZ 6A	#N/A	#N/A	#N/A	#N/A	#N/A
52	FSB 89D	#N/A	#N/A	#N/A	#N/A	#N/A
53	FSP-12A	#N/A	#N/A	#N/A	#N/A	#N/A
54	FOB 2D	#N/A	4	#N/A	12.50%	#N/A
55	FSB116D	8	#N/A	25.00%	#N/A	#N/A

Table 22. "With Preset" Well Selection Results

Rank	well name	W preset Run (Count)	W preset Run (%)
Preset	FSB126D	32	100.00%
Preset	FSB130D	32	100.00%
Preset	FSB 97D	32	100.00%
Preset	FSB 79	32	100.00%
Preset	FSB 95DR	32	100.00%
Preset	FPZ 6A	32	100.00%
Preset	FPZ 4A	28	87.50%
Preset	FSP-12A	28	87.50%
Preset	FSB131D	24	75.00%
1	FSB 92D	18	56.25%
2	FSB108D	16	50.00%
3	FSB116D	16	50.00%
4	FSB124D	15	46.88%
5	FSB 91D	14	43.75%
6	FSB 93D	13	40.63%
7	FSB 94DR	13	40.63%
8	FSB 87D	12	37.50%
9	FSB132D	12	37.50%
10	FSB 99D	12	37.50%
11	FSB138D	12	37.50%
12	FOB 14D	12	37.50%
13	FSB123D	12	37.50%
14	FSB134D	11	34.38%
15	FBI 17D	10	31.25%
16	FOB 13D	10	31.25%
17	FSB129D	9	28.13%
18	FEX 4	8	25.00%
19	FSB112DR	8	25.00%
20	FSB118D	8	25.00%
21	FSB 78	8	25.00%
22	FSB120D	8	25.00%
23	FSB122D	8	25.00%
24	FSB 88D	8	25.00%
25	FSB115D	8	25.00%
26	FSB109D	8	25.00%
27	FSB135D	7	21.88%
28	FSB 98D	7	21.88%
29	FSB125DR	7	21.88%
30	FSB104D	6	18.75%
31	FSB117D	6	18.75%
32	FBI 15D	6	18.75%
33	FSB114D	6	18.75%
34	FSB128D	4	12.50%
35	FSB136D	4	12.50%
36	FSB137D	4	12.50%
37	FSB133D	4	12.50%
38	FSB127D	4	12.50%
39	FSB 76	4	12.50%
40	FBI 14D	4	12.50%
41	FSB 90D	4	12.50%
42	FSB 89D	2	6.25%
43	FOB 15D	#N/A	#N/A
44	FIB 1	#N/A	#N/A
45	FIB 8	#N/A	#N/A
46	FOB 2D	#N/A	#N/A

To make better sense of the results of the two versions and to help the ALTEMIS team make a decision based on the results, the color-coding is performed for the rows with the following meaning:

- **Green:** The given well in the top 20 of the "with preset" version falls **within** the top 20 of the "without preset" version. (**Best** similarity).
- **Yellow:** The given well in the top 20 of the "with preset" version falls **below** the top 20 of the "without preset" version. (**Medium** similarity).
- **Red:** The given well in the top 20 of the "with preset" version does not appear/does not have enough data in the "without preset" version (**No** similarity).
- **Blue:** The **preselected well** falls **within** the top 20 of the "without preset" version. (5/9 = 56%).

The above-mentioned results were helpful to the ALTEMIS team's experts in the field of geostatistics in making an informed decision as to where to place new sensors. The well selections were influenced mainly by the "without preset" version results. They selected to place the new In-Situ Aqua TROLL 500 sensors at the following wells: 'FSB 97D', 'FSB 95DR', 'FSB 78', 'FSB126D', 'FSB130D', 'FSB 79', 'FEX 4', 'FSB 99D', 'FSB 91D', 'FSB118D', 'FSB124D', 'FSB128D', 'FSB135D', 'FSB132D', 'FSB138D'. From these 15 listed wells, 13 of them appeared in the top 20 of the selection made by the algorithmic approach and other two were in the top 22. This selection of wells demonstrates a successful delivery of the optimization task.

Task 8: Conclusions

The combination of the different components from the first two subtasks contributed greatly to the final results of subtask 8.3. The exploratory data analysis and the proxy variable analysis helped to provide a foundation for the sensor placement optimization. The majority voting approach combining the results of multiple optimized spatial estimation maps generated a successful list of recommendations for the placement of new sensors at the SRS F-Area.

Task 8: References

Denham, Miles E., et al. "A New Paradigm for Long Term Monitoring at the F-Area Seepage Basins, Savannah River Site." 2019, DOI: 10.2172/1504623.

Schmidt, Franziska, et al. "In Situ Monitoring of Groundwater Contamination Using the Kalman Filter." *Environmental Science & Technology*, vol. 52, no. 13, 2018, pp. 7418–7425., DOI: 10.1021/acs.est.8b00017.

Wainwright, Haruko, et al. "Objective." *ALTEMIS*, 19 Aug. 2020, altemis.lbl.gov/about/.

CONFERENCE PARTICIPATION, PUBLICATIONS, AWARDS & ACADEMIC MILESTONES

Professional Conference Presentations and Proceedings

**M. Komninakis, J. Sinicrope, J. Nicholson, L. Lagos. *Certifying the Performance of Fixative Technologies Under Impact Stress for D&D Activities*. Waste Management 2021 Virtual Conference, Phoenix, AZ, March 2021.

** NOTE: Awarded "Superior Paper" rating by WM Symposia.

J. Sinicrope, J. Nicholson, M. Komninakis, L. Lagos. *Strategic Integration of Consensus-based Standards to Improve Technology Acceptance and Return on Investment in Federally-funded Applied R&D Programs*. Waste Management 2021 Virtual Conference, Phoenix, AZ, March 2021.

**H. Upadhyay, W. Quintero, L. Lagos. *Waste Information Management System with 2020-21 Waste Streams*. Waste Management 2021 Virtual Conference, Phoenix, AZ, March 2021.

** NOTE: Awarded "Best Poster Presentation in Track #3" by WM Symposia.

W. Quintero, H. Upadhyay, L. Lagos. *D&D KM-IT Responsive Design*. Waste Management 2021 Virtual Conference, Phoenix, AZ, March 2021.

H. Upadhyay, L. Lagos, S. Joshi. *Artificial Intelligence & Machine Learning Framework for DOE-EM Problem Sets*. Waste Management 2021 Virtual Conference, Phoenix, AZ, March 2021.

Student Conference Presentations and Awards

**A. Meray, H. Wainwright, H. Upadhyay. *pyLEnM: Machine Learning and Analytics Toolkit for Long-term Water Quality Monitoring Using a Remote Sensing Network (21420).* Waste Management 2021 Virtual Conference, Phoenix, AZ, March 2021. (Student Poster)

**D. Gabaldon. *Assessing the Effects of Vibrational Forces on the Performance of Fixative Materials in Mitigating Risk During D&D Activities.* Waste Management 2021 Virtual Conference, Phoenix, AZ, March 2021. (Student Poster)

R. Boza, H. Upadhyay, N. Prabakar, L. Lagos. Robust Anomaly Detection of Nuclear Facility Structures with Convolutional Autoencoder (21425). Waste Management 2021 Virtual Conference, Phoenix, AZ, March 2021. (Student Poster)

** NOTE: DOE Fellows Derek Gabaldon and Aurelien Meray were awarded "Best Undergraduate Student Poster" and "Best Graduate Student Poster", respectively, by WM Symposia.

Academic Milestones

DOE Fellow Alejandro Koszarycz (class of 2017) graduated with a B.S. degree in computer science in Fall 2020 and DOE Fellow, Derek Gabaldon graduated with B.S. degree in mechanical engineering in Summer 2021.

ACKNOWLEDGEMENTS

Funding for this research was provided by U.S. DOE Cooperative Agreement #DE-EM0005213. FIU's Applied Research Center would like to acknowledge the commitment of DOE-EM to this Waste and D&D Engineering and Technology Development project and to all the research being conducted as part of the Cooperative Agreement. The partnership between DOE EM and FIU has resulted in the development and training of outstanding minority STEM students that will benefit this country as a whole.

APPENDIX

The following documents are available at the DOE Research website for the Cooperative Agreement between the U.S. Department of Energy Office of Environmental Management and the Applied Research Center at Florida International University: https://doeresearch.fiu.edu

FIU Year 1 Annual Research Review Presentations:

1. FIU Research Review - Project 1
2. FIU Research Review - Project 2
3. FIU Research Review - Project 3 – D&D
4. FIU Research Review - Project 3 – IT ML
5. FIU Research Review - Project 4 & 5
6. FIU Research Review - Project 4 - DOE Fellow Aurelien Meray
7. FIU Research Review - Project 4 - DOE Fellow Gisselle Gutierrez
8. FIU Research Review - Project 4 - DOE Fellow Jeff Natividad
9. FIU Research Review - Project 4 - DOE Fellow Mariah Doughman
10. FIU Research Review - Project 4 - DOE Fellow Philip Moore
11. FIU Research Review - Project 4 - DOE Fellow Sebastian Story
12. FIU Research Review - Project 5 - DOE Fellow Eduardo Rojas
13. FIU Research Review - Project 5 - DOE Fellow Olivia Bustillo
14. FIU Research Review - Wrap Up - Project 1
15. FIU Research Review - Wrap Up - Project 2
16. FIU Research Review - Wrap Up - Project 3 – D&D
17. FIU Research Review - Wrap Up - Project 3 – IT ML
18. FIU Research Review - Wrap Up - Project 4
19. FIU Research Review - Wrap Up - Project 5